UNIVERSITY OF CALIFORNIA SAN DIEGO

Momentum and Heat Transport in MHD Turbulence in Presence of Stochastic Magnetic Fields

A dissertation submitted in partial satisfaction of the
requirements for the degree Doctor of Philosophy

in

Physics

by

Changchun Chen

Committee in charge:

Professor Patrick H. Diamond, Chair
Professor George M. Fuller
Professor Dusan Keres
Professor Sutanu Sarkar
Professor George R. Tynan

2022

The Dissertation of Changchun Chen is approved, and it is acceptable in quality and form for publication on microfilm and electronically.

University of California San Diego

2022

DEDICATION

To my husband, *Hsiu-Chung Yeh*, and my parents.

EPIGRAPH

A wave is never found alone, but is mingled with as many other waves
as there are uneven places in the object where said wave is produced.
At one and the same time there will be moving over the greatest wave of
a sea innumerable other waves, proceeding in different directions.

Leonardo da Vinci

TABLE OF CONTENTS

LIST OF FIGURES

LIST OF TABLES

ACKNOWLEDGEMENTS

Firstly, I would like to express my sincere gratitude to Prof. Patrick H. Diamond for the continuous support of my PhD study in the last five and a half years. Pat is knowledgeable in the field of plasma, fluid, and nonlinear physics. I am thankful for all the support he has given me over the years, whether explaining a concept to me, spent tremendous time in discussing my results, polishing manuscripts, or writing letters on my behalf for conferences, fellowships, and other opportunities. His guidance helped me complete a successful PhD degree and present a decent scientific research.

I would like to thank our collaborator Prof. Steven Tobias in University of Leeds and colleague Rameswar Singh in UCSD for the help with the simulation code. I also thank my committee members: Prof. George M. Fuller, Prof. Dusan Keres, Prof. Sutanu Sarkar, and Prof. George R. Tynan, for valuable comments and suggestions on my dissertation.

Nobody has been more important to me in the pursuit of the PhD degree than my husband Hsiu-Chung Yeh. He is the one encouraging me to pursue a PhD degree in Physics, and being the most important companion during my stressful PhD life. I am thankful for his constant love, support, and encouragement, near and far.

There are countless other people in my life over the past few years who have made the past few years joyful—too many to name. Here, I thank my parents' support in the past years. My sincere thanks also go to people discussed research with me—Dr. Xavier Garbet in CEA France, Prof. Taik Soo Hahm in Seoul University, Prof. George Mckee in UW Madison, Dr. Lothar Schmitz in UCLA, Dr. Mikhail Malkov, Dr. Xiang Fan, Dr. Norman Cao, Dr. Robin Heinonen, and Mingyun Cao. I also have special thanks to all the members in NTHU Hangout Gang for distressing me during the pandemic.

Chapter 2, in full, is a reprint of the material as it appears in Chang-Chun Chen & Patrick H. Diamond, *The Astrophysical Journal* 892, 24(2020). The dissertation author was the primary investigator and author of this paper.

Chapter 3, in full, is a reprint of the material as it appears in Chang-Chun Chen, Patrick

H. Diamond, Rameswar Singh, and Steven M. Tobias, *Physics of Plasmas* 28, 042301 (2021). The dissertation author was the primary investigator and author of this paper.

Chapter 4, in full, is a reprint of the material as it appears in Chang-Chun Chen, Patrick H. Diamond, and Steven M. Tobias, *Plasma Physics and Controlled Fusion* 64, 015006 (2022). The dissertation author was the primary investigator and author of this paper.

Chapter 5, in full, is currently being prepared for submission for publication of the material. Chang-Chun Chen & Patrick H. Diamond (2022). The dissertation author was the primary investigator and author of this material.

VITA

2015	Bachelor of Science in Physics, National Tsing Hua University, Hsinchu, Taiwan
2015–2016	Research Assistant, National Tsing Hua University, Hsinchu, Taiwan
2018–2022	Research Assistant, University of California, San Diego
2022	Doctor of Philosophy in Physics, University of California, San Diego

PUBLICATIONS

Chang-Chun Chen, Patrick H. Diamond, and Steven M. Tobias. "Ion Heat and Parallel Momentum Transport by Stochastic Magnetic Fields and Turbulence", *Plasma Physics and Controlled Fusion* 64, 015006 (2022)

Chang-Chun Chen, Patrick H. Diamond, Rameswar Singh, and Steven M. Tobias. "Potential vorticity transport in weakly and strongly magnetized plasmas", *Physics of Plasmas* 28, 042301 (2021)

Chang-Chun Chen & Patrick H. Diamond. "Potential Vorticity Mixing in a Tangled Magnetic Field", *The Astrophysical Journal* 892, 24(2020)

ABSTRACT OF THE DISSERTATION

Momentum and Heat Transport in MHD Turbulence in Presence of Stochastic Magnetic Fields

by

Changchun Chen

Doctor of Philosophy in Physics

University of California San Diego, 2022

Professor Patrick H. Diamond, Chair

Tangled magnetic fields, often coexisting with an ordered mean field, have a major impact on turbulence and momentum transport in many plasmas, including those found in the solar tachocline and magnetic confinement devices. In this dissertation, we present research on the turbulent transport in presence of a stochastic magnetic field, and the discuss implications on the formation of astronomical objects and on the turbulence in edge plasma in fusion devices.

The research is divided into three projects. First, we present a novel mean field theory of potential vorticity mixing in β-plane magnetohydrodynamic (MHD). Our results show that mean square stochastic fields strongly reduce Reynolds stress coherence. This decoherence of potential

vorticity flux due to stochastic field scattering leads to suppression of momentum transport and zonal flow formation. We discuss a model of stochastic fields as a resisto-elastic network.

In second project, we shows the breaking of the shear-eddy tilting feedback loop by stochastic fields is the key underlying physics mechanism. A simple calculation suggests that the breaking of the shear-eddy tilting feedback loop by stochastic fields is the key underlying physics mechanism. A dimensionless parameter that quantifies the increment in power threshold is identified and used to assess the impact of stochastic field on the L-H transition in fusion devices.

Finally, we study the turbulent transport of parallel momentum and ion heat by the interaction of stochastic magnetic fields and turbulence in third project. Attention is focused on determining the kinetic stress and the compressive energy flux. A critical parameter is identified as the ratio of the turbulent scattering rate to the rate of parallel acoustic dispersion. For the parameter large, the kinetic stress takes the form of a viscous stress. For the parameter small, the quasilinear residual stress is recovered. In practice, the viscous stress is the relevant form, and the quasilinear limit is not observable. This is the principal prediction of this project.

Chapter 1

Introduction

1.1 Turbulence and Stochastic Fields in β-plane MHD and in Fusion Devices

Turbulent momentum transport plays a key role in the dynamics of astrophysical and geophysical fluids, in the formation of astrophysical objects, and in the formation of shear flows and transport barriers in fusion physics. And tangled magnetic fields, often coexisting with an ordered mean field, have a major impact on turbulence momentum transport in these plasma. In space, examples can be found in the generation of differential rotation in the sun and stars, magnetic dynamos, and atmospheric phenomena in the solar system and exoplanets. The dynamics of the turbulence in several cases is effectively two-dimensional (2D)—usually due to rapid rotation, strong stratification (i.e. low effective Rossby number or large Richardson number), or strong mean field. Hence, a classic β-plane or quasi-geostrophic magnetohydrodynamic (MHD) model is useful to describe these systems.

The solar tachocline is one such quasi-2D astrophysical object—a weakly magnetized system where turbulent transport is critical for its very existence. Specifically, the tachocline may be thought to form by 'burrowing' driven by large meridional cells. These, in turn, are driven by baroclinic torque (i.e. $\nabla p \times \nabla \rho$). Moreover, in this application, turbulence will co-exist with a stochastic field—the disordered magnetic field pumped by the convective overshoot from the convective zone which leads to large magnetic Reynolds number (Rm)[15]. We can expect

the intensity of root-mean-square (rms) magnetic field surpasses that of mean field B_0 in the tachocline from Zel'dovich relation for 2D MHD [29, 32, 16]. As a result, even though the tachocline is surely magnetized, its field is neither smooth nor uniform. And this *stochasticity of magnetic fields* thickens the plot. Hence, the physics of transport in a state of coexisting turbulence and stochastic magnetic field is aa topic of intense interest in astrophysics. There are two main models explains the existence and stability of the tachocline. In one leading model—that of Spiegel & Zahn (1992) [91]—burrowing is opposed by turbulent viscous diffusion of momentum in latitude, but the true nature of 2D tachocline dynamics is ignored. In another model—proposed by Gough & McIntyre (1998) [31]—burrowing is opposed by PV mixing and by a hypothetical fossil magnetic field in the solar radiation zone, but the effects of magnetic fields in turbulent momentum transport and the implication for Alfvén's theorem are ignored. And neither of these studies tackle the strong stochasticity of the ambient tachocline field. In this vein, Chen & Diamond et al. [9] aims to build an analytical model *beyond* quasi-linear (QL) theory and study the momentum transport in highly disordered magnetic fields. Details are discussed later in Chapter 2.

Another application is to tokamaks, where the heat transport, momentum transport, and the formation of shear flows in presence of a stochastic field has long been recognized as a fascinating, though complex, problem. Here, we consider that the stochasticity of magnetic fields is induced by Resonant magnetic perturbations (RMPs) generated by the external RMP coils. RMPs are applied to the edge of tokamak plasma to mitigate Edge Localized Modes (ELMs) [26, 25], which produce unacceptably high transient heat loads on plasma-facing components, and can damage wall components of a fusion device. As a result, stochastic field effects on turbulent transport is a 'paradigm problem' in magnetic fusion physics and has stimulated the writing of many well-known papers, most notably Rosenbluth et al. [82] and Rechester and Rosenbluth [77]. The synergetic effect of stochastic fields on heat/momentum transport and the turbulence is especially true for L-mode plasmas, with resonant magnetic perturbations RMP (before the L-H transition), where the predominantly electrostatic turbulence is strongest

just before transition. Experiments and simulations shows that the RMPs rais the transition threshold [54, 30, 46, 84, 64, 85, 86] and that the Reynolds stress burst in pre-L-H transition drops significantly when RMPs are applied to the edge of DIII-D [50]. But no analytical model has shed light on this stochastic-fields-induced mechanism for Reynolds stress. Hence, studies on stochastic-field-induced effects *analytically* in the presence of strong turbulence are of importance in fusion plasma. Chen et al (2021) [10] aims to calculate the poloidal momentum transport and derive a critical parameter for the power threshold increment in L-H transition in presence of stochastic fields induced by RMPs (see Chapter 3).

In addition to mean poloidal flow, the evolution of mean parallel flow and ion pressure will also be affected by the *co-existing* backgrounds of turbulence and stochastic magnetic fields. This can be realized by observing the radial balance equation $\langle E_r \rangle = \frac{\nabla \langle p_i \rangle}{ne} - \langle \mathbf{u} \rangle \times \langle \mathbf{B} \rangle$. Motivated by studies of rotation damping due to ergodic magnetic limiter operation on the TEXT [102], Finn et al. [28] (hereafter referred to as FGC) addressed the 'stochastic field only' limit of the problem. The FGC analysis start with the equation of mean parallel and pressure

$$\frac{\partial}{\partial t}\langle u_\parallel \rangle + \frac{\partial}{\partial r}\langle \widetilde{u}_r \widetilde{u}_\parallel \rangle = -\frac{1}{\rho}\frac{\partial}{\partial r}\langle \widetilde{b}_r \widetilde{p} \rangle \tag{1.1}$$

$$\frac{\partial}{\partial t}\langle p \rangle + \frac{\partial}{\partial r} + \frac{\partial}{\partial r}\langle \widetilde{u}_r \widetilde{p}_\parallel \rangle = -\rho c_s^2 \frac{\partial}{\partial r}\frac{\partial}{\partial r}\langle \widetilde{b}_r \widetilde{u}_\parallel \rangle, \tag{1.2}$$

where $\widetilde{b} \equiv \sqrt{\langle \widetilde{B}^2 \rangle / B_0^2}$ is a root-mean-square (rms) of normalized disordered fields, B_0 is the mean toroidal field, and the bracket average is an ensemble average over symmetry direction, i.e. $\langle\rangle \equiv \frac{1}{2\pi r}\int r d\theta \frac{1}{L_\parallel}\int dL_\parallel$. Here, $c_s \equiv \sqrt{\gamma p/\rho}$ is the sound speed, γ is the adiabatic index, and ρ is the mass density. And hereafter we define the RHS term as derivative of kinetic stress (K) and compressive energy flux (H)

$$K \equiv \frac{\langle \widetilde{b}_r \widetilde{p} \rangle}{\rho} \tag{1.3}$$

$$H \equiv \rho c_s^2 \langle \widetilde{b}_r \widetilde{u}_\parallel \rangle. \tag{1.4}$$

In FGC's study [28], the familiar advective fluxes of the parallel flow and pressure are ignored. We note in passing that the kinetic stress has been linked directly to plasma rotation by studies on the Madison Symmetric Torus reverse field pinch. By a combination of probes and polarimetry, Ding et al. (2013) demonstrated a clear correlation between the divergence of the measured kinetic stress and the profile of mean parallel flow (see figure 2 of Ding et al [22]). This result shows a compelling insight into the connection among fluctuation measurements, parallel flow dynamics, and momentum transport. FGC, however, didn't address this relation between the microscopic and macroscopic facets of the momentum transport problem. Our work [8] aims to calculate the relation between the kinetic stress and the compressive energy flux *explicitly*. A *hybrid diffusivity* is also derived—this depicts how stochastic fields and turbulent flows *interact together* and hence induce the energy and parallel momentum transport. Details are discussed later in and 4.

1.2 Potential Vorticity

Given the effective 2D structure of the tachocline and the fusion devices (due to strong mean toroidal magnetic field), it is natural to treat its dynamics using classical shallow water theory and formulate its description in terms of potential vorticity (PV) evolution and transport. In such systems, Reynolds forces are equivalent to vorticity fluxes via the Taylor identity [93] . For this and other reasons—the most fundamental being the freezing-in law for fluid vorticity [72]——it is natural to describe such systems in terms of PV. Generally, $PV \equiv \zeta = \zeta_a \cdot \nabla\psi/\rho$, where ζ_a is the absolute vorticity, ψ is a conserved scalar field, and ρ is the fluid density. The advantage of a PV description of the dynamics is that ζ is conserved along fluid particle trajectories, up to dissipation, much like phase space density is conserved in the Vlasov plasma. Another advantage to consider PV is because it can be expressed as a 'charge density element', i.e. $\zeta \equiv \rho_{PV}$, floating in the fluid threaded by stretched magnetic fields. And the PV phase-space

conservation will lead to the charge density continuity, i.e.

$$\frac{\partial}{\partial t}\rho_{PV} + \nabla \cdot \mathbf{J}_{PV} = 0. \tag{1.5}$$

Figure 1.1 shows a cartoon of how the PV charge density is related to 'plucking' magnetic lines. In β-plane MHD, zonal flows are produced by inhomogeneous PV mixing (i.e. an inhomogeneous flux of PV 'charge density') and by the inhomogeneous tilting of magnetic field lines (weighted by current density). In simple words, there are two ways to redistribute the charge density (in this case, the absolute vorticity) — one is through advection, and the other is by bending the magnetic field lines, along which current flows. These two processes together determine the net change in local PV charge density.

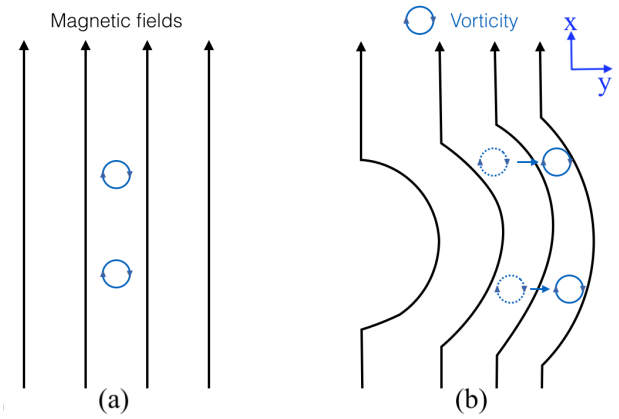

Figure 1.1. Evolution of PV threaded by magnetic field lines in a frame moving with the flow. Aside from the advection of flow, the distribution of PV charge density also changed under the influence of inhomogeneous magnetic fields. (a) PV uniformly distributed in the moving frame. (b) PV distribution is changed by the tilted magnetic field lines. Dashed circles are undisturbed vortices. Solid circles are new locations of PV charge density.

Examples of conserved PV are:

- Pure fluid: $PV \equiv \nabla \times \mathbf{u}$, where $\mathbf{u}$ is the flow velocity.
- On β-plane: $PV = \zeta = \beta y - \nabla^2 \psi$. β is the Rossby parameter given by $\beta = df/dy|_{\phi_0} = 2\Omega\cos(\phi_0)/a$, where f is angular frequency at latitude ϕ_0 on β-plane (see figure 1.2).

- Hasegawa-Mima system [34]: $PV = (1-\rho_s^2\nabla^2)|e|\phi/T + \ln n_0$, where ϕ is electric potential and n_0 is a background mass density.

In these system, momentum transport and flow formation are determined by inhomogeneous PV mixing [55, 101] (see figure 1.3 and 1.4). The mechanism for the PV mixing is closely related to the coherence and cross phase of the vorticity flux. Mechanisms include viscous dissipation, wave-flow resonance, nonlinear mode interaction, and beat wave-flow interaction, akin to nonlinear Landau damping [1].

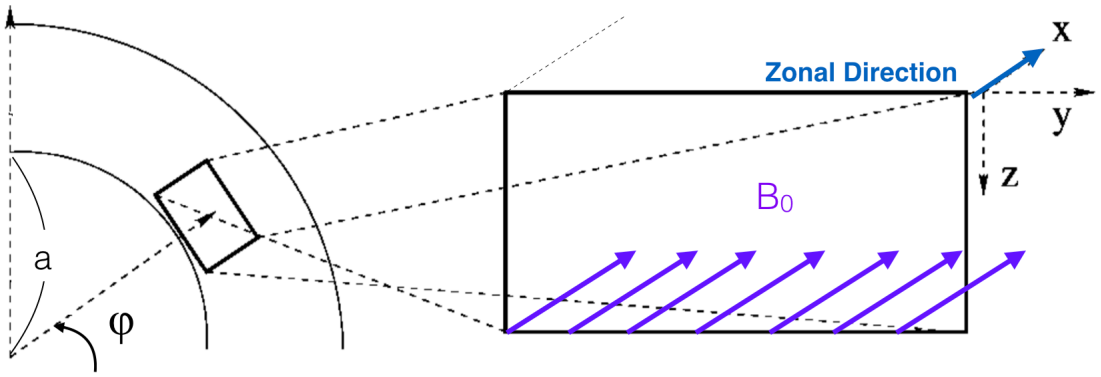

Figure 1.2. Geometry and computational domain for the local Cartesian model. The x- and y-axes are local longitudinal and latitudinal directions, respectively. The z-axis represents the depth of the β-plane. The mean magnetic field B_0 is zonal direction (x-axis)

This points to the topic of *PV transport in a tangled field*—the main study in this dissertation [9, 10, 8]—as being crucial to understanding momentum transport in the tachocline and fusion devices. Previous studies of flow dynamics for β-plane MHD have focused on PV transport and jet (zonal flow) formation [16, 17, 55]. Computational studies have noted that even weak mean magnetic fields can inhibit the expected negative viscosity phenomena such as jet formation [61, 62, 95, 33]. Results indicate that for fixed forcing and dissipation, jets form for $B_0^2/\eta < (B_0^2/\eta)_{crit}$, but are inhibited for $B_0^2/\eta > (B_0^2/\eta)_{crit}$. These findings are interpreted in terms of the idea that the mean field, B_0, tends to 'Alfvénize' the turbulence , i.e. converts Rossby wave turbulence to Alfvén wave turbulence. For Alfvénic turbulence, fluid and magnetic stresses tend to compete, thus restricting PV mixing and inhibiting zonal flow formation [16]. When

the freezing-in law is not violated (Poincare 1893), the strong field-fluid coupling prevents PV mixing, and loosely put, the 2D inverse energy cascade [49, 40, 5]. When the resistive diffusion is sufficiently large to break freezing-in, PV mixing occurs.

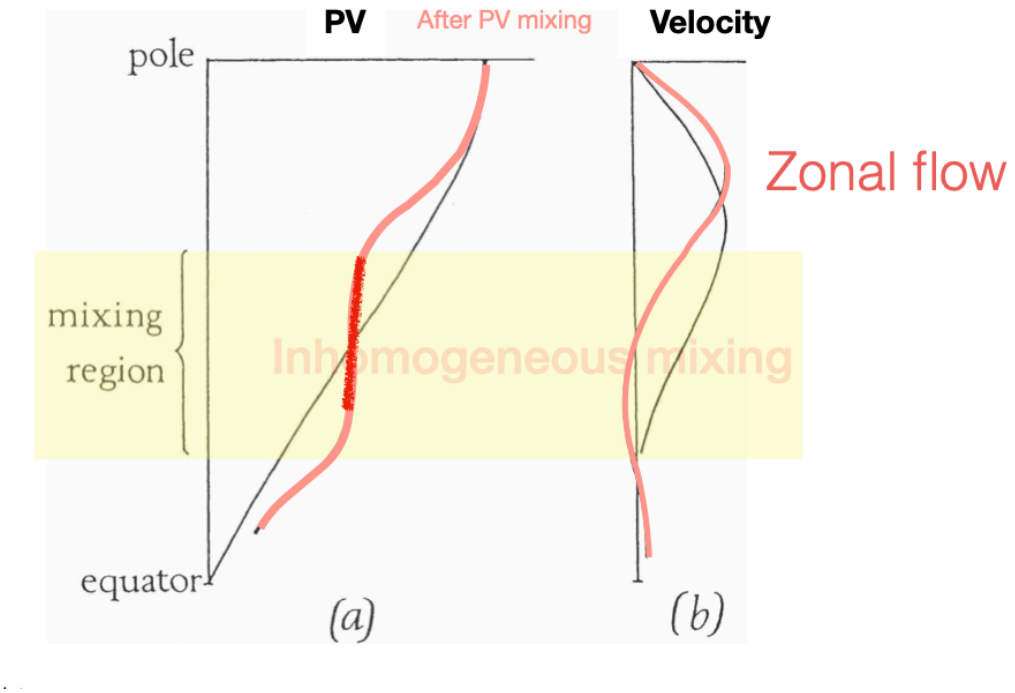

Figure 1.3. A cartoon for PV mixing on β-plane. (a) The PV intensity along a longitudinal line. (b) The velocity intensity along a longitudinal line. The inhomogeneous PV mixing occurs in the yellow shaded region. The pink line indicate the new PV and velocity intensity after the PV mixing.

1.3 A model Beyond Quasilinear Theory

Recent progress on the β-plane MHD has exploited theoretical approaches based on quasi-linear (QL) theory or wave turbulence theory [13]. These are unable to take into account of the stochasticity of the ambient field; i.e. the fact that $|\widetilde{B}^2|/B_0^2 \gg 1$ in the tachocline, where fields are strongly tangled.

Since the system we are interested in is highly *nonlinear*—it consists turbulence and a

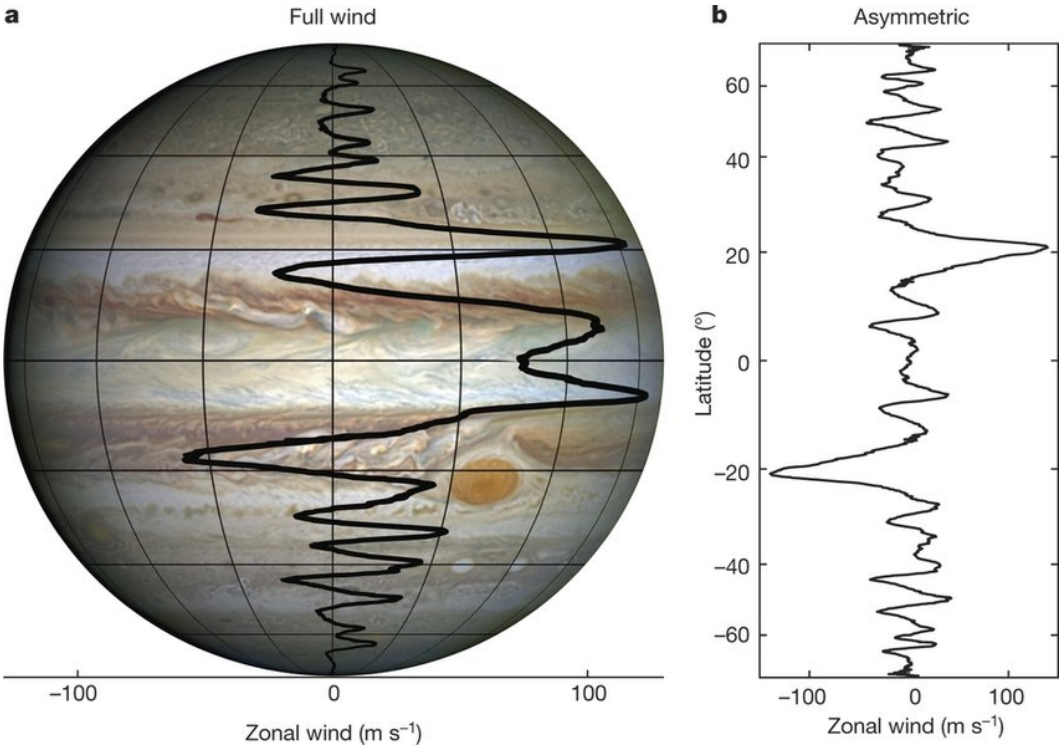

Figure 1.4. Jupiter's asymmetric zonal velocity field. (a) The cloud-level zonal flows (thick black line) as a function of latitude, as measured during Juno's third perijove pass on 11 December 2016. The image of Jupiter was taken by the Hubble Wide Field Camera in 2014 (https://en.wikipedia.org/wiki/Jupiter). Grid latitudes are as in b and the longitudinal spread is 45°. Grid latitudes are as in b and the longitudinal spread is 45°. Zonal flow scale is the same as the longitudinal grid on the sphere. b, The asymmetric component of the flow, taken as the difference between the northern and southern hemisphere cloud-level flows. Reprint from [45].

stochastic magnetic field—a key to check the 'non-linearity', or validity for for the QL closure, is Kubo number (i.e. *Ku* [52]), is introduced. The **fluid Kubo number**, which quantifies the effective memory of the flow and the field, is defined as

$$Ku_{fluid} \equiv \frac{\delta_l}{\Delta_\perp} \sim \frac{\widetilde{u}\tau_{ac}}{\Delta_\perp} \sim \frac{\tau_{ac}}{\tau_{eddy}}, \tag{1.6}$$

where δ_l is the characteristic scattering length, τ_{ac} is the velocity autocorrelation time, and τ_{eddy} is the eddy turn-over time. The eddy turn-over time is $\tau_{eddy} = \Delta_\perp/\widetilde{u}$, where $\Delta_\perp$ is the eddy size (see Figure 1.5). In practice, the validity of QL theory requires small fluid Kubo number

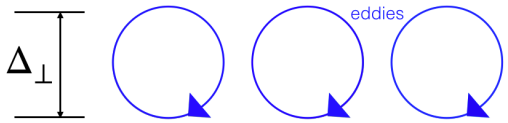

Figure 1.5. Eddy size $\Delta_\perp$. In this figure, the shear flow is in the left-right direction. The eddy size is measured perpendicular to the flow.

$Ku_{fluid} \ll 1$. As a particle traverses an eddy length, it experiences several random kicks by the flow perturbations, as in a diffusion process. In this limit, trajectories of particles don't deviate significantly from unperturbed trajectories. Note that in the case of wave turbulence, the autocorrelation time (τ_{ac}) is sensitive to dispersion. The autocorrelation time can be expressed as:

$$\frac{1}{\tau_{ac}} = \Delta\omega = \frac{d\omega}{d\mathbf{k}} \cdot \Delta\mathbf{k}. \tag{1.7}$$

However, when the turbulence is strong, we have $\delta_l \gg \Delta_\perp$. Here, particles deviate strongly from the original trajectories in an autocorrelation time, indicating a failure of QL theory (i.e. $Ku_{fluid} > 1$). However, it is clear that β-plane MHD is not a purely fluid system; hence the validity of QL theory depends not only on the fluid Kubo number but also on the **magnetic Kubo number**. This can be written as:

$$Ku_{mag} \equiv \frac{\delta_l}{\Delta_\perp} \tag{1.8}$$

$$\delta_l \sim \frac{l_{ac}|\widetilde{\mathbf{B}}|}{B_0}, \tag{1.9}$$

where δ_l is the deviation of a field line, l_{ac} is the magnetic autocorrelation length, and $|\widetilde{B}|$ is the magnetic field intensity of the wave turbulence. If a particle travels a coherence length $\Delta_\perp$ and experiences several random kicks in weak magnetic perturbations, it undergoes a process of magnetic diffusion, which can be treated using QL theory [78]. In contrast, when magnetic perturbations are strong, particle trajectories are sharply deflected by strong $\widetilde{B}$-induced scattering

within an autocorrelation length.

One indication [95, 9] of the deficiency in the conventional wisdom is the observation from theory and computation that values of B_0^2 well *below* that for Alfvénization are sufficient to result in a the reduction in Reynold stress and thus PV mixing (see Figure 1.6). This suggests that tangled magnetic fields act to reduce the phase correlation between $\widetilde{u}_x$ and $\widetilde{u}_y$ in the turbulent Reynolds stress $\langle \widetilde{u}_y \widetilde{u}_x \rangle$. Note that, as we will show here, this effect is one of *dephasing*, not suppression, and not due to a reduction of turbulence intensity. It resembles the well-known effect of quenching of turbulent resistivity in 2D MHD, which occurs for weak B_0^2 but large $\langle \widetilde{B}^2 \rangle$ (i.e. large Rm), at fixed drive and dissipation. Thus, it appears that Alfvénization — in the usual sense of the $\rho_0 \langle \widetilde{v}^2 \rangle = \langle \widetilde{B}^2 \rangle / \mu_0$ balance intrinsic to linear Alfvén waves—and the associated stress cancelation are *not* responsible for the inhibition of PV mixing in β-plane MHD at high magnetic Reynolds number. This observation reinforces the need to revisit the problem with a fresh approach.

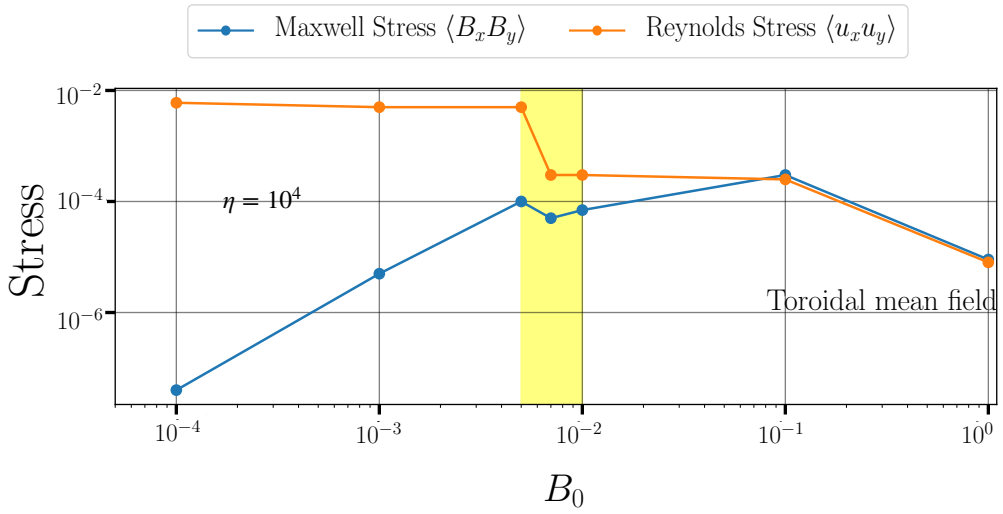

Figure 1.6. Average Reynolds stresses (orange line) and Maxwell stresses (blue line) for $\beta = 5$, $\eta = 10^{-4}$ from [9]. Full Alfvénization happens when B_0 intensity is larger than $B_0 = 10^{-1}$ and $B_0 = 6 \times 10^{-2}$, respectively. The yellow-shaded area is where zonal flows cease to grow. This is where the random-field suppression on the growth of zonal flow becomes noticeable.

In Chen & Diamond (2020) [9], we present a theory of PV mixing in β-plane MHD. A

mean field theory is developed for the weak perturbation regime, and a novel model is derived for the case of a strong tangled field ($\langle \widetilde{B}^2 \rangle > B_0^2$). The latter is rendered tractable by considering the fluid dynamics to occur in a prescribed static, stochastic field. For $\langle \widetilde{B}^2 \rangle < B_0^2$, the quasi-linear calculation reveals that PV mixing evolves by both advection and by inhomogeneous tilting of field lines correlated with fluctuations. The presence of B_0 converts Rossby waves to Rossby-Alfvén waves so the system exhibits a stronger Alfvénic character for larger B_0. When turbulence Alfvénizes, PV mixing is quenched by the competition between fluid and magnetic stresses. However, the issue is more subtle, since numerical calculations reported here indicate that *magnetic fields affect the Reynolds stress well below the intensity of B_0 for which Alfvénization occur*. This suggests that magnetic fluctuations affect the phase *correlation* of velocity fluctuation in the stress, in addition to producing the competing magnetic stress. By the Zel'dovich theorem, however, we expect that $|\widetilde{B}^2| \gg B_0^2$, so QL theory formally *fails*, for magnetic Kubo number can be large, i.e. $Ku_{mag} \propto |\widetilde{B}^2|/B_0^2 \gg 1$. To address the $|\widetilde{B}^2| \gg B_0^2$ limit, we go beyond QL theory and consider an effective medium theory, which allows calculation of PV mixing in a resisto-elastic fluid, where the elasticity is due to $\langle \widetilde{B}^2 \rangle$. The resisto-elasticity of the system acts to reduce the phase correlation in the Reynolds stress. Physically, fluid energy is coupled to damped waves, propagating through a disordered magnetic network. The dissipative nature of the wave-field coupling induces a drag on the mesoscale flows. We show that PV mixing is quenched at large Rm, for even a weak B_0. The implications for momentum transport in the solar tachocline and related problems are discussed in Chapter 2.

Note that for the drift-wave turbulence at the edge of a fusion device, the magnetic perturbation caused by RMPs are much smaller than the toroidal mean field by a factor 10^{-7}. So, the magnetic Kubo number there is small, i.e. $Ku_{mag} \ll 1$.

1.4 Drift-wave turbulence and Zonal Flow

As discussed in previous sections, one can notice that zonal flow has tight relation with turbulence when analyzing the turbulent momentum transport. In this section, we explain the underlying physics for the production of turbulence, of the zonal flow, and also their interaction.

The production of turbulence is driven the inhomogeneity—for the β-plane MHD turbulence, the inhomogeneity is rotation (or Rossby parameter β) and buoyancy frequency $\mathscr{B}$ (i.e. Rossby number Ro and Richardson number R_i); while for drift-wave turbulence in fusion devices, the free energy comes from density or temperature gradient (i.e. ∇n and ∇T). Detailed comparison between β-plane MHD turbulence and drift-wave turbulence can be found in Table 2.1. Interactions among turbulent wave modes, in turn, form the zonal modes (hereafter referred to as zonal flows).

In real space perpective, the Taylor Identity [93] an useful tool to understand this mechanism:

$$\underbrace{\frac{\partial}{\partial t}\langle u_x\rangle}_{\text{large scale}} = \langle \widetilde{u_y}\widetilde{\zeta}\rangle = -\frac{\partial}{\partial y}\underbrace{\langle \widetilde{u_y}\widetilde{u_x}\rangle}_{\substack{\text{small-scale}\\ \text{coupling}}}, \tag{1.10}$$

where the $\langle u_x\rangle$ is the zonal flow. This equation shows that the cross-flow flux of potential velocity underpins the Reynolds stress and that the gradient of the Reynolds stress (a shear force) then drives the large-scale zonal flow. From the Taylor Identity, the link between inhomogeneous, cross-flow PV transport (i.e., local PV mixing) and mean flow generation is established. Also, a *non-local* (in wavenumber space), *non-linear* interaction from wave-wave interactions (i.e. three-wave/triad interaction) drives zonal flows. The three-wave interaction mechanism is shown in Figure 1.7. As a result, *strongly nonlinear processes like PV mixing and wave breaking yield turbulent PV flux, and form a large-scale zonal flow*.

Then, how do the zonal flow and turbulence interact in model perspective? Given that the kinetic energy is deposit from turbulence to the zonal flow, it is useful to view turbulence

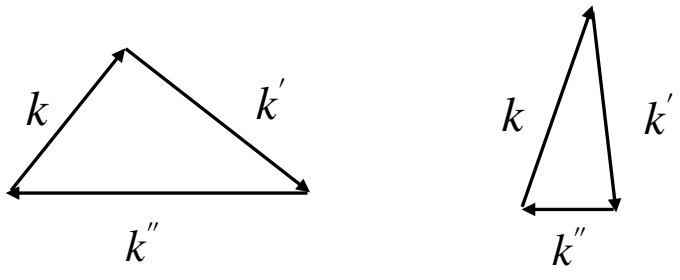

Figure 1.7. Three-wave (triad) interaction where $\mathbf{k}+\mathbf{k}^{'}+\mathbf{k}^{"}=0$. (a) Local transport. The wave-numbers of the three waves are similar. (b) Non-local transport. The resultant wave (zonal flow mode) has wavenumber much smaller than that of the other two waves.

and zonal flows as predators and preys in predator-prey model. Here, the turbulences is the prey, growing from the free energy source (i.e. the environmental nutrients). And the zonal flow (i.e. the predator) 'feeds' upon turbulence (see Figure 1.8).

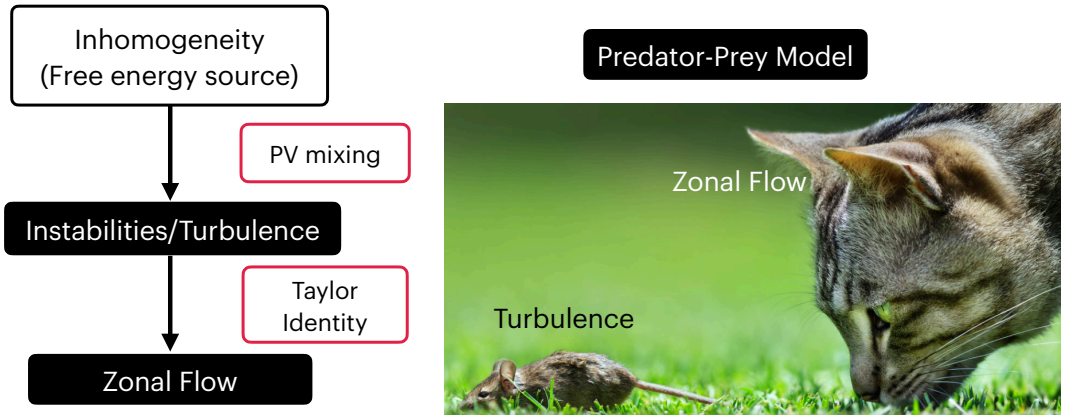

Figure 1.8. Reprint from [88].

Recall the theme of this dissertation is understanding the momentum transport in presence of a stochastic field; consequently, one can expect the predator-prey story becomes complicated when stochastic fields thicken the plot. First, the stochastic effect suppresses the production of

zonal flow. This can be observed by considering the *extented* Taylor Identity:

$$\langle \widetilde{B}_y \nabla^2 \widetilde{A} \rangle = \frac{\partial}{\partial y} \langle \widetilde{B}_y \widetilde{B}_x \rangle, \tag{1.11}$$

and therefore the evolution of zonal flow becomes

$$\frac{\partial}{\partial t} \langle u_x \rangle = -\frac{\partial}{\partial y} \left[\langle \widetilde{u_y} \widetilde{u_x} \rangle - \frac{\langle \widetilde{B}_y \widetilde{B}_x \rangle}{\mu_0 \rho} \right], \tag{1.12}$$

This equation states that the mean PV transport is determined by the difference between the Reynolds and Maxwell stresses, in which the stochastic-field enters. Moreover, the Reynolds stress itself is determined by the cross-phase (i.e. $\langle k_y k_x \rangle$), which will be *decorrelated* by stochastic fields—the effect of this Alfvénic coupling (due to the stochastic fields) induces the decoherence of the Reynolds stress (or vorticity flux), thus reducing momentum transport and flow generation. I proposed [10] that physical insight into this decoherence can be obtained by considering the effect of a stochastic magnetic field on the "shear-eddy tilting feedback loop." To see this, we observe Snell's law:

$$\frac{d}{dt} k_x = -\frac{\partial(\omega_0 + u_y k_y)}{\partial x} \simeq 0 - \frac{\partial(k_y u_y)}{\partial x}, \tag{1.13}$$

and obtain the Reynolds stress

$$\langle \widetilde{u}_x \widetilde{u}_y \rangle = -\sum_k \frac{|\widetilde{\phi}|^2}{B_0^2} \langle \widetilde{k}_x \widetilde{k}_y \rangle, \tag{1.14}$$

where, and hereafter in fusion device geometry, x-, y-, and z-direction is defined in radial, poloidal, and toroidal direction (see Figure 1.9). By considering this feedback loop in presence of a stochastic field, I show [10] explicitly that sufficiently strong coupling of drift waves to a stochastic magnetic field can *break* the "shear-eddy tilting feedback loop". This underpins flow generation by modulational instability. Note that the interaction of Alfvén waves with a tangled

magnetic field differs from that of Alfvén waves with an ordered field. Here, the effect is to strongly couple the flow perturbations to an effective elastic medium threaded by the chaotic field. More details are discussed in Chapter 3.

In fusion device, several studies [20, 47, 57, 23] suggest that the L-H transition is triggered by edge shear flows, implying that the transition dynamics are modified by the effects of stochastic fields on poloidal zonal flow ($E \times B$ mean flow) evolution. Indeed, analyses suggests that RMPs may "randomize" the edge layer. Stochasticity results from $\mathbf{k} \cdot \mathbf{B} = 0$ resonance overlap, and the field line separation increases exponentially. Hence, a central question is one of phase—i.e., the effect of the stochastic field on the coherence of fluctuating velocities, which enters the Reynolds stress and PV. In physical terms, the disordered field tends to couple energy from fluid motion to Alfvénic and acoustic waves, which radiate energy away and disperse wave packets.

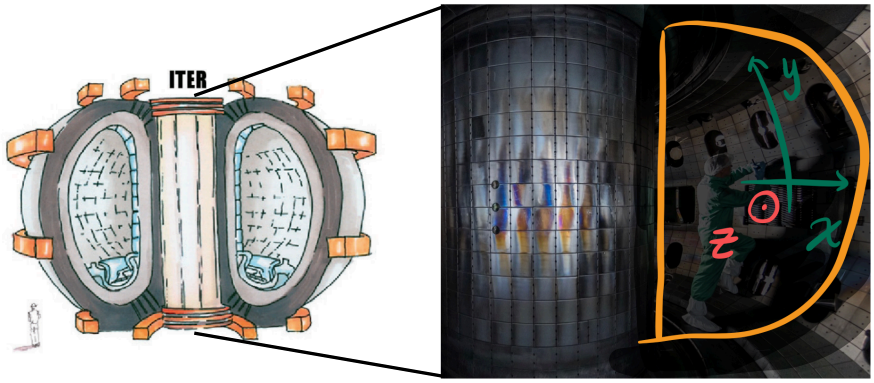

Figure 1.9. Coordinate in fusion device. We define x-, y-, and z-direction is defined in radial, poloidal, and toroidal direction.

Also, by noting the ion radial force balance equation at the edge of fusion device

$$\langle E_r \rangle = \frac{\nabla \langle p_i \rangle}{ne} - \langle \mathbf{u} \rangle \times \langle \mathbf{B} \rangle, \tag{1.15}$$

one should notice that mean parallel (toroidal) flow and ion pressure are also under the influence

of stochastic fields decorelation effect. Hence, in addition to the effect of stochastic on the mean shear flow, I revisited [8] the mean toroidal (i.e. in the direction parallel to the mean field $\mathbf{B_0}$) flow in the context of *co-existing* grounds of turbulence and stochastic magnetic fields. Given the clear resemblance of this problem to aspects of gas dynamics, a natural approach is to cast the analysis in terms of the familiar Riemann variables $u_{\parallel} \pm p$ [53]. A quasilinear analysis then gives an estimate of the relaxation rate for excitation on a perpendicular scale length $l_{\perp}$ as $c_s D_M / l_{\perp}^2$, here D_M is conventional magnetic diffusivity. This rate may be thought of as characteristic of acoustic pulse decorrelation due to propagation along stochastic field lines. However, it should be said that the dynamics here are fundamentally *non-diffusive*. In particular, the kinetic stress actually is *residual stress* driven by $\nabla\langle p\rangle$, i.e. $K = -c_s D_M \partial_r \langle p\rangle$. Likewise, the compressive energy flux is a non-diffusive contribution to the energy flux driven by $\nabla\langle u_{\parallel}\rangle$, i.e. $H = -c_s D_M \partial_r \langle u_{\parallel}\rangle$. These relations are not addressed in FGC. Moreover, the FGC analysis was quasilinear. But to address the strong turbulence regime *together* with stochastic field, the response of pressure and parallel flow must be computed in the presence of a scattering field of electrostatic fluctuations, which were present as a spectrum of fluctuating velocities $\langle \widetilde{\mathbf{u}}\,\widetilde{\mathbf{u}}\rangle_{k,\omega}$. This requires for *a significant and qualitative departure from the quasilinear analysis*. I calculated [8] the explicit form of the stochastic-field-induced transports (i.e. from kinetic stress and the compressive energy flux), and obtained different transports mechanisms in strong and weak electrostatic turbulence regimes. Moreover, we are interested in how the synergetic effect of stochastic and turbulence influence the particle transport. FGC refers to the density evolution in this problem as 'sound wave transport', yet it is clear that no sound wave dynamics is involved. To clarify this question, we consider electron particle transport in a stochastic magnetic field. Here, we consider the stochastic field as co-existing with plasma current perturbations which generate it, so that Ampère's law is satisfied. I obtain an additional term, $\langle \widetilde{b}_x \widetilde{u}_z\rangle$, for the electron particle flux. This is an effect due to *ion* flow along tilted lines and shows stochastic lines and parallel ion flow gradient drive a net electron particle flux. Calculations for the mechanism that mean parallel flow and mean pressure are driven via the *hybrid diffusivity* that involves effect

Table 1.1. Comparison MHD Turbulence of the solar tachocline and fusion devices.

	β-plane MHD Turbulence (Solar tachocline)	Drift Wave Turbulence (tokamak)
Linear Wave	Rossby-Alfvén waves	Drift waves
Conserved PV	$PV = -\nabla^2\psi + \beta y$	$PV = -\nabla^2\phi + n$
Inhomogeneity (free energy source)	Rossby Parameter β and flow buoyancy $\mathscr{B}$	$\mathbf{B_0}$, ∇n, and ∇T
Rossby number (Ro)	$Ro = 0.1 \sim 1$	$Ro = \frac{u}{L\Omega_i} \ll 1$
Reynolds number (Re)	$Re = 10^{16} \sim 10^{17}$	$Re = 10^1 \sim 10^2$ (Landau Damping)
Magnetic Reynolds number (Rm)	$Rm = 10^5 \sim 10^6$	$Rm = \frac{Lv_A}{\eta} = 10^5 \sim 10^7$ (Lundquest number)
Zonal flow	Jets, zonal bands (toroidal)	$E \times B$ shear flow (poloidal)

of stochastic field and turbulent scattering, and the stochastic-field-induced effect on electron particle flux are shown in Chapter 4.

1.5 Overview of Chapters

In this dissertation, we focus on three main topics: the stochastic magnetic fields effect on momentum transport in β-plane MHD turbulence, the mechanism of the breaking of shear-eddy tilting feedback loop due to the RMPs at the edge of a tokamak, and the turbulent transport of parallel momentum and ion heat by the interaction of stochastic magnetic fields and turbulence. These topics are discussed in Chapter 2, 3, and 4 respectively. A summary and future work are discussed in Chapter 5.

Chapter 2 addresses a mean field theory for a tangled "in-plane" field in b-plane magnetohydrodynamic (MHD), which is used to compute the Reynolds force and magnetic drag in this weak mean field (B_0) system. The validity of QL theory of β-plane MHD and the Kubo numbers

are calculated. The mean square stochastic magnetic field $\overline{B_{st}^2}$ was shown to be the dominant element, controlling the coherence in the PV flux and Reynolds force. Of particular interest is the finding that the Reynolds stress degrades for weak B_0, at a level well below that required for Alfvénization. The effective medium theory of PV mixing in a tangled magnetic field is also detailed. The phase correlation in the Reynolds stress and the onset of magnetic drag are calculated. Finally, a physical model of the effective resisto-elastic medium is discussed—the small-scale field defines an effective Young's modulus for elastic waves, rather than a turbulent dissipation.

Chapter 3 presents the study of Reynolds stress decoherence in tokamak edge turbulence due to the RMPs coils. Notice that the stochastic fields here is 3D. It offers insights of how drift-Alfvén wave propagation along stochastic fields induces an ensemble averaged frequency shift that breaks the "shear-eddy tilting feedback loop." It also shows that Reynolds stress decoherence occurs for a modest level of stochasticity. The ratio of the stochastic broadening effect to the natural linewidth defines a critical parameter that determines the concomitant L-H transition power threshold increment. With intrinsic toroidal rotation in mind, the decoherence of the parallel Reynolds stress is explored. This mechanism is demonstrated to be weaker than for the poloidal momentum transport case since the propagation speed which enters parallel flow dynamics is acoustic in stead of Alfvénic. The intertwined mechanisms of symmetry breaking, stochasticity, and residual stress are discussed.

In Chapter 4, the explicit calculation of particle flux and the parallel momentum transport in a steady stochastic magnetic field is presented. Chapter 4 also analyzes the physics of kinetic stress (K) and compressive energy flux (H), which play important roles in momentum and density evolution—these are calculated under the interplay between $E \times B$ turbulence and stochastic magnetic fields. A critical parameter is identified as the ratio of the turbulent scattering rate to the rate of parallel acoustic dispersion. For the parameter large, the kinetic stress takes the form of a viscous stress. For the parameter small, the quasilinear residual stress is recovered. In practice,

the viscous stress is the relevant form, and the quasilinear limit is not in practice observable.

In Chapter 5, the key results of the chapters above are summarized, and possible future directions of study are discussed.

Chapter 2

β-Plane MHD Turbulence and the Solar Tachocline

The β-plane MHD system at high *Rm* with *weak* mean field supports a strong disordered magnetic field. Hence, analyzing this problem is a daunting task, on account of the chaotic field and strong non-linearity. Zel'dovich [105] suggested the 'whole' problem consists of a random mix of two components: a weak, constant field (B_0) and a random ensemble of magnetic 'cells' (B_{st}), for which the lines are closed loops ($\nabla \cdot \mathbf{B_{st}} = 0$). Assembling these two parts gives a field configuration which may be thought of as randomly distributed 'cells' of various sizes, threaded by 'sinews' of open lines (Fig. 2.1). Hence, the magnetic fields can be decomposed to $\mathbf{B} \equiv \mathbf{B_0} + \mathbf{B_{st}}$, where B_0 is modest (i.e. $|B_{st}| > B_0$). This system with strong, tangled field cannot be described by linear responses involving B_0 only, and so is not amenable to traditional quasilinear theory. Linear closure theory allows analysis in a diffusive regime, where fluid Kubo

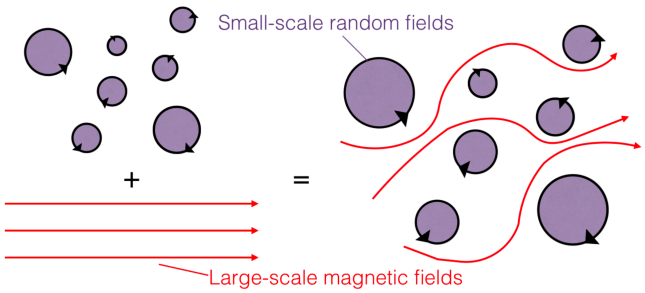

Figure 2.1. The large-scale magnetic field is distorted by the small-scale fields. The system is the 'soup' of cells threaded by sinews of open field lines.

number [52] $Ku_{fluid} < 1$ and magnetic Kubo number $Ku_{mag} < 1$. The **fluid Kubo number** is defined as

$$Ku_{fluid} \equiv \frac{\delta_l}{\Delta_\perp} \sim \frac{\widetilde{u}\tau_{ac}}{\Delta_\perp} \sim \frac{\tau_{ac}}{\tau_{eddy}}, \tag{2.1}$$

where δ_l is the characteristic scattering length, τ_{ac} is the velocity autocorrelation time, and τ_{eddy} is the eddy turn-over time. The eddy turn-over time is $\tau_{eddy} = \Delta_\perp/\widetilde{u}$, where $\Delta_\perp$ is the eddy size (see Figure 1.5).

In practice, the validity of QL theory requires small fluid Kubo number $Ku \ll 1$. To understand this, we compare autocorrelation rate ($1/\tau_{ac} \equiv \Delta\left(-\beta k_x/k^2\right) = \left|-\beta/k^2 + 2\beta k_x^2/k^4\right|\Delta k_x + \left|2\beta k_x k_y/k^4\right|\Delta k_y$) with decorrelation rate ($1/\tau_{eddy} = k\widetilde{u}$) on β-plane. This gives $\tau_{ac} < \tau_{eddy}$ (or equivalently $l_{ac} < \Delta_\perp$), leading to $Ku_{fluid} < 1$.

For weak mean field, we have $Ku_{mag} \equiv l_{ac}|B_{st}/B_0|/\Delta_\perp > 1$, rendering standard closure method inapplicable. Here l_{ac} is magnetic auto-correlation length. Hence, we employ the simplifying assumption of $l_{ac} \to 0$ so $Ku_{mag} \simeq l_{ac}|B_{st}/B_0|/\Delta_\perp < 1$. This approximation allows us to peek at the mysteries of the strong perturbation regime by assuming delta-correlated fields. In a system with strong random fields (B_{st}; such that ensemble average of squared stochastic magnetic field $\overline{B_{st}^2} > B_0^2$), this approximation comes at the price of replacing the full β-plane MHD problem with a model problem. Results for this model problem, where $|B_{st}| > B_0$, are discussed.

2.1 Model setup

In this Section, we present the β-plane MHD model and discuss its relevance to the solar tachocline. The physics of PV transport in β-plane MHD is described. Both mixing by fluid advection and magnetic tilting are accounted for.

The solar tachocline is a thin layer inside the Sun, located at a radius of at most 0.7 $R_\odot$, with a thickness of $\lesssim 0.04\ R_\odot$ [12]. Dynamics on this thin shell can be modeled using the β-plane, following a model proposed by [83], for the thin atmosphere. In this model, β is defined

Table 2.1. Summary of the properties of fluid and magnetic Kubo numbers. All models in this paper are set up to make Kubo numbers small to ensure the QLT is valid. This is fulfilled by assuming flows and fields are delta correlated in time and space, respectively.

	Fluid Kubo number	Magnetic Kubo number
Operator	$\mathbf{u}\cdot\nabla$	$\lvert\widetilde{B}/B_0\rvert\ \mathbf{u}_A\cdot\nabla$
Ratio	$\delta_l/\Delta_\perp \lesssim 1$	$\widetilde{B}/B_0 \gg 1$
QL Theory Validity	$\tau_{ac}\to 0$	$l_{ac}\to 0$
Kubo number in this model	$Ku_{fluid}\lesssim 1$	$Ku_{mag}\ll 1$

as the **Rossby Parameter**, given by $\beta = \frac{df}{dy}|_{\phi_0} = 2\Omega cos(\phi_0)/a$. The angular frequency f is also known as the **Coriolis parameter**. Notice that ϕ_0 increases from the equator (see Figure 1.2).

The simplified β-plane MHD model extends the hydrodynamic model to include the effects of MHD and comprises two basic scalar equations:

$$\left(\frac{\partial}{\partial t}+\mathbf{u}\cdot\nabla\right)\zeta-\beta\frac{\partial\psi}{\partial x}=-\frac{(\mathbf{B}\cdot\nabla)(\nabla^2 A)}{\mu_0\rho}+\nu\nabla^2\zeta, \tag{2.2}$$

$$\frac{\partial}{\partial t}A=(\mathbf{B}\cdot\nabla)\psi+\eta\nabla^2 A. \tag{2.3}$$

These two scalar equations are from the Navier-Stokes equation and the induction equation, respectively. Here, η, μ_0, and ρ are the magnetic diffusivity, the permeability, and the density, respectively. The scalar ψ is the z-component of the stream function $\Psi=(0,0,\psi)$ for 2D incompressible flow, so that $\mathbf{u}=(\frac{\partial}{\partial y}\psi,-\frac{\partial}{\partial x}\psi,0)$, and A is the scalar potential for the magnetic field $\mathbf{A}=(0,0,A)$. We also define the vorticity $\zeta\equiv-\nabla^2\psi$, similar to the relationship between the current and the potential $J\equiv-\mu_0\nabla^2 A$. Eq. 2.2 and 2.3 show that the vorticity and the potential field A are conserved in β-plane, up to the Lorentz force, resistivity, and viscosity.

The 2D hydrodynamic inviscid shallow water equation illustrates physics of the solar tachocline. The **PV Freezing-in Law** describes how the PV is frozen into the fluid. In β-plane

model, the generalized PV that frozen into fluid is the potential vorticity $PV \equiv \zeta + f$, where ζ is the vorticity as defined, and f is the Coriolis parameter. This freezing-in of the PV is broken by body forces, such as the Lorentz force, and by the viscosity. To illustrate how the PV freezing-in law is broken, we first split the parameters into two parts, representing two-scale dependences. The shorter length is the turbulence wavelength and the longer length is the scale over which we perform the spatial average. Applying this mean field theory to Eq. 2.2 and 2.3 leads to:

$$\frac{D}{Dt}\langle\zeta\rangle = \frac{\partial}{\partial y}\frac{\langle\widetilde{J}_z\widetilde{B}_y\rangle}{\rho} + \nu\nabla^2\langle\zeta\rangle \neq 0. \tag{2.4}$$

In this form, we can interpret PV density as a 'charge density element' ($\zeta \equiv \rho_{PV}$), floating in the fluid threaded by stretched magnetic fields (see Figure 1.1).

We first consider the simple case where the large-scale magnetic field B_0 is stronger than the small-scale magnetic fields (i.e. $|\widetilde{B}^2|/B_0^2 \ll 1$). Here, the fluid turbulence is weak (restricted by B_0), and the tilt of the magnetic field lines are small, corresponding to a small magnetic Kubo number. To construct the QL equations, we linearize Eq. 2.2 and 2.3:

$$\frac{\partial}{\partial t}\widetilde{\zeta} + \widetilde{u}_y\frac{\partial\langle\zeta\rangle}{\partial y} + \beta\widetilde{u}_y = -\frac{B_0}{\mu_0\rho}\frac{\partial(\nabla^2\widetilde{A})}{\partial x} + \nu\nabla^2\widetilde{\zeta} \tag{2.5}$$

$$\frac{\partial}{\partial t}\widetilde{A} = B_0\widetilde{u}_y + \eta\nabla^2\widetilde{A}, \tag{2.6}$$

and obtain the linear responses of vorticity and magnetic potential at wavenumber k_x in the zonal direction to be:

$$\widetilde{\zeta}_k = -\left(\frac{i}{\omega + i\nu k^2 + \left(\frac{-B_0^2}{\mu_0\rho}\right)\frac{k_x^2}{\omega+i\eta k^2}}\right)\left(\widetilde{u}_y\frac{\partial}{\partial y}\langle\zeta\rangle + \beta\widetilde{u}_y\right),$$

$$\widetilde{A}_k = \frac{\widetilde{\zeta}_k}{k^2}\left(\frac{B_0 k_x}{-\omega - i\eta k^2}\right),$$

where $k \equiv k_x^2 + k_y^2$. From these, the dispersion relation for the ideal Rossby-Alfvén wave follows:

$$\left(\omega - \omega_R + i\nu k^2\right)\left(\omega + i\eta k^2\right) = \omega_A^2. \tag{2.7}$$

Here, ω_A is **Alfvén frequency** (i.e. $\omega_A \equiv B_0 k_x/\sqrt{\mu_0\rho}$), and ω_R is **Rossby frequency** (i.e. $\omega_R \equiv -\beta k_x/k^2$). We also derive the QL evolution equation for mean vorticity:

$$\frac{\partial}{\partial t}\langle\zeta\rangle = -\frac{\partial}{\partial y}\left(\langle\widetilde{u}_y\widetilde{\zeta}\rangle + \frac{\langle\widetilde{B}_y\nabla^2\widetilde{A}\rangle}{\mu_0\rho}\right) + \nu\nabla^2\langle\zeta\rangle. \tag{2.8}$$

Using the Taylor identity, the averaged PV flux ($\langle\Gamma\rangle \equiv \langle\widetilde{u}_y\widetilde{\zeta}\rangle + \langle\widetilde{B}_y\nabla^2\widetilde{A}\rangle/\mu_0\rho$) can be expressed with two coefficients, the fluid and magnetic diffusivities (D_{fluid} and D_{mag}):

$$\frac{\partial}{\partial t}\langle\zeta\rangle = -\frac{\partial}{\partial y}\langle\Gamma\rangle \equiv -\frac{\partial}{\partial y}\left(-(D_{fluid} - D_{mag})\frac{\partial}{\partial y}\langle PV\rangle\right), \tag{2.9}$$

Note two aspects of Eq. 2.9. One is that the anisotropy and inhomogeniety of vorticity flux (i.e. $\frac{\partial}{\partial y}\langle\zeta\rangle$) leads to the formation of zonal flow. For a not-fully-Alfvénized case ($D_{mag} < D_{fluid}$), zero PV transport occurs when $\frac{\partial}{\partial y}\langle\zeta\rangle = -\beta$. This states that β provides the symmetry breaking necessary to define zonal flow orientation. The second aspect is the well-known competition between Reynolds and Maxwell stresses that determines the total zonal flow production. These two diffusivities are related to the Reynolds and Maxwell stress by:

$$D_{fluid}\frac{\partial}{\partial y}PV = \frac{\partial}{\partial y}\langle\widetilde{u}_x\widetilde{u}_y\rangle \tag{2.10}$$

$$D_{mag}\frac{\partial}{\partial y}PV = \frac{\partial}{\partial y}\frac{\langle\widetilde{B}_x\widetilde{B}_y\rangle}{\mu_0\rho}. \tag{2.11}$$

To calculate the turbulent diffusivities, we express terms $\widetilde{u}_y\widetilde{\zeta}$ and $\widetilde{B}_{y,k}\nabla^2\widetilde{A}_k$ in Eq. 2.8 as

summations over components in the k space, i.e. $\widetilde{u}_y\widetilde{\zeta} = \sum_k \widetilde{u}^*_{y,k}\widetilde{\zeta}_k$. Thus, from Eq. 2.7 :

$$\widetilde{u}^*_{y,k}\widetilde{\zeta}_k = \left(\frac{-i}{\omega + i\nu k^2 + \frac{-B_0^2}{\mu_0\rho}\frac{k_x^2}{\omega+i\eta k^2}}\right)|\widetilde{u}_y|^2\frac{\partial}{\partial y}PV, \tag{2.12}$$

$$\widetilde{B}^*_{y,k}\nabla^2\widetilde{A}_k = \left(\frac{-B_0^2k_x^2}{\omega^2+\eta^2k^4}\right)\widetilde{u}^*_{y,k}\widetilde{\zeta}_k. \tag{2.13}$$

Equation 2.13 links the magnetic and fluid diffusivities such that

$$D_{mag}\frac{\partial}{\partial y}PV = \frac{1}{\mu_0\rho}\left(\frac{B_0^2k_x^2}{\omega^2+\eta^2k^4}\right)D_{fluid}\frac{\partial}{\partial y}PV,$$

leading to

$$D_{mag} = \frac{1}{\mu_0\rho}\left(\frac{B_0^2k_x^2}{\omega^2+\eta^2k^4}\right)D_{fluid}. \tag{2.14}$$

Hence,

$$D_{fluid} = \sum_k C_{k,\,fluid}|\widetilde{u}_{y,k}|^2$$
$$D_{mag} = \frac{1}{\mu_0\rho}\sum_k C_{k,mag}|\widetilde{u}_{y,k}|^2,$$

where the phase coherence coefficients C_k are given by

$$C_{k,\,fluid} = \frac{\nu k^2 + \frac{\omega_A^2\eta k^2}{\omega^2+\eta^2k^4}}{\omega^2\left(1-\frac{\omega_A^2}{\omega^2+\eta^2k^4}\right)^2 + \left(\nu k^2 + \omega_A^2\frac{\eta k^2}{\omega^2+\eta^2k^4}\right)^2}, \tag{2.15}$$

$$C_{k,mag} = \frac{\omega_A^2\left(\frac{\nu k^2}{\omega^2+\eta^2k^4} + \frac{\omega_A^2\eta k^2}{(\omega^2+\eta^2k^4)^2}\right)^2}{\omega^2\left(1-\frac{\omega_A^2}{\omega^2+\eta^2k^4}\right)^2 + \left(\nu k^2 + \omega_A^2\frac{\eta k^2}{\omega^2+\eta^2k^4}\right)^2}. \tag{2.16}$$

Note that, in the term $\nu k^2 + \omega_A^2\eta k^2/(\omega^2+\eta^2k^4)$ of Eq. 2.15, which defines the width of the response function in time, the resistive and viscous damping rates ηk^2 and νk^2 should be taken as representing eddy scattering (as for resonance broadening) on small scales. Also, notice that the mean magnetic field modifies *both* PV diffusivities, via ω_A^2 contributions. Comfortingly, on one

hand, we recover the momentum flux of 2D fluid turbulence on a β-plane when we let the large-scale mean magnetic field vanish ($B_0 = 0$). On the other hand, when the mean magnetic field is strong enough ($\omega_A \gg \omega_R$), the fluctuations are *Alfvénic*. In this limit $\omega \sim \omega_A \gg \eta k^2 \gg \nu k^2$ (i.e. magnetic Prandtl number $Pm \ll 1$), we have $D_{fluid} \simeq D_{mag}$ and the vorticity flux vanishes, i.e. $\Gamma = 0 + \mathscr{O}\big((\frac{\eta k^2 - \nu k^2}{\omega_A})^2\big)$. This is the well-known 'Alfvénization' condition, for which the Reynolds and the Maxwell stress cancel, indicating that the driving of the zonal flow vanishes in the Alfvénized state. There, the MHD turbulence *plays no role in transporting momentum*. Between these two extremes, we are interested in the case of the solar tachocline, where the stretching of mean field by Rossby wave turbulence generates $\widetilde{B}$ and the large-scale magnetic field is not strong enough to Alfvénize the system, but remains nonnegligible (i.e. $|\widetilde{B}^2| > B_0^2$ but $B_0 \neq 0$). In this case, the large-scale field lines of the near-constant field will be strongly perturbed by turbulence. Thus, the magnetic Kubo number is large, for any finite autocorrelation length. Understanding the physics here requires a model beyond simple QL theory. Here we develop a new, nonperturbative approach that we term an 'effective medium' approach. Zel'dovich [105] gave a physical picture of the effect of magnetic fields with $|\widetilde{B}^2| \gg B_0^2$. He interpreted the 'whole' strongly perturbed problem as consisting of a random mix of two components: a weak, constant field and a random ensemble of magnetic cells, for which the lines are closed loops ($\nabla \cdot \mathbf{B} = 0$). Assembling these two parts gives a field configuration of randomly distributed cells, threaded by sinews of open lines (see figure 2.1). Wave energy can propagate along the open sinews and will radiate to a large distance if the open lines form long-range connections. As noted above, this system with strong stochastic fields cannot be described by the simple linear responses retaining B_0 only, since $|\widetilde{B}^2| \gg B_0^2$

Thus, a 'frontal assault' on calculating PV transport in an ensemble of tangled magnetic fields is a daunting task. Facing a similar task, Rosenbluth [78] suggested replacing the 'full' problem with one where waves, instabilities, and transport are studied in the presence of an ensemble of prescribed, static, stochastic fields. Inspired by this idea, we replace the full model with one where PV mixing occurs in an ensemble of stochastic fields that need not be weak

— i.e. $|\widetilde{B}^2|/B_0^2 > 1$ allowed. This is accomplished by taking the small-scale fields as spatially uncorrelated ($l_{ac} \to 0$), i.e. with spatial coherence small. In simple terms, we replace the 'full' problem with one in which stochastic fields are static and uncorrelated, though possibly strong. *This way, the magnetic Kubo number remains small—*$Ku_{mag} = l_{ac}|\widetilde{B}|/(\Delta_\perp B_0) < 1$ *— even though* $|\widetilde{B}^2| \gg B_0^2$. By employing this ansatz, calculation of PV transport in the presence of stochasticity for an ensemble of Rossby waves is accessible to a mean field approach, even in the large perturbation limit. Based on this idea, we uncover several new effects including the crucial role of the small-tangled-field (B_{st}) in the modification of the cross-phase in the PV flux and a novel drag mechanism that damps flows. Together, these regulate the transport of mean PV [44]. We stress again that these effects are not apparent from simple QL calculations.

We approach the problem with strongly perturbed magnetic fields ($|\widetilde{B}^2| \gg B_0^2$) by considering an environment with stochastic fields (B_{st}) coexisting with an ordered mean toroidal field (B_0) of variable strength. The mean toroidal field is uniformly distributed on the β-plane, while the stochastic component is a set of prescribed, small-scale fields taken as static. These small-scale magnetic fields are randomly distributed, and the amplitudes are distributed statistically. We order the magnetic fields and currents by spatial scales as:

$$\begin{aligned} \text{potential field} \quad \mathbf{A} &= \mathbf{A_0} + \widetilde{\mathbf{A}} + \mathbf{A_{st}} \\ \text{magnetic field} \quad \mathbf{B} &= \mathbf{B_0} + \widetilde{\mathbf{B}} + \mathbf{B_{st}} \\ \text{magnetic current} \quad \mathbf{J} &= \mathbf{0} + \widetilde{\mathbf{J}} + \mathbf{J_{st}}, \end{aligned} \tag{2.17}$$

where $\mathbf{J_0} = 0$ for $\mathbf{B_0}$ is a constant.

The waves are described hydrodynamically by:

$$\begin{aligned} \text{stream function} \quad \psi &= \langle\psi\rangle + \widetilde{\psi} \\ \text{flow velocity} \quad \mathbf{u} &= \langle\mathbf{u}\rangle + \widetilde{\mathbf{u}} \\ \text{vorticity} \quad \zeta &= \langle\zeta\rangle + \widetilde{\zeta}, \end{aligned} \tag{2.18}$$

where, as before, the $\langle\ \rangle$ is an average over the zonal scales $(1/k_{zonal})$ and fast timescales. For the ordering of wavenumbers of stochastic fields k_{st}, Rossby turbulence k_{Rossby}, and zonal flows k_{zonal}, respectively, we take the scale of spatial average larger than that of Rossby waves. A length scale cartoon is given in figure 2.2.

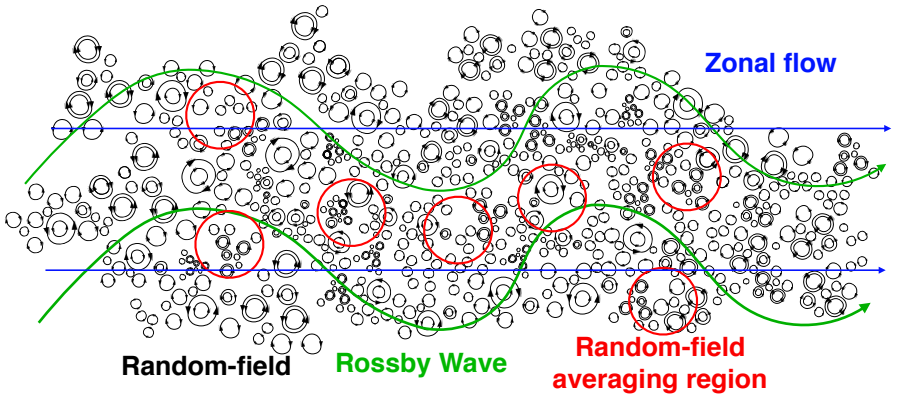

Figure 2.2. Length scale ordering. The smallest length scale is that of the random field (l_{st}). The random-field averaging region is larger than the length scale of random fields but smaller than that of the Rossby waves.

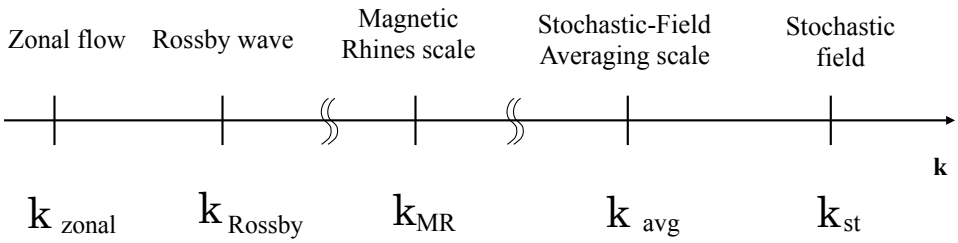

Figure 2.3. Multi-scale Ordering. The Magnetic Rhines scale separates the regimes of large- and small-length scale. MHD turbulences dominate the system on a smaller length scale and is comprised of Alfévn waves and eddies. In this regime, wavenumbers k from high to low are ordered as $k_{st} > k_{avg}$. On a larger length scale, however, Rossby waves dominate. Here, the scale ordering from high to low wavenumber is: $k_{Rossby} > k_{zonal}$.

Following the argument above, a model which circumvent the problem of simple quasi-linear theory for this highly disordered system is presented. This is accomplished by considering

the scale ordering. In the *two-scale average method* proposed [9], an average over an area is performed, with a scale ($1/k_{avg}$) larger than the scale of the stochastic fields ($1/k_{st}$) but smaller than the Magnetic Rhines scale [79] (k_{MR}), and Rossby wavelength (k_{Rossby}). This average is denoted as $\overline{F} \equiv \int dR^2 \int dB_{st} \cdot P_{(B_{st,x},B_{st,y})} \cdot F$, where F is arbitrary function, dR^2 denotes integration over the region, and $P_{(B_{st,x},B_{st,y})}$ is probability distribution function for the random fields. This random-field average allows us to replace the total field due to MHD turbulence (something difficult to calculate) by moments of a prescribed probability distribution function (PDF) of the stochastic magnetic field. The latter *can* be calculated. Another ensemble average— over zonal flow scales k_{zonal}, denoted as bracket average $\langle\rangle \equiv \frac{1}{L}\int dx \frac{1}{T}\int dt$—is conducted. Hence the scale ordering is ultimately $k_{st} > k_{avg} \gtrsim k_{MR} \gtrsim k_{Rossby} > k_{zonal}$ See figure 2.3 and 2.2, and also Tobias et al. (2007) [95].

The novelty and utility of the random-field average method is that it allows the replacement of the total field due to MHD turbulence (which is difficult to calculate) by moments of the distribution of a static, stochastic magnetic field, which *can* be calculated. This is based on the tacit assumption that the perturbation in magnetic fields on the Rossby scale has a negligible effect on the structure of the imposed random fields and its stress-energy tensor. Put simply, $\overline{(B_{tot})^2} \simeq \overline{B_{st}^2}$ (i.e. first order correction term vanishes, upon averaging), where $\overline{B_{tot}}$ is the averaged total field, regulated by Rossby waves.

We apply random-field averaging to the vorticity equation first, so as to deal with the nonlinear magnetic term. This yields

$$\frac{\partial}{\partial t}\overline{\zeta} - \beta\frac{\partial\overline{\psi}}{\partial x} = -\frac{\overline{(\mathbf{B}\cdot\nabla)\nabla^2 A}}{\mu_0\rho} + \nu\nabla^2\overline{\zeta}. \tag{2.19}$$

However, we don't apply the random-field average to the induction equation at this stage, as A_{st} is static so that the induction equation for stochastic fields reduces to

$$\nabla^2 A_{st} = \frac{-1}{\eta}(\mathbf{B_{st}}\cdot\nabla)\psi. \tag{2.20}$$

We hold, nonetheless, the general induction equation for mean field, such that $\frac{\partial}{\partial t}A_0 = \mathbf{B}_0 \cdot \nabla\psi + \eta\nabla^2 A_0$. Combining Eq. 2.19 and 2.20, we have

$$\frac{\partial}{\partial t}\overline{\zeta} - \beta\frac{\partial\overline{\psi}}{\partial x} = \frac{1}{\eta\mu_0\rho}\frac{\partial}{\partial y}(\overline{B^2_{st,y}}\frac{\partial}{\partial y}\overline{\psi}) - \frac{B_0}{\mu_0\rho}\frac{\partial(\nabla^2\overline{A}_0)}{\partial x} + \nu\nabla^2\overline{\zeta}. \tag{2.21}$$

Next, we consider the vorticity wave perturbation after applying the random-field average:

$$\frac{\partial}{\partial t}\widetilde{\zeta} + \beta\widetilde{u}_y + \widetilde{u}_y\frac{\partial}{\partial y}\overline{\zeta} = \frac{\partial}{\partial y}\frac{\overline{B^2_{st,y}}\frac{\partial}{\partial y}\widetilde{\psi}}{\eta\rho\mu_0} - \frac{B_0}{\mu_0\rho}\frac{\partial(\nabla^2\widetilde{A}_0)}{\partial x} + \nu\nabla^2\widetilde{\zeta}. \tag{2.22}$$

Equation 2.22 is formally linear in pertubations and allows us to calculate the response of the vorticity in the presence of tangled fields, namely

$$\widetilde{\zeta}_k = \left(\frac{-i}{\omega + i\nu k^2 + \frac{i\overline{B^2_{st,y}}k_y^2}{\mu_0\rho\eta k^2} + \frac{-B_0^2k_x^2}{\mu_0\rho(\omega+i\eta k^2)}}\right)\widetilde{u}_{y,k}\left(\frac{\partial}{\partial y}\overline{\zeta} + \beta\right). \tag{2.23}$$

The effective medium Rossby-Alfvén dispersion relation can be derived from this Eq. 2.23, and is given by

$$\left(\omega - \omega_R + \frac{i\overline{B^2_{st,y}}k_y^2}{\mu_0\rho\eta k^2} + i\nu k^2\right)\left(\omega + i\eta k^2\right) = \frac{B_0^2k_x^2}{\mu_0\rho}. \tag{2.24}$$

This model [9] with its two-average method allows insights into the physics of how the evolution of zonal flows is suppressed by disordered fields both via reduced PV flux (Γ) and by an induced magnetic drag, i.e.

$$\frac{\partial}{\partial t}\langle u_x\rangle = \langle\overline{\Gamma}\rangle - \frac{1}{\eta\mu_0\rho}\langle\overline{B^2_{st,y}}\rangle\langle u_x\rangle + \nu\nabla^2\langle u_x\rangle. \tag{2.25}$$

Here, $\langle u_x\rangle$ is mean velocity in the zonal direction, $\langle\overline{\Gamma}\rangle$ is the double-average PV flux, η is resistivity, ρ is mass density, and ν is viscosity. Here $\frac{1}{\eta\mu_0\rho}\langle\overline{B^2_{st,y}}\rangle$ is the magnetic drag coefficient.

Several important results are obtained. First, stochastic fields suppress PV flux by

reducing the PV diffusivity (D_{PV})

$$\overline{\Gamma} = -D_{PV}\left(\frac{\partial}{\partial y}\overline{\zeta} + \beta\right), \tag{2.26}$$

where β is the Rossby parameter and the PV diffusivity can be written as

$$D_{PV} = \sum_k |\widetilde{u}_{y,k}|^2 \times \frac{\nu k^2 + \left(\frac{B_0^2 k_x^2}{\mu_0 \rho}\right)\frac{\eta k^2}{\omega^2 + \eta^2 k^4} + \frac{\overline{B_{st,y}^2} k^2}{\mu_0 \rho \eta k^2}}{\left(\omega - \left(\frac{B_0^2 k_x^2}{\mu_0 \rho}\right)\frac{\omega}{\omega^2 + \eta^2 k^4}\right)^2 + \left(\nu k^2 + \left(\frac{B_0^2 k_x^2}{\mu_0 \rho}\right)\frac{\eta k^2}{\omega^2 + \eta^2 k^4} + \frac{\overline{B_{st,y}^2} k^2}{\mu_0 \rho \eta k^2}\right)^2}. \tag{2.27}$$

Eq. (2.27) shows that strong mean-square stochastic field ($\overline{B_{st}^2}$) acts to reduce the correlation of the vorticity flux, thus reducing PV mixing. This explains the Reynolds stress suppression observed in simulation[9] (Fig. 1.6). Note that this reduction in Reynolds stress sets in for values of B_0 *well below that required for Alfvénization* (i.e. Alfvénic equi-partition $\langle \widetilde{u}^2 \rangle \simeq \langle \widetilde{B}^2 \rangle / \mu_0 \rho$).

Second, magnetic drag physics is elucidated via the mean-field dispersion relation for waves in an inertial frame ($\beta = 0$), on scales $l \gg k_{avg}^{-1}$,

$$\left(\omega + \frac{i\overline{B_{st,y}^2} k_y^2}{\mu_0 \rho \eta k^2} + i\nu k^2\right)\left(\omega + i\eta k^2\right) = \frac{B_0^2 k_x^2}{\mu_0 \rho}. \tag{2.28}$$

The drag coefficient $\chi \equiv \overline{B_{st,y}^2} k_y^2 / \mu_0 \rho \eta k^2$, emerges as approximately proportional to an effective spring constant/dissipation. The 'dissipation' and 'drag' effects suggest that mean-square stochastic fields $\overline{B_{st}^2}$ form an effective resisto-elastic network, in which the dynamics evolve. The fluid velocity is redistributed by the drag of small-scale stochastic fields. Ignoring viscosity ($\nu \to 0$), we have

$$\omega^2 + i \underbrace{(\chi + \eta k^2)}_{\text{drag + dissipation}} \omega - \underbrace{\left(\frac{\overline{B_{st,y}^2} k_y^2}{\mu_0 \rho} + \frac{B_0^2 k_x^2}{\mu_0 \rho}\right)}_{\text{effective spring constant}} = 0. \tag{2.29}$$

Note that this is effectively the dispersion relation of dissipative Alfvén waves, where the 'stiffness' (or magnetic tension) is determined by *both* the ordered and the mean-square stochastic field ($\overline{B_{st}^2}$). In practice, the latter is dominant, as $\overline{B_{st}^2} \simeq RmB_0^2$ and $Rm \gg 1$. So, the ensemble of Alfvénic loops can be viewed as an network of springs (Fig. 2.4). Fluid couples to network elastic elements, thus exciting collective elastic modes. The strong elasticity, due to Alfvénic loops, increases the effective memory of the system, thus reducing mixing and transport and ultimately causes Reynolds stress decoherence.

Finally, this network is fractal and is characterized by a 'packing factor', which determines the effective Young's Modulus. It is important to note that the 'stochastic elasticized' effect is one of increased memory (*not* one of enhanced dissipation) as in the familiar cases of turbulent viscosity or resistivity.

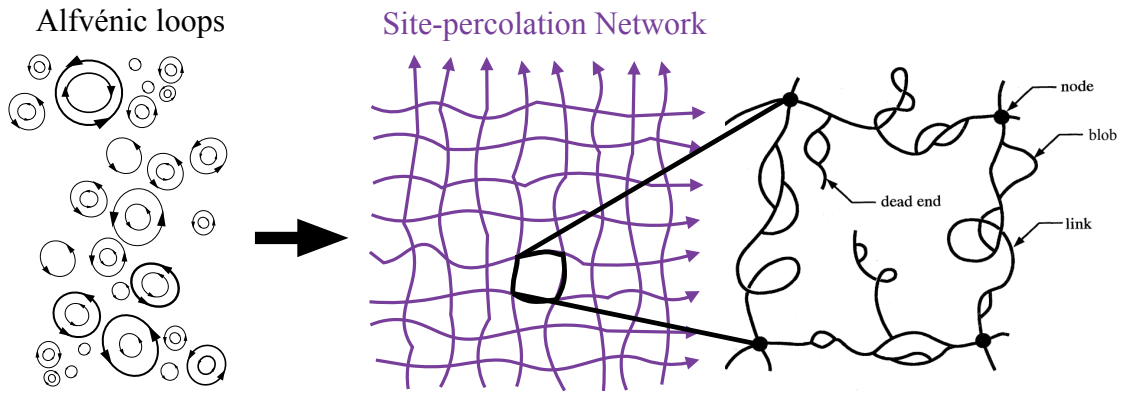

Figure 2.4. Site-Percolation Network. Schematic of the nodes-links-blobs model (or SSdG model, see [90, 14, 65]). This depicts the resisto-elastic medium formed by small-scale stochastic fields.

2.2 Conclusion for the β-plane MHD in presence of stochastic magnetic filed

In this Chapter (and presented in Chen & Diamond (2020)[9]), we have developed and elucidated the theory of PV mixing and zonal flow generation, for models of Rossby–Alfvén turbulence with two different turbulence intensities. The balance between Reynolds and Maxwell

stress in a fully Alfvénized system where fluid and magnetic energy reach near equi-partition is the conventional wisdom. Simulation results (Fig. 1.6), however, show that Reynolds stress is suppressed by stochastic fields *well before* the mean field is strong enough to fully Alfvénize the system [9]—-at which the magnetic field is strongly disordered. Our most novel model considered the large fluctuation regime ($\langle\widetilde{B}^2\rangle/B_0^2 > 1$) — where the field is tangled, not ordered. For this, we developed a theory of PV mixing in a static, stochastic magnetic field. It is striking that this model problem is amenable to rigorous, systematic analysis yet yields novel insights into the broader questions asked.

Our main results can be summarized as follows. First, we have defined the *magnetic Kubo number* and demonstrated the importance of ensuring $Ku \ll 1$ for the application of QL theory to a turbulent magnetized fluid. In this regime, we have derived the relevant QL model for turbulent transport and production of jets and shown the utility of the *critical damping parameter* in determining the transition between jet drive and suppression by the magnetized turbulence.

A striking result is that numerical experiments show how magnetic fields may significantly reduce the Reynolds stresses, which drives jets, well before the critical mean field strength needed to bring the Maxwell and Reynolds stresses into balance, i.e. before Alfvénization. This is important and demonstrates that the magnetic field acts in a subtle way to change the transport properties — indeed, even more subtle than was previously envisaged. The explanation of this effect required the development of a new model of PV mixing in a tangled, disordered magnetic field. This tractable model has $Ku_{mag} < 1$, because the tangled field is delta correlated and allows the consideration of strong stochastic fields $\overline{B_{st}^2}/B_0^2 > 1$. We use a 'double average' procedure over random-field scales and mesoscales that allows treatment of the wave and flow dynamics in an effective resistive-elastic medium.

We identify two principle effects as the crucial findings:

1. A modification (reduction) of the cross-phase in the PV flux by the *mean-square* field $\overline{B_{st}^2}$. This is in addition to ω_A^2 effects, proportional to B_0^2, which appears in QL theory. Note that

this is not a fluctuation quench effect.

2. A magnetic drag, which is proportional to $\langle\overline{B_{st}^2}\rangle$, on the mean zonal flow. The scaling of $\langle\overline{B_{st}^2}\rangle/\eta$ resembles that of the familiar magnetic drag in the 'electrostatic' limit, with $\overline{B_{st}^2}$ replacing B_0^2. Note that the appearance of such a drag is not surprising, as stochastic fields are *static*, so $\frac{\partial}{\partial t}A_{st} \to 0$.

Finally, in the specific context of modeling tachocline formation and dynamics, this analysis yields a tractable model of PV transport, which can incorporate magnetic effects into hydrodynamic models. In this Chapter, we ignore the perturbation of random fields $\widetilde{B}$ (see Appendix I). Here $\widetilde{B}^2$ can be replaced by $\langle\overline{B_{st}^2}\rangle$ and be estimated using the Zel'dovich value $\overline{B_{st}^2} \sim B_0^2 Rm$. The model suggests that the 'burrowing' due to meridional cells that drives tachocline formation will be opposed by relaxation of PV gradients (not shears!) and the resisto-elastic drag. The magnetic-intensity-induced phase modification will reduce PV mixing relative to the prediction of pure hydrodynamics.

These results suggest that turbulent momentum transport in the tachocline is suppressed by the enhanced memory of stochastically induced elasticity. This leaves no viscous or mixing mechanism to oppose 'burrowing' of the tachocline due to meridional cells driven by baroclinic torque $\nabla p \times \nabla \rho$[60]. This finding suggests that the Spiegel & Zahn (1992) [91] scenario of burrowing opposed by latitudinal viscous diffusion, and the Gough & McIntyre (1998) [31] suggestion of that PV mixing opposed burrowing *both fail*. Finally, by process of elimination, the enhanced memory-induced suppression of momentum transport allows the Gough & McIntyre (1998) [31] suggestion that a residual fossil field in the radiation zone is what ultimately limits tachocline burrowing. Thus, it seems fair to comment that neither the model proposed by Spiegel & Zahn (1992) [91], nor that by Gough & McIntyre (1998) [31] is fully "correct". The truth here is still elusive, and 'neither pure nor simple' (apologies to Oscar Wilde).

2.3 Implications for the solar tachocline

The picture discussed in this paper is analogous to that of dilute polymer flows, in which momentum transport via Reynolds stresses is reduced, at roughly constant turbulence intensity, leading to drag reduction. The similarity of the Oldroyd-B model of polymeric liquids and MHD is well known [69, 70, 4, 73, 67, 6]. A Reynolds stress phase coherence reduction related to mean-square polymer extension is a promising candidate to explain the drag reduction phenomenology.

More generally, this paper suggests a novel model of transport and mixing in 2D MHD turbulence derived from considering the coupling of turbulent hydrodynamic motion to a fractal elastic network [7, 76, 74, 75, 58, 3]. Both the network connectivity and the elasticity of the network elements can be distributed statistically and can be intermittent and multiscale. These would introduce a packing fractional factor to C_k in the cross-phase, i.e. $\langle \widetilde{B}^2 \rangle \to p \langle \widetilde{B}^2 \rangle$ in C_k, where $0 < p < 1$ is probabilities of sites. This admittedly crude representation resembles that of the mean field limit for 'fractons' [2]. Somewhat more sophisticated might be the form $\langle \widetilde{B}^2 \rangle \to (p - p_c)^\gamma |\widetilde{B}|^{2\varepsilon}$, where p_c is the magnetic activity percolation threshold, and γ, ε are scaling exponents to be determined [92]. We also speculate that the back-reaction (at high Rm) of the small-scale magnetic field on the fluid dynamics may ultimately depend heavily on whether or not the field is above the packing 'percolation threshold' for long-range Alfvén wave propagation. Such long-range propagation would induce radiative damping of fluid energy by Alfvénic propagation through the stochastic network.

We also note that this study has yielded results of use in other contexts, most notably that of magnetized plasma confinement where the field is stochastic, as for a tokamak with resonant magnetic perturbations (RMP). Indeed, recent experiments [51, 66, 86] have noted a reduction in shear flow generation in plasmas with RMP. This reduction causes an increase in the low/high confinement regime power threshold.

Chapter 2, in full, is a reprint of the material as it appears in Chang-Chun Chen & Patrick

H. Diamond, *The Astrophysical Journal* 892, 24(2020). The dissertation author was the primary investigator and author of this paper.

Chapter 3

The Stochastic Field on Momentum Transport in Fusion Devices

This section focuses on the effect of stochastic fields on zonal flow suppression, such as in the case of RMPs at the edge of tokamak. Experimental results shows that pre-L-H transition Reynolds stress bursts drop significantly when RMPs are applied to the edge of DIII-D [50]. The power threshold for L-H transition increases, as the normalized intensity of radial RMPs ($\delta B_r/B_0$) increases [54, 30, 46, 84, 64, 85, 39, 86]. This paper aims to shed light on these two phenomena, and to address the more general question of Reynolds stress decoherence in a stochastic magnetic field.

To begin, we explore the timescale ordering for the physics. Consider a generalized diffusivity D_0

$$D_0 = Re\{\sum_k \int d\omega \frac{k_\theta^2}{B_0^2}|\phi_{k\omega}|^2 \frac{i}{\omega - v_A k_z + iDk^2}\} \tag{3.1}$$

where the D is a spatial diffusivity under the influence of stochastic field, defined as $D \equiv v_A D_M$, and $v_A \equiv B_0/\sqrt{\mu_0 \rho}$ is Alfvén speed[106]. As discussed below, v_A appears as the characteristic velocity for signal propagation along the stochastic field, since zonal flows follow from the need to maintain $\underline{\nabla} \cdot \underline{J} = 0$, in the face of ambipolarity breaking due to polarization fluxes. Here $D_M \simeq l_{ac} b^2$ (hearafter $b^2 \equiv \langle B_{st,\perp}^2 \rangle / B_0^2$) is the magnetic diffusivity, first derived by Rosenbluth [82]. Here, the bracket average is a stochastic ensemble average $\langle\rangle \equiv \int dR^2 \int dB_{st} \cdot P_{(B_{st,x}, B_{st,y})} \cdot F$. But here dR^2 is an averaging area (at scale $1/k_{st}$) over y- and z- direction. $|\phi_{k\omega}|^2$ is the electric

potential spectrum, such that

$$|\phi|^2_{k\omega} = \phi_0^2 S_{(k)} \frac{|\Delta\omega_k|}{(\omega-\omega_{0,k})^2+(\Delta\omega_k)^2}, \tag{3.2}$$

where $S_{(k)}$ is the k-spectrum of the potential field, $\omega_{0,k}$ is the centroid of the frequency spectrum, and $|\Delta\omega|$ is the natural linewidth of potential field. Performing the frequency integration, we have

$$\begin{aligned} D_0 &= Re\{\sum_k \phi_0^2 S_{(k)} \int d\omega \{\tfrac{i}{(\omega-\omega_{0,k})+i|\Delta\omega_k|} \tfrac{i}{\omega-v_A k_z+iDk^2}\} \\ &= Re\{\sum_k \phi_0^2 S_{(k)} \tfrac{-2\pi i}{\omega_{0,k}+i|\Delta\omega_k|-v_A k_z+iDk^2}\}. \end{aligned} \tag{3.3}$$

Now consider a Lorentzian k-spectrum

$$S_{(k)} = \frac{S_0}{(k-k_0)^2+(\Delta k_\parallel)^2}. \tag{3.4}$$

We have

$$\begin{aligned} D_0 &= Re\{\int dk_\parallel \phi_0^2 \tfrac{S_0}{(k-k_0)^2+(\Delta k_\parallel)^2} \cdot \tfrac{-2\pi i}{\omega_{0,k}-v_A k_z+i|\Delta\omega_k|+iDk^2}\} \\ &\simeq Re\left(S_0\phi_0^2(2\pi)^2 \frac{i}{\omega_{0,k_0}-k_{0,z}v_A+i|\Delta k_\parallel|v_A+i|\Delta\omega_{k_0}|+iDk_\perp^2}\right), \end{aligned} \tag{3.5}$$

assuming $|\Delta k_\parallel| \ll k_\perp$ and $\partial\Delta\omega/\partial k \simeq 0$. The ordering of these broadenings ($|\Delta k_\parallel|v_A$, $|\Delta\omega_{k_0}|$, and $Dk_\perp^2$) in the denominator is the key to quantifying stochastic field effects. The first term, $|\Delta k_\parallel|v_A$, is the bandwidth of an Alfvén wave packet excited by drift-Alfvén coupling. Here $v_A|\Delta k_\parallel| \lesssim v_A/Rq$, where R is major radius and $q \equiv rB_t/RB_p$ is the safety factor. The bandwidth $|\Delta k_\parallel|v_A$ is a measure of the dispersion rate of an Alfvén wave packet. The second term is the rate of nonlinear coupling or mixing—due to ambient electrostatic micro-instability $|\Delta\omega_{k_0}| \equiv \Delta\omega \simeq \omega_* = k_\theta\rho_s C_s/L_n$, where the ω_* is drift wave turbulence frequency, ρ_s is gyro-radius, C_s is

sound speed, and L_n is density scale length. $\Delta\omega$ is comparable to $k_\perp^2 D_{GB}$, where $D_{GB} \equiv \omega_*/k_\perp^2 \simeq \rho_s^2 C_s/L_n$ is the gyro-Bohm diffusivity (for $k_\theta \rho_s \sim 1$). The third is the stochastic field scattering rate $Dk_\perp^2 \simeq k_\perp^2 v_A D_M$. Ultimately, we will show that $k_\perp^2 v_A D_M \gtrsim \Delta\omega_k$ (or $v_A D_M > D_{GB}$) is required for Reynolds stress decoherence (see Figure 3.1). In practice, this occur for $k_\perp^2 v_A D_M \gtrsim v_A |\Delta k_\parallel|$, i.e. $Ku_{mag} \simeq 1$ is required. The condition $k_\perp^2 v_A D_M > \Delta\omega_k$ requires that *stochastic field broadening exceeds the natural turbulence linewidth* [86], so that $k_\perp^2 v_A D_M > \Delta\omega$. Satisfying this requires $b^2 > \sqrt{\beta}\rho_*^2 \varepsilon/q \sim 10^{-7}$, where $l_{ac} \simeq Rq$, $\varepsilon \equiv L_n/R \sim 10^{-2}$, $\beta \simeq 10^{-2\sim-3}$, and normalized gyro-radius $\rho_* \equiv \rho_s/L_n \simeq 10^{-2\sim-3}$. It is believed that b^2 at the edge due to RMP is $\sim 10^{-7}$ for typical parameters; hence, the stochastic broadening effect is likely sufficient to dephase the Reynolds stress. Following from this condition, we propose a dimensionless parameter $\alpha \equiv b^2 q/\rho_*^2\sqrt{\beta}\varepsilon$—defined by the ratio $k_\perp^2 v_A D_M/\Delta\omega_k$—to quantify the broadening effect. The increment in L-I and I-H power thresholds as α varies are explored using a *modified* Kim-Diamond L-H transition model [47] in Sec. 3.2. We also give a physical insight into stress decoherence by showing how stochastic fields break the 'shear-eddy tilting feedback loop', which underpins zonal flow growth by modulational instability.

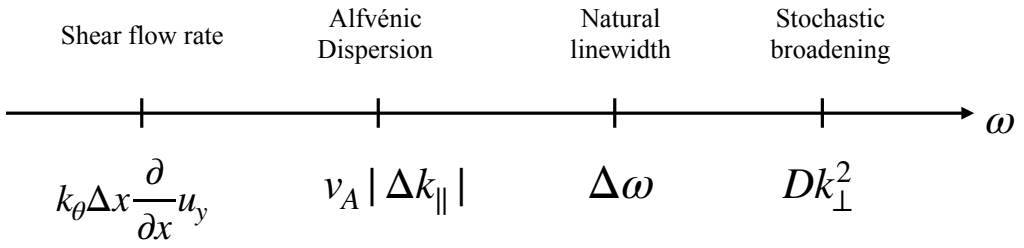

Figure 3.1. Timescale ordering for drift-wave turbulence in fusion devices. We are interested in a regime where stochastic field effect becomes noticeable, which requires $\Delta\omega < Dk_\perp^2$. The comparison between Alfvénic dispersion rate $v_A|\Delta k_\parallel|$ and stochastic broadening rate $Dk_\perp^2$ gives a magnetic Kubo number $Ku_{mag} \simeq 1$.

3.1 Model Setup

We construct a model in Cartesian (slab) coordinates—x is radial, y is poloidal, and z is toroidal direction, in which the mean toroidal field lies (Fig. 3.2). A current flows in the toroidal

direction, producing a mean poloidal field. In contrast to the tachocline, here the magnetic field is 3D, and stochasticity results from the overlap of magnetic islands located at the resonant $\underline{k}\cdot\underline{B}=0$ surfaces. The stochasticity is attributed to the external RMP field, and typically occurs in a layer around the separatrix. The distance between neighboring magnetic field trajectories diverges exponentially, as for a positive Lyapunov exponent. Stochastic fields due to RMPs resemble Zel'dovich 'cells' [105] (Fig. 2.1), lying in $x-y$ plane with a mean toroidal field (on z-axis), threading through perpendicularly. Of course, once overlap occurs, the coherent character of the perturbations is lost, due to finite Kolmogorov-Sinai entropy (i.e. there exists a positive Lyapunov exponent for the field). In this case, the magnetic Kubo number is modest $Ku_{mag} \lesssim 1$.

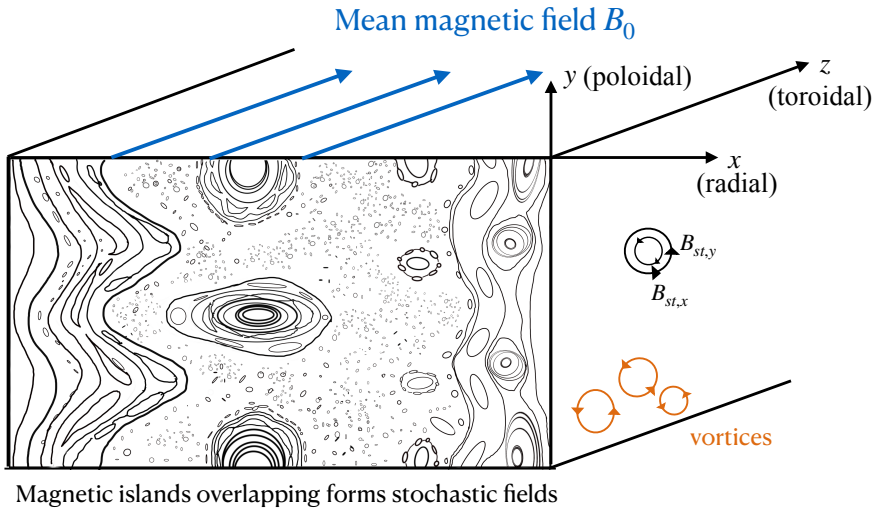

Figure 3.2. Magnetic fields at the edge of tokamak. RMP-induced stochastic fields (black loops) lie in radial (x) and poloidal (y) plane. Mean toroidal field is treading through stochastic fields perpendicular in z-direction (blue arrows).

We start with 4 field equations—

1. Vorticity evolution—$\underline{\nabla}\cdot\underline{J}=0$

$$\frac{\partial}{\partial t}\zeta_z + u_y\frac{\partial}{\partial y}\zeta_z + u_z\frac{\partial}{\partial z}\zeta_z = \frac{1}{\rho}B_0\frac{\partial}{\partial z}J_z + \frac{1}{\rho}B_{x,st}\frac{\partial}{\partial x}J_z + \frac{2\kappa}{\rho}\frac{\partial}{\partial y}P, \tag{3.6}$$

where ζ is the vorticity, u_y is $E \times B$ shear flow, u_z is intrinsic rotation, and κ is curvature.

2. Induction evolution

$$\frac{\partial}{\partial t}A_z + u_y \frac{\partial}{\partial y}A_z = -\frac{B_{x,st}}{B_0}\frac{\partial}{\partial x}\phi - \frac{\partial}{\partial z}\phi + \eta \nabla^2 A_z, \tag{3.7}$$

where ϕ is electric potential field ($\zeta \equiv \nabla \times v = \frac{1}{B_0}\nabla^2\phi$).

3. Pressure evolution

$$\frac{\partial}{\partial t}p + (\mathbf{u}\cdot\nabla)p = -\gamma p(\nabla\cdot\mathbf{u}), \tag{3.8}$$

where γ is the adiabatic index .

4. Parallel acceleration

$$\frac{\partial}{\partial t}u_z + (\mathbf{u}\cdot\nabla)u_z = -\frac{1}{\rho}\frac{\partial}{\partial z}p, \tag{3.9}$$

where p is pressure.

3.2 Calculation and Results

We define a Elsässer-like variable $f_{\pm,k\omega} \equiv \widetilde{\phi}_{k\omega} \pm v_A \widetilde{A}_{k\omega}$, and combine Eq. (3.6) and (3.7) to obtain

$$\begin{aligned}&(-i\omega + \langle u_y\rangle i k_y) f_{\pm,k\omega} \pm v_A (ik_z + ik_j \frac{B_{j,st}}{B_0}) f_{\pm,k\omega} \\ &= \frac{\widetilde{u}_x}{k^2}\frac{\partial}{\partial x}\nabla^2\langle\phi\rangle + \frac{2\kappa}{\rho} i k_y (\frac{B_0}{-k^2})\widetilde{p} \equiv S_f,\end{aligned} \tag{3.10}$$

where S_f is the source function for $f_{\pm,k\omega}$. Eq. 3.10 is the evolution equation for the Elsässer response to a vorticity perturbation. Note that this response is defined by

1. Propagation along the total magnetic field, i.e. $ik_z + ik_j B_{j,st}/B_0$. Note this includes propagation along the wandering magnetic field component.

2. Advection by mean flow $ik_y\langle u_y\rangle$.

3. Finite frequency $i\omega$.

Hence, the Elsässer response for $f_{\pm,k\omega}$ is be obtained by integrating along trajectories of total magnetic field lines (including perturbations), i.e.

$$f_{\pm,k\omega} = \int d\tau e^{i(\omega - \langle u_y\rangle k_y \mp v_A k_z)\tau} e^{\mp i v_A \int d\tau' (\frac{B_{i,st}}{B_0} k_i)} \times S_f \tag{3.11}$$

Integration along the perturbed field trajectory can be implemented using the stochastic average over an scale $(1/k_{st})$

$$e^{\mp i v_A \int d\tau' (\frac{B_{i,st}}{B_0} k_i)} \to \langle e^{\mp i v_A \int d\tau' (\frac{B_{i,st}}{B_0} k_i)} \rangle, \tag{3.12}$$

where the bracket denotes an average over random radial excursions $\delta x_i = \int d\tau v_A B_{i,st}/B_0$. This yields the Elsässer response

$$\langle f_{\pm,k\omega}\rangle = \int d\tau e^{i(\omega - \langle u_y\rangle k_y \mp v_A k_z)\tau} \langle e^{\mp i v_A \int d\tau' (\frac{B_{i,st}}{B_0} k_i)} \rangle \times S_f, \tag{3.13}$$

where i, j are indexes for perpendicular components and $Dk^2 = D_x k_x^2 + D_y k_y^2$ and M_f is the propagator. Here, $\langle e^{\mp i v_A \int d\tau' (\frac{B_{i,st}}{B_0} k_i)} \rangle$ is set by the diffusivity tensor $\underline{\underline{D}} = v_A^2 \int d\tau" b^2_{j,st(\tau")}$ so

$$\langle e^{\mp i v_A \int d\tau' (\frac{B_{i,st}}{B_0} k_i)} \rangle \simeq 1 - k_i D_{ij} k_j \tau \simeq e^{-\underline{k}\cdot\underline{\underline{D}}\cdot\underline{k}\tau}, \tag{3.14}$$

where τ is the decorrelation time due to field stochasticity, such that $\tau \simeq \int d\tau" \simeq l_{ac}/v_A$. We assume no correlation between x- and y-direction of stochastic field (i.e. and $\langle B_{x,st} B_{y,st}\rangle = 0$) and $\langle B_{i,st}\rangle = 0$. Hence, only diagonal terms of $\underline{\underline{D}}$ survive (i.e. $D_{ij} = \delta_{ij} v_A l_{ac} b_i^2$). A number of important comments are in order here. First, $D \simeq v_A D_M$, indicating that vorticity response decorrelation occurs by Alfvénic pulse diffusion along wandering magnetic fields. This is a consequence of the fact that PV (or polarization charge) perturbations (which determine the PV or polarization charge flux—i.e. the Reynolds force) are determined via $\underline{\nabla}\cdot\underline{J} = 0$, the characteristic

signal speed for which is v_A. Second, $v_A D_M$ is actually *independent of* B_0 and is a set only by b^2. To see this, observe that $b^2 \equiv \langle B_{st}^2 \rangle / B_0^2$, $v_A = B_0/\sqrt{\mu_0 \rho}$, and $l_{ac} = Rq$. Thus, $D \propto b^2$ reflects the physics that decorrelation occurs due to pulses traveling along stochastic fields, *only*. In this respect, the result here closely resembles the 2D case (i.e. β-plane MHD in Chapter 2). Third, v_A for the mean field enters only via the linear vorticity response—which is used to compute the vorticity flux—and thus the Reynolds force.

Now we have the averaged Elsässer response

$$\langle f_{\pm,k\omega} \rangle = \frac{i}{(\omega - \langle u_y \rangle k_y \mp v_A k_z) + iDk^2} \times S_f \equiv M_f S_f, \tag{3.15}$$

where $Dk^2 = D_x k_x^2 + D_y k_y^2$. And M_f is a propagator defined as

$$M_f = \frac{1}{2}\left(\frac{i}{(\omega_{sh} - v_A k_z) + iDk^2} + \frac{i}{(\omega_{sh} + v_A k_z) + iDk^2} \right), \tag{3.16}$$

where $\omega_{sh} \equiv \omega - \langle u_y \rangle k_y$ is the shear flow Doppler shifted frequency. From Eq. (3.10), we have the fluctuating vorticity

$$\widetilde{\zeta} = \frac{1}{B_0} \nabla^2 \widetilde{\phi} = \sum_{k\omega} Re[M_f (\frac{-k^2}{B_0} S_f)] \tag{3.17}$$

Hence, the response of vorticity ($\widetilde{\zeta}$) to the vorticity gradient and curvature term in the presence of stochastic fields is:

$$\widetilde{\zeta} = \sum_{k\omega} \left[Re(M_f)(-\frac{\widetilde{u}_{x,k\omega}}{B_0} \frac{\partial}{\partial x} \nabla^2 \langle \phi \rangle) + Re\left(i k_y M_f \frac{2\kappa}{\rho} \widetilde{p}_{k\omega} \right) \right] \tag{3.18}$$

The first term determines the diffusive flux of vorticity. The second sets the off-diagonal stress, or *residual stress*, that depends on the pressure perturbation and the curvature of the mean magnetic field. We calculate the residual stress term in Eq. (3.18) by using another set of Elsässer-like variables $g_{\pm,k\omega} \equiv \frac{\widetilde{p}_{k\omega}}{\rho C_s^2} \pm \frac{\widetilde{u}_{z,k\omega}}{C_s}$, defined from Eq. (3.8) and (3.9), and follow the approach discussed

above. This yields $\widetilde{p}_{k\omega} = M_g \widetilde{u}_x \frac{\partial}{\partial x}\langle p\rangle$ and M_g is defined as

$$M_g = \frac{1}{2}\left(\frac{i}{(\omega_{sh} - C_s k_z) + iD_s k^2} + \frac{i}{(\omega_{sh} + C_s k_z) + iD_s k^2}\right) \simeq \frac{i}{\omega_{sh}}. \tag{3.19}$$

where $D_s \equiv C_s D_M$ (for pressure decorrelation rate $\tau_c = l_{ac}/C_s$) is the diffusivity due to an acoustic signal propagating along stochastic fields. Notice that $\widetilde{p}$ is the pressure perturbation set by the acoustic coupling. Hence, it has slower speed $C_s \ll v_A$ (or $\beta \ll 1$) as compared to Alfénic coupling. An ensemble average of total vorticity flux yields

$$\begin{aligned}\langle \widetilde{u}_x \widetilde{\zeta}\rangle = &-\sum_{k\omega} |\widetilde{u}_{x,k\omega}|^2 Re(M_f) \frac{\partial}{\partial x}\langle \zeta\rangle \\ &+ \underbrace{\sum_{k\omega}\left[|\widetilde{u}_{x,k\omega}|^2 Re(ik_y M_f M_g)\frac{2\kappa}{\rho}\frac{\partial}{\partial x}\langle p\rangle\right]}_{\textit{Residual Stress}}.\end{aligned} \tag{3.20}$$

Notice that $D_s k^2 \simeq C_s D_M k^2$. Hence, the broadening effect of random acoustic wave propagation itself is negligible as compared to the natural linewidth, since the plasma $\beta \ll 1$. Now, we have

$$\langle \widetilde{u}_x \widetilde{\zeta}\rangle = -D_{PV}\frac{\partial}{\partial x}\langle \zeta\rangle + F_{res}\kappa \frac{\partial}{\partial x}\langle p\rangle, \tag{3.21}$$

where $D_{PV} \equiv \sum_{k\omega} |\widetilde{u}_{x,k\omega}|^2 Re(M_f)$ is PV diffusivity, and $F_{res} \simeq \sum_{k\omega} \frac{-2k_y}{\omega_{sh}\rho} D_{PV,k\omega}$ is the residual stress. Notice that there is no parity issue lurking in the term $2k_y/\omega_{sh}\rho$ since $2k_y/\omega_{sh}\rho \propto 2\cancel{k_y}/\cancel{k_y}\rho \propto 2/\rho$ (i.e. even) for $k_y\langle u_y\rangle \ll \omega \simeq \omega_*$. By using the Taylor Identity[93], we rewrite the PV flux as Reynolds force $\langle \widetilde{u}_x \widetilde{\zeta}\rangle = \frac{\partial}{\partial x}\langle \widetilde{u}_x \widetilde{u}_y\rangle$. In the limit of the D_{PV} and F_{res} slowly varying as compared with vorticity $\langle \zeta\rangle$ and pressure $\langle p\rangle$, respectively, the poloidal Reynolds stress is

$$\langle \widetilde{u}_x \widetilde{u}_y\rangle = -D_{PV}\frac{\partial}{\partial x}\langle u_y\rangle + F_{res}\kappa\langle p\rangle, \tag{3.22}$$

where the effective viscosity is

$$D_{PV} = \sum_{k\omega} |\widetilde{u}_{x,k\omega}|^2 \frac{v_A b^2 l_{ac} k^2}{\omega_{sh}^2 + (v_A b^2 l_{ac} k^2)^2}. \tag{3.23}$$

This indicates that *both the PV diffusivity and residual stress (and thus the Reynolds stress) are suppressed as the stochastic field intensity b^2 increases*, so that $v_A b^2 l_{ac} k^2$ exceeds ω_{sh}. This result is consistent with our expectations based upon scaling and with the Reynolds stress burst suppression in presence of RMPs, observed in Kriete et al. [50]. This model is build on gyro-Bohm scaling and hence the stochastic dephasing effect is insensitive to the details of the turbulence mode (e.g. ITG, TEM,... etc.), within that broad class.

Physical insight into the physics of Reynolds stress decoherence can be obtained by considering the effect of a stochastic magnetic field on the 'shear-eddy tilting feedback loop'. Recall that the Reynolds stress is given by

$$\langle \widetilde{u}_x \widetilde{u}_y \rangle = -\sum_k \frac{|\widetilde{\phi}_k|^2}{B_0^2} \langle k_y k_x \rangle. \tag{3.24}$$

Thus, a non-zero stress requires $\langle k_y k_x \rangle \neq 0$, i.e. a spectrally averaged wave vector component correlation. This in turn requires a spectral asymmetry. In the presence of a seed shear, k_x tends to align with k_y, producing $\langle \rangle \neq 0$ (Fig. 3.3). To see this, observe that Snell's law states

$$\frac{dk_x}{dt} = -\frac{\partial(\omega_{0,k} + k_y u_y)}{\partial x} \simeq 0 - \frac{\partial(k_y u_y)}{\partial x}. \tag{3.25}$$

So, to set a non-zero phase correlation $\langle k_y k_x \rangle \neq 0$, we take $k_x \simeq k_x^{(0)} - k_y \frac{\partial \langle u_y \rangle}{\partial x} \tau_c$, where τ_c is a ray scattering time that limits ray trajectory time integration. Ignoring $k_x^{(0)}$, we then find

$$\langle \widetilde{u}_x \widetilde{u}_y \rangle \simeq 0 + \sum_k \frac{|\widetilde{\phi}_k|^2}{B_0^2} k_y^2 \frac{\partial \langle u_y \rangle}{\partial x} \tau_{c,k}. \tag{3.26}$$

Note that the existence of correlation is unambiguous, and the Reynolds stress is manifestly non-

zero. Here, *eddy tilting* (i.e. k_x evolution) has aligned wave vector components. Once $\langle u_x u_y \rangle \neq 0$, flow evolution occurs due to momentum transport. Then, flow shear amplification further amplifies the Reynolds stress, etc. This process constitutes the 'shear-eddy tilting feedback loop', and underpins modulational instability amplification of zonal shears. Central to shear-eddy tilting feedback is the proportionality of stress cross-phase to shear. However, in the presence of stochastic fields, the correlation $\langle k_x k_y \rangle$ is altered. To see this, consider drift-Alfén turbulence, for which

$$\omega^2 - \omega_* \omega - k_\parallel^2 v_A^2 = 0. \tag{3.27}$$

Let ω_0 be the frequency of the drift wave roots. Now, let $k_\parallel = k_\parallel^{(0)} + \underline{k}_\perp \cdot (\underline{B}_{st,\perp}/B_0)$ due to stochastic field wandering, and $\delta\omega$ the corresponding ensemble averaged correction to ω_0—i.e. $\omega = \omega_0 + \delta\omega$. After taking an ensemble average of random fields from Eq. (3.27), we obtain $\langle \delta\omega \rangle \simeq v_A^2 (2k_\parallel \frac{\langle \underline{B}_{st,\perp} \rangle}{B_0} \cdot \underline{k}_\perp + \langle (\frac{\underline{B}_{st,\perp}}{B_0} \cdot \underline{k}_\perp)^2 \rangle)/\omega_0$, where $\langle B_{i,st} \rangle = 0$ so the first term vanishes. The ensemble averaged frequency shift is then

$$\langle \delta\omega \rangle \simeq \frac{1}{2} \frac{v_A^2}{\omega_0} b^2 k_\perp^2. \tag{3.28}$$

Here, $\langle \omega_0 \rangle \simeq \omega_*$, corresponding to the drift wave. Note that $\delta\omega \propto \langle B_{st}^2 \rangle$ is independent of B_0, except for ω_0. Thus, in the presence of shear flow, the Reynolds stress becomes

$$\langle \widetilde{u}_x \widetilde{u}_y \rangle \simeq \sum_k \frac{|\widetilde{\phi}_k|^2}{B_0^2} (k_y^2 \frac{\partial \langle u_y \rangle}{\partial x} \tau_{c,k} + \frac{1}{2} k_y \frac{v_A^2 k_\perp^2}{\omega_0} \frac{\partial b^2}{\partial x} \tau_{c,k}). \tag{3.29}$$

This indicates that for $\frac{\partial \langle u_y \rangle}{\partial x} < \frac{v_A^2 k_\perp^2}{\omega_0} \frac{\partial b^2}{\partial x}$, the shear-eddy tilting feedback loop is broken, since the $\langle k_x k_y \rangle$ correlation is no longer set by flow shear. In practice, this requires $b^2 \gtrsim 10^{-7}$, as deduced above.

We modify a well-known predator-prey model of the L-H transition, the Kim-Diamond model [47] to include the effects of stochastic fields. The Kim-Diamond model is a zero-dimensional reduced model, which evolves fluctuation energy, Reynolds stress-driven flow

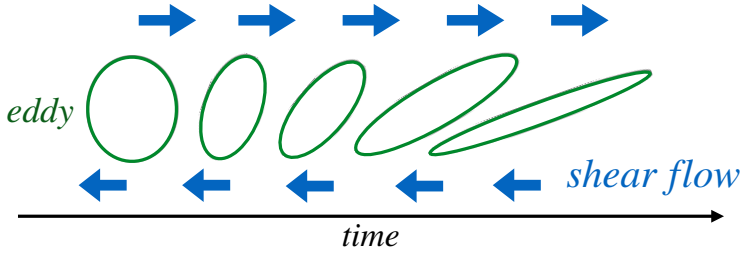

Figure 3.3. Shear-eddy tilting feedback loop. The $E \times B$ shear generates the $\langle k_x k_y \rangle$ correlation and hence support the non-zero Reynolds stress. And the Reynold stress, in turns, modifies the shear via momentum transport. Hence, the shear flow reinforce the self-tilting.

shear, and the mean pressure gradient. As heat flux is increased, a transition from L-mode to Intermediate phase (I-phase) and to H-mode occurs. Here, we include the principal stochastic field effect—Reynolds stress decoherence. This is quantified by the dimensionless parameter $\alpha \equiv qb^2/\sqrt{\beta}\rho_*^2\varepsilon$. The aim is to explore the changes in L-H transition evolution (i.e. power threshold increment) due to magnetic stochasticity. This dimensionless parameter α quantifies the strength of stochastic dephasing relative to turbulent decorrelation. As shown in the previous paragraph, the $E \times B$ shear feedback loop that forms the zonal flow is broken by the stochastic fields. Hence, the modification enters the *shear decorrelation term* in the turbulence (ξ) evolution, the corresponding term in the zonal flow energy (v_{ZF}^2) evolution, and the pressure gradient ($\mathcal{N}$) evolution. The third term is smaller by $\sqrt{\beta}$ (i.e. $\alpha \to \alpha\sqrt{\beta}$), due to the fact that *acoustic* wave scatting is what causes decoherence in the pressure evolution. A factor $1/(1+c\alpha)$ captures the modification due to the effect of stochastic suppression effect, where c a constant. The *modified*

Kim-Diamond model becomes

$$\frac{\partial \xi}{\partial t} = \xi \mathscr{N} - a_1 \xi^2 - a_2 (\frac{\partial \langle u_y \rangle}{\partial x})^2 \xi - \underbrace{a_3 v_{ZF}^2 \xi \cdot \frac{1}{(1+a_4\alpha)}}_{\textit{Reynolds stress decoherence}} \tag{3.30}$$

$$\frac{\partial v_{ZF}^2}{\partial t} = \underbrace{a_3 v_{ZF}^2 \xi \cdot \frac{1}{(1+a_4\alpha)}}_{\textit{Reynolds stress decoherence}} - b_1 v_{ZF}^2 \tag{3.31}$$

$$\frac{\partial \mathscr{N}}{\partial t} = \underbrace{-c_1 \xi \mathscr{N} \cdot \frac{1}{(1+a_4\alpha\sqrt{\beta})}}_{\textit{turbulent diffusion of pressure}} - c_2 \mathscr{N} + Q, \tag{3.32}$$

where a_i, b_i, and c_i ($a_1 = 0.2$, $a_2 = 0.7$, $a_3 = 0.7$, $a_4 = 1$, $b_1 = 1.5$, $c_1 = 1$, $c_2 = 0.5$, $\sqrt{\beta}$=0.05) are model-dependent coefficients, and Q is the input power.

We find that stochastic fields raise the L-I and I-H transition power thresholds, linearly in proportion to α (Fig. 3.5). And recall that α is proportional to stochastic fields intensity b^2 (Fig. 3.4). This is a likely candidate to explain the L-H power threshold increment in DIII-D [86].

We are also interested in stochastic field effects on the toroidal Reynolds stress $\langle \widetilde{u}_x \widetilde{u}_z \rangle$, which determines intrinsic toroidal rotation. Consider toroidal Eq. (3.9) with the stochastic fields effect $\frac{\partial}{\partial z} = \frac{\partial}{\partial z}^{(0)} + \underline{b} \cdot \nabla_\perp$. We have

$$\frac{\partial}{\partial t}\langle u_z \rangle + \frac{\partial}{\partial x}\langle \widetilde{u}_x \widetilde{u}_z \rangle = -\frac{1}{\rho}\frac{\partial}{\partial x}\langle b\widetilde{p} \rangle, \tag{3.33}$$

The second term on the LHS is the toroidal Reynold stress $\langle \widetilde{u_r} \widetilde{u_z} \rangle$. The RHS contains the $\langle b\widetilde{p} \rangle$ the kinetic stress. Both of these terms can be dephased by stochastic fields, but the dephasing of the former is of primary importance. In the context of intrinsic rotation, we follow the method for the derivation of decoherence of the poloidal residual stress—i.e. using Elässer-like variables $g_{\pm,k\omega} \equiv \frac{\widetilde{p}_{k\omega}}{\rho C_s^2} \pm \frac{\widetilde{u}_{z,k\omega}}{C_s}$ from Eq. (3.8) and (3.9). The only difference from the previous residual stress calculation is the presence term of $\frac{\partial}{\partial x}\langle u_z \rangle$, and hence the source of toroidal stress becomes

$S_{g,\pm} \equiv -\frac{\widetilde{u}_{x,k\omega}}{\rho C_s^2}\frac{\partial}{\partial x}\langle p\rangle \mp \frac{\widetilde{u}_x}{C_s}\frac{\partial}{\partial x}\langle u_z\rangle$. We find $\widetilde{u}_{z,k\omega} = M_{g,-}C_s$, where $M_{g,-}$ is a propagator such that

$$M_{g,-} = \frac{i}{2}\Big(\frac{S_{g,+}}{(\omega_{sh} - C_s k_z) + iD_s k^2} - \frac{S_{g,-}}{(\omega_{sh} + C_s k_z) + iD_s k^2}\Big), \tag{3.34}$$

Noted that when $\frac{\partial}{\partial x}\langle u_z\rangle = 0$, the propagator $M_{g,-}$ reduces to M_g. Thus, the toroidal Reynold stress is

$$\begin{aligned}\langle \widetilde{u}_x \widetilde{u}_z\rangle = \sum_{k\omega} |\widetilde{u}_{x,k\omega}|^2 \Big[&\frac{-2D_s k^2}{\omega_{sh}^2 + (2D_s k^2)^2}\frac{\partial\langle u_z\rangle}{\partial x} \\ &+ \frac{-2D_s k^2}{\omega_{sh}^2 + (2D_s k^2)^2}\frac{k_z}{\omega_{sh}\rho}\frac{\partial\langle p\rangle}{\partial x}\Big].\end{aligned} \tag{3.35}$$

The first term in RHS contains the *turbulent viscosity* (ν_{turb}), which we define as

$$\begin{aligned}\nu_{turb} &\equiv \sum_{k\omega} |\widetilde{u}_{x,k\omega}|^2 \frac{2D_s k^2}{\omega_{sh}^2 + (2D_s k^2)^2} \\ &= \sum_{k\omega} |\widetilde{u}_{x,k\omega}|^2 \frac{2C_s b^2 l_{ac} k^2}{\omega_{sh}^2 + (2C_s b^2 l_{ac} k^2)^2}.\end{aligned} \tag{3.36}$$

This turbulent viscosity has a form similar to D_{PV} in Eq. (3.23). However, decorrelation of ν_{turb} is set by C_s while that of D_{PV} is set by v_A. Thus, decoherence effects here are weaker. The second term in Eq. (3.35) contains the *toroidal residual stress* ($F_{z,res}$)

$$F_{z,res} \equiv \sum_{k\omega}\Big(\frac{-k_z}{\omega_{sh}\rho}\Big)|\widetilde{u}_{x,k\omega}|^2 \frac{(2D_s k^2)}{\omega_{sh}^2 + (2D_s k^2)^2} \sim \sum_{k\omega}\frac{-k_z}{\omega_{sh}\rho}\nu_{turb,k\omega}. \tag{3.37}$$

Notice that non-zero value of $F_{z,res}$ requires symmetry breaking (i.e. $\langle k_z k_y\rangle \neq 0$) since $\frac{k_z}{\omega_{sh}\rho} \propto \frac{k_z}{k_y}$. Thus, *a symmetry breaking condition—non-zero $\langle k_z k_y\rangle$—must be met for finite residual toroidal residual stress ($F_{z,res}$)* . Here, $\langle k_z k_y\rangle$ must now be calculated in the presence of the stochastic field. The details of this calculation involve determining the interplay of stochastic field effects with spectral shifts (i.e. symmetry breaking by $E \times B$ shear) and inhomogeneities (i.e. spectral symmetry breaking by intensity gradient). This will involve competition between the radial

scale length of stochastic fields and the scales characteristic of the spectral shift (induced by $E \times B$ shear) and the spectral intensity gradient. This detailed technical study is left for a future publication. We rewrite the toroidal stress as

$$\langle \widetilde{u}_x \widetilde{u}_z \rangle = -\nu_{turb} \frac{\partial}{\partial x} \langle u_z \rangle + F_{z,res} \frac{\partial}{\partial x} \langle p \rangle, \tag{3.38}$$

which has similar form to that of poloidal Reynolds stress in Eq. (3.22). This shows that stochastic fields reduce the toroidal stress and hence slow down the intrinsic rotation. However, from Eq. (3.36) and (3.37), the stochastic suppression effect on toroidal stress and residual stress depends on $C_s D_M$ (not $v_A D_M$), and so is weaker than for zonal flows.

3.3 Conclusion for Drift-Wave Turbulence in Fusion Devices

RMPs are applied to the edge of tokamak plasma to mitigate Edge Localized Modes (ELMs), which produce unacceptably high transient heat loads on plasma-facing components. The 'cost' of this benefit is an increase in the Low to High confinement mode transition (L-H transition) threshold power, as observed with RMPs. Because several studies suggest that the L-H transition is triggered by edge shear flows, it implies that the transition dynamics are modified by the effects of stochastic fields on shear flow evolution. Stochasticity results from $\underline{k} \cdot \underline{B} = 0$ resonance overlap, and field line separations diverge exponentially. And the magnetic Kubo number is modest. Hence, a key question is the effect of stochastic fields on self-generated shear flows. In this chapter, the system is the L-mode tokamak edge plasma, in the presence of a stochastic magnetic field induced by external RMP coils. We showed that the 'shear-eddy tilting feedback loop' is broken by a critical b^2 intensity, and that $k_\perp^2 v_A D_M$ characterizes the rate of stress decoherence. Note that the Alfvén speed follows from charge balance, which determines Reynolds stress. A natural threshold condition for Reynolds stress decoherence emerges as $k_\perp^2 v_A D_M / \Delta\omega > 1$. In turn, we show that this defines a dimensionless ratio α, which quantifies the effect on zonal flow excitation, and thus power thresholds. $\alpha \simeq 1$ occurs for $b^2 \simeq 10^{-7}$,

consistent with stochastic magnetic field intensities for which a significant increment in power threshold occurs. Note that this scaling is somewhat pessimistic (i.e. ρ_*^{-2}).

3.4 Future work for the drift-wave turbulence in presence of stochastic fields

This study has identified several topics for future work. These include developing a magnetic stress—energy tensor evolution equation, for representing small-scale fields in real space. Fractal network models of small-scale magnetic field are promising in the context of intermittency. A better understanding of stochastic field effects on transport for $Ku_{mag} \geq 1$ is necessary as a complement to our $Ku_{mag} \leq 1$ model-based understanding. For MFE plasmas, an 1D model for the L-H transition evolution is required. This study will introduce a new length scale (M. Jiang & W. Guo et al. in press), which quantifies the radial extent of the stochastic region. Finally, the bursty character of pre-transition Reynolds work, suggests that a statistical approach to the transition is required. The challenge here is to identify the physics of the noise and flow bursts, and how the presence of stochasticity quenches them. The stochasticity-induced change in 'shear-eddy tilting feedback loop' discussed herein is a likely candidate for the quenching of the noise and flow burst.

Chapter 3, in full, is a reprint of the material as it appears in Chang-Chun Chen, Patrick H. Diamond, Rameswar Singh, and Steven M. Tobias, *Physics of Plasmas* 28, 042301 (2021). The dissertation author was the primary investigator and author of this paper.

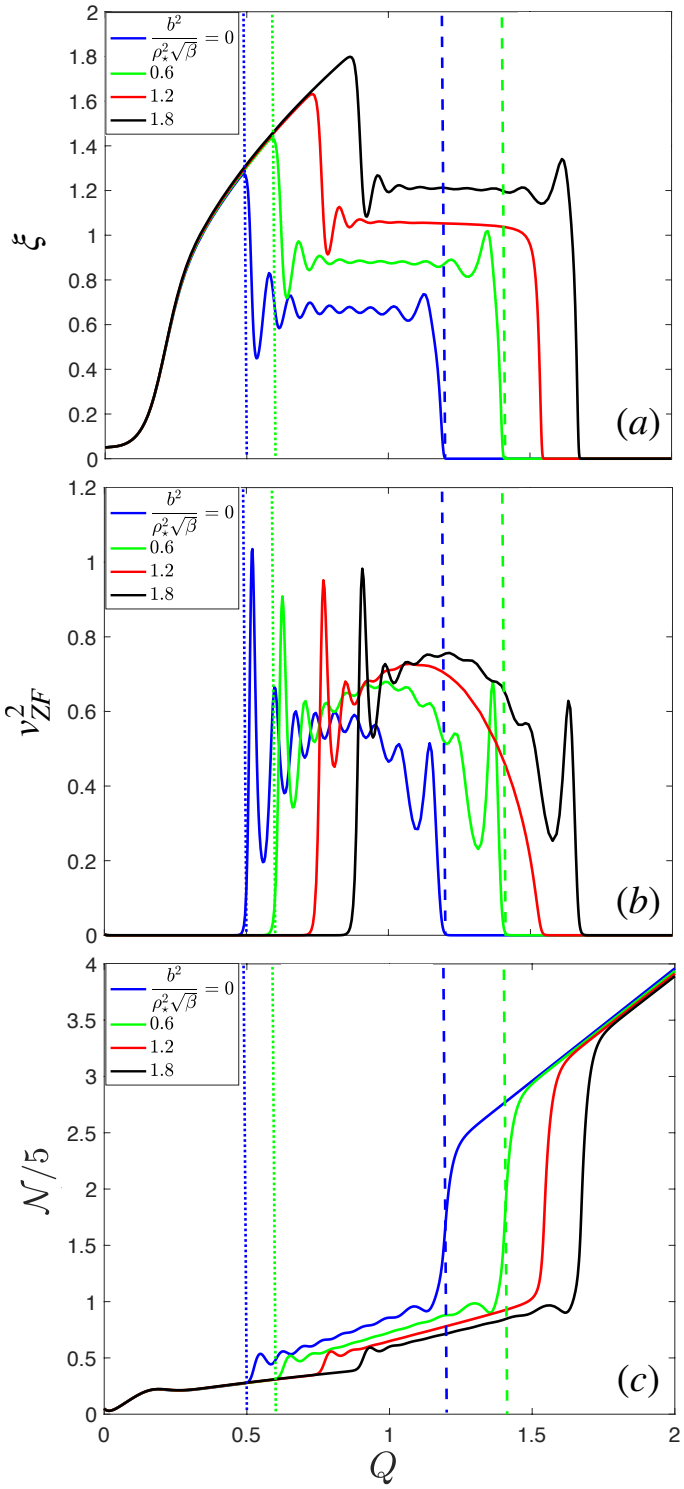

Figure 3.4. Modified Kim-Diamond model. (a) Turbulent intensity ξ. (b) Zonal flow energy v_{ZF}^2. (c) Pressure gradient $\mathcal{N}$ evolution with increasing input power Q. Dotted lines indicate L-I transitions, dashed lines indicate I-H transitions. As we increase the mean-square stochastic field (b^2), L-I and I-H transitions power threshold shift to the right, i.e. from $b^2/\rho_*^2\sqrt{\beta} = 0$ (blue) to 0.6 (green).

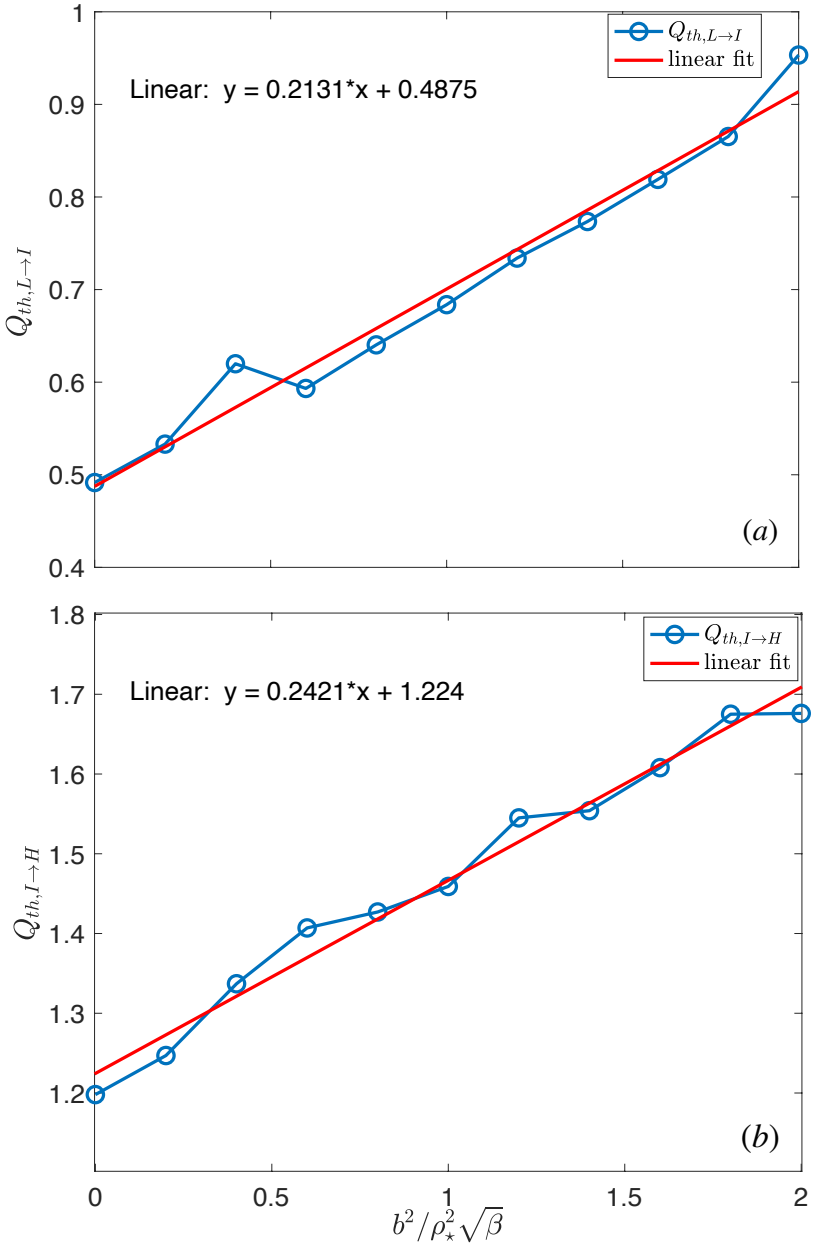

Figure 3.5. Power threshold increments in modified Kim-Diamond model. (a) L-I transition power threshold increment. (b) I-H transition power threshold increment. Mean-square stochastic fields (b^2) shift L-H and I-H transition thresholds to higher power, in proportional to $b^2/\rho_*^2\sqrt{\beta}$.

Chapter 4

Ion Heat, Parallel Momentum Transport and the Hybrid Diffusivity

Transport in a stochastic field has long been recognized as a fascinating though complex problem. It is one of the classic 'paradigm problems' of magnetic fusion physics and has stimulated the writing of many well-known papers, most notably Rosenbluth et. al 1966 [82] and Rechester & Rosenbluth1978 [77]. The bulk of previous work on the subject is concerned with *electron thermal transport* in a stochastic magnetic field [43, 87, 38, 68]—this is on account of the tiny electron inertia, which is thought to allow long-distance electron streaming along wandering field lines. However, the more recent awareness of the need to achieve both good confinement and good power handling (and boundary control) has driven a resurgence of interest in the stochastic-field-induced transport problem—this time in new contexts. Topics of interest include, but are not limited to:

- L-H transition dynamics in a stochastic magnetic field, as produced by resonant magnetic perturbations (RMPs) [24]. It's now well known that the application of an RMPs raises the transition threshold[54, 30, 46, 84, 64, 85, 86, 50] while it 'stochasticizes' the edge layer.
- Intrinsic rotation in a stochastic magnetic field, as for the H-mode pedestal torque with RMPs [80, 81, 19, 96, 18].
- Internal transport barrier transitions triggered by magnetic islands[11, 36, 99, 42, 37, 35].

Note that most or all of these phenomena are rooted in *ion* transport and flow physics—topics rarely associated with stochastic magnetic fields. The related questions of the effect of magnetic stochasticity on the mean radial electric field and its shear are also of great interest in this context. To this end, this paper addresses aspects of ion energy and parallel momentum transport in a stochastic magnetic field.

The theory of turbulent transport of parallel momentum and ion heat by the interaction of stochastic magnetic fields and turbulence is presented. Attention is focused on determining the kinetic stress and the compressive energy flux. In this Chapter, a critical parameter is identified as the ratio of the turbulent scattering rate to the rate of parallel acoustic dispersion. For the parameter large, the kinetic stress takes the form of a viscous stress. For the parameter small, the quasilinear residual stress is recovered. In practice, the viscous stress is the relevant form, and the quasilinear limit is not observable. This is the principal prediction of this paper. A simple physical picture is developed and shown to recover the results of the detailed analysis.

4.1 A heuristic model

A heuristic but enlightening model of the pressure response $\delta p/\delta b$ is presented here and serves to guide the reader through the subsequent detailed analysis. The parallel flow response $\delta u_\parallel/\delta b$ can be estimated in a similar way. Hence, we discuss only $\delta p/\delta b$. Here, it is helpful for the reader to consult Figure 4.2 and 4.1. One can 'pluck' a magnetic field line by $\widetilde{b}$. Since a mean radial pressure gradient $\partial_r\langle p\rangle$ is present, the magnetic perturbation will generate a localized slug of pressure excess-per-length $\widetilde{b}_r\partial_r\langle p\rangle$. To balance this local pressure excess, there are two possibilities:

- If the rate of turbulent (i.e. viscous) mixing of the parallel flow response is large (i.e. $\nu_T/l_\perp^2 >$ other rates), then a turbulent viscosity ν_T will dissipate the parallel flow perturbation $\widetilde{u}_\parallel$, produced in response to the magnetic perturbation and pressure slug (see Figure 4.1). In this case, $\nu_T\nabla_\perp^2\widetilde{u}_\parallel \simeq \widetilde{b}_r\partial_r\langle p\rangle/\rho$, where ν_T is the turbulent viscosity

due to the electrostatic turbulence. In this limit, perturbed pressure is replaced by a dynamic balance of the turbulent Reynolds force with the local pressure excess. Here, $\nu_T \simeq D_T \simeq \int dt' \langle \widetilde{u}_\perp(0)\widetilde{u}_\perp(t')\rangle \simeq \langle \widetilde{u}_\perp^2 \rangle \tau_{ac}$, where τ_{ac} is the autocorrelation time of the electrostatic fluctuation and D_T is the turbulent fluid diffusivity.

- If the rate of sound propagation along the perturbed field is large (i.e. $c_s/l_\parallel >$ other rates), then a pressure gradient will build up along the mean field, so as to cancel the initial imbalance due to the slug (see Figure 4.2). In this case, $\widetilde{p}c_s/l_\parallel \simeq -c_s\widetilde{b}_r\partial_r\langle p\rangle$, which leads to the quasilinear result for $\widetilde{p}$ and K.

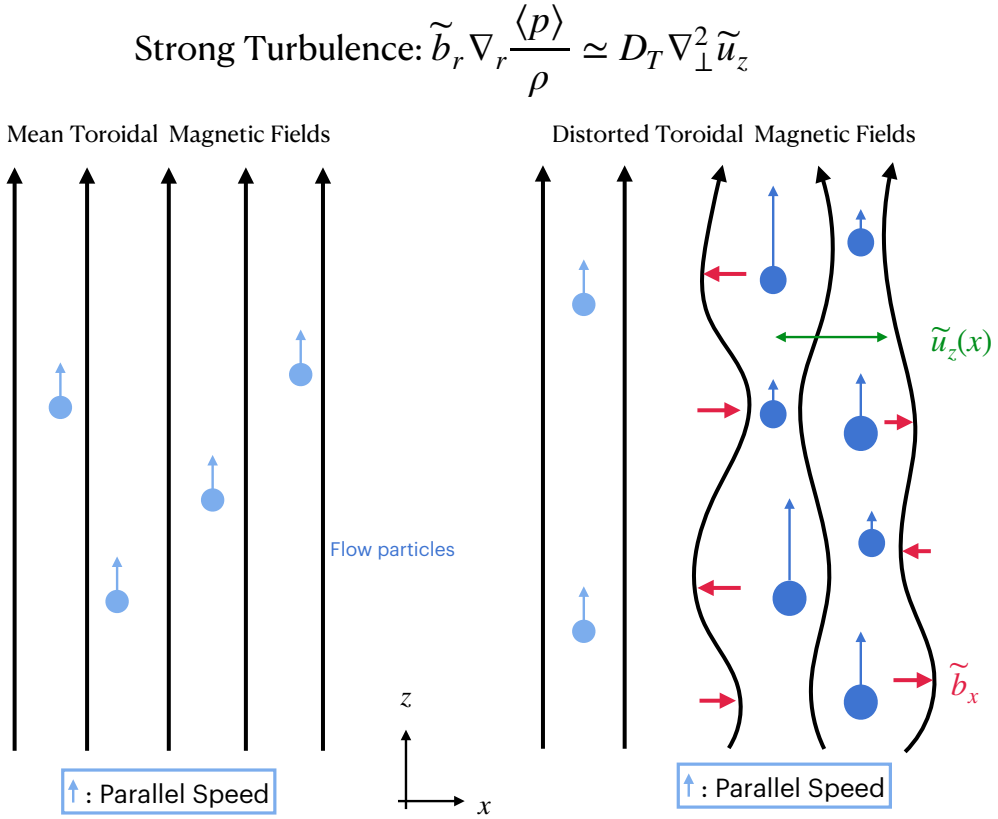

Figure 4.1. Left: Mean magnetic field in the parallel direction with fluid flow speed. Right: The magnetic field is perturbed by the stochastic field $\widetilde{b}_r$. In response to magnetic perturbation and pressure slug, turbulent viscosity ν_T will dissipate the parallel flow perturbation. In this chapter, we obtain that the change in mean pressure $(\partial_x\langle p\rangle/\rho)$ is balanced by turbulent mixing of parallel flow, i.e. $\nabla_\perp^2\widetilde{u}_z$. Blue arrows indicate the change of parallel speed.

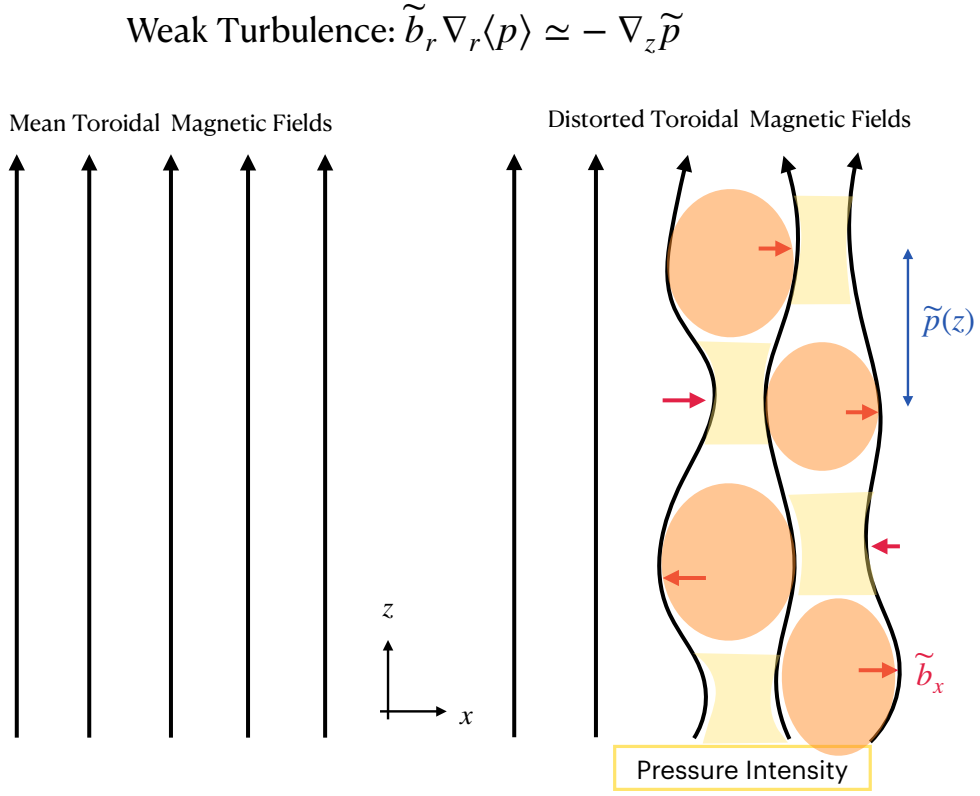

Figure 4.2. Left: Mean magnetic field in toroidal direction with constant pressure in z-direction. Right: The magnetic field is perturbed by the stochastic field $\widetilde{b}_r$. In response to magnetic perturbation and pressure slug, the pressure gradient will build up along the mean field. Regions with higher and lower pressure intensity are colored orange and yellow, respectively.

Here, the critical competition (highlighted in Figure 4.2 and 4.1) is that between the parallel acoustic transit rate $c_s/l_\parallel \simeq c_s \Delta k_\parallel$ and the perpendicular diffusive mixing rate $\simeq \nu_T/l_\perp^2 \simeq k_\perp^2 D_T$. Hereafter, we take $k_\parallel \simeq |\Delta k_\parallel|$. In most relevant cases (i.e. as for drift wave turbulence), $k_\perp^2 D_T \simeq \omega > k_\parallel c_s$, so the dynamic balance regime is relevant. Note that in this regime, the *qualitative* form of the response to $\widetilde{b}$ differs from the quasilinear case. In particular, a hybrid viscous stress replaces the residual stress and involves turbulent decorrelation resulting from scattering by electrostatic fluctuation. In the weak turbulence regime, we recover perturbed pressure balance. The detailed analysis supports the conclusion derived from heuristics here.

4.2 Models setup and Transport by Static Stochastic Fields

Here, we construct a model for the evolution of density and parallel flow in presence of stochastic fields in Cartesian (slab) coordinates used in previous chapter [10]—x is radial, y is poloidal, and z is toroidal direction, in which the mean toroidal field lies (Figure 3.2). In this 3D system, the stochasticity of magnetic fields, given by a response to an external excitation such as an RMP coil, results from the overlap of magnetic islands located at resonant $\underline{k}\cdot\underline{B}=0$ surfaces [97]. Once overlap occurs, the coherent character of the perturbations is lost, due to finite Kolmogorov-Sinai entropy (i.e. there exists a positive Lyapunov exponent for the field) [48, 89]. Hence, the total magnetic field can be decomposed into the mean toroidal (parallel) field on the z-axis plus the stochastic field lying in $x-y$ plane. In this case, we take the magnetic Kubo number [52] to be modest $Ku_{mag} \lesssim 1$—so mean field theory is valid. This is consistent with reported experimental values of magnetic perturbations $\widetilde{b}$ [103, 100, 27, 39]. We decompose the magnetic fields, magnetic potential, velocities, electrical potential, pressure, and density

$$\begin{cases} \text{magnetic fields} & \mathbf{B} = (\widetilde{B}_x, \widetilde{B}_y,\, B_0) \\ \text{potential fields} & \mathbf{A} = (-\frac{1}{2}B_0 y,\, \frac{1}{2}B_0 x,\, \widetilde{A}_{(x,y)}) \\ \text{velocities} & \mathbf{u} = (\widetilde{u}_x,\, \langle u_y\rangle + \widetilde{u}_y,\, \langle u_z\rangle + \widetilde{u}_z) \\ \text{electric potential} & \phi = \langle\phi\rangle + \widetilde{\phi} \\ \text{pressure} & p = \langle p\rangle + \widetilde{p} \\ \text{particle density} & n = \langle n\rangle + \widetilde{n}. \end{cases} \tag{4.1}$$

Here $\langle u_y\rangle$ is the mean poloidal flow, $\langle u_z\rangle$ is the parallel flow. The tilde $\widetilde{}$ denotes the perturbations of the mean.

4.3 Non-diffusive Effect for Electron Particle Flux

In this section, we discuss the transport of parallel momentum and particles due to stochastic fields. One aim here is to make contact with and clarify the FGC result [28] as a baseline for later studies of stochastic scattering along with turbulence. Another is to elucidate the contribution to the physics of particle transport in a stochastic magnetic field—i.e. to determine the physical significance of the result. Following FGC, here, we assume an isothermal plasma, so the basic equations reduce to:

$$n\frac{\partial}{\partial t}u_z = -c_s^2\nabla_z n \tag{4.2}$$

$$\frac{\partial}{\partial t}n = -n\nabla_z u_z \tag{4.3}$$

where $\nabla_z = \nabla_z^{(0)} + \widetilde{b}\cdot\nabla_\perp$. Then the mean fields $\langle u_z\rangle$ and $\langle n\rangle$ evolve according to

$$n_0\frac{\partial}{\partial t}\langle u_z\rangle = -c_s^2\frac{\partial}{\partial x}\langle\widetilde{b}_x\widetilde{n}\rangle \tag{4.4}$$

$$\frac{\partial}{\partial t}\langle n\rangle = -n_0\frac{\partial}{\partial x}\langle\widetilde{b}_x\widetilde{u}_z\rangle, \tag{4.5}$$

where n_0 is a static, uniform background density. Thus, determining the effect of a stochastic field on density evolution (i.e. particle transport) requires a calculation of the flux $\langle\widetilde{b}_x\widetilde{u}_z\rangle$. Likewise, for the effect on parallel flow, the kinetic stress $c_s^2\langle\widetilde{b}_x\widetilde{n}\rangle$ is needed. The physical interpretation of how the density evolution discussed here is related to the particle flux is discussed at the end of this section.

To calculate $\langle\widetilde{b}_x\widetilde{u}_z\rangle$ and $\langle\widetilde{b}_x\widetilde{n}\rangle$, we proceed by quasilinear theory. Proceeding from Eq. 4.4 and Eq. 4.4, these equations can be written as

$$\frac{\partial}{\partial t}\frac{\widetilde{u}_z}{c_s} = -c_s\nabla_z^{(0)}\frac{\widetilde{n}}{n_0} - c_s\widetilde{b}_x\frac{\partial}{\partial x}\frac{\langle n\rangle}{n_0} \tag{4.6}$$

$$\frac{\partial}{\partial t}\frac{\widetilde{n}}{n_0} = -c_s\nabla_z^{(0)}\frac{\widetilde{u}_z}{c_s} - c_s\widetilde{b}_x\frac{\partial}{\partial x}\frac{\langle u_z\rangle}{c_s}. \tag{4.7}$$

We combine Eq. 4.6±Eq. 4.7 and obtain the Riemann-like variables $h_\pm \equiv \frac{\widetilde{u}_z}{c_s} \pm \frac{\widetilde{n}}{n_0}$, and the Riemann equation

$$\frac{\partial}{\partial t}h_\pm \pm c_s\frac{\partial}{\partial z}h_\pm = -c_s\widetilde{b}_x\frac{\partial}{\partial x}\frac{\langle n\rangle}{n_0} \mp c_s\widetilde{b}_x\frac{\partial}{\partial x}\frac{\langle u_z\rangle}{c_s}. \tag{4.8}$$

Note that $h_\pm$ propagate at c_s in opposite directions. Now, the magnetic perturbations here are *static*, so we can immediately take $\partial_t h_\pm = 0$. No acoustic wave dynamics enters, though the acoustic speed appears in the problem. From Eq. 4.8, we can then immediately write

$$h_{\pm,k} = \mp\int dl[\widetilde{b}_x\frac{\partial}{\partial x}\frac{\langle n\rangle}{n_0} \pm \widetilde{b}_x\frac{\partial}{\partial x}\frac{\langle u_z\rangle}{c_s}]. \tag{4.9}$$

Here, l parameterizes the distance along a magnetic field line, and the solution of Eq. 4.8 is affected by integrating along static stochastic field lines. Now, $\widetilde{u}_z/c_s$ and $\widetilde{n}/n_0$ can be recovered noting

$$\frac{\widetilde{u}_z}{c_s} = (h_+ + h_-)/2 = -\int dl\widetilde{b}_x\frac{\partial}{\partial x}\frac{\langle u_z\rangle}{c_s} \tag{4.10}$$

$$\frac{\widetilde{n}}{n_0} = (h_+ - h_-)/2 = -\int dl\widetilde{b}_x\frac{\partial}{\partial x}\frac{\langle n\rangle}{n_0} \tag{4.11}$$

It then follows that

$$\langle\widetilde{b}_x\widetilde{u}_z\rangle = -D_M\frac{\partial}{\partial x}\langle u_z\rangle \tag{4.12}$$

$$\langle\widetilde{b}_x\widetilde{n}\rangle = -D_M\frac{\partial}{\partial x}\langle n\rangle, \tag{4.13}$$

where

$$D_M = \int dl\langle\widetilde{b}_x(0)\widetilde{b}_x(l)\rangle = \langle\widetilde{b}_x^2\rangle l_{ac} \tag{4.14}$$

and $\langle \widetilde{b}_x(0)\widetilde{b}_x(l)\rangle$ is the magnetic perturbation correlation function, D_M is the usual stochastic field diffusivity, and l_{ac} is magnetic perturbation auto-correlation length. The mean field equations then are

$$\frac{\partial}{\partial t}\frac{\langle u_z\rangle}{c_s} = \frac{\partial}{\partial x} c_s D_M \frac{\partial}{\partial x}\frac{\langle n\rangle}{n_0} \tag{4.15}$$

$$\frac{\partial}{\partial t}\frac{\langle n\rangle}{n_0} = \frac{\partial}{\partial x} c_s D_M \frac{\partial}{\partial x}\frac{\langle u_z\rangle}{c_s}. \tag{4.16}$$

Several aspects of these results merit some discussion. First, Eq. 4.15 and Eq. 4.16 are transport equations with a characteristic transport coefficient $c_s D_M$. Thus, the rate for perturbations on scale $l_\perp$ is $1/\tau(l_\perp) \simeq c_s D_M / l_\perp^2$ as noted by FGC. However, the actual fluxes in Eq. 4.15 and Eq. 4.16 are *not* diffusive, but rather off-diagonal, leading to cross-coupling of $\langle n\rangle$ and $\langle u_z\rangle$ evolution. In particular, $\langle \widetilde{b}_x \widetilde{n}\rangle$ contributes to a fundamentally non-diffusive *residual stress* but not a viscosity. Here, $\partial_x\langle n\rangle$ drives the residual stress. Likewise, $\langle \widetilde{b}_x \widetilde{u}_z\rangle$ yields an off-diagonal convective flux driven by $\partial_x\langle u_z\rangle$ but not particle diffusion. FGC overlooked these points since that analysis never transformed back from Riemann variables (referred to as Elsässer variables by FGC) to physical variables. We note also that the results of Eq. 4.12 and Eq. 4.13 may be obtained directly from linearizing

$$B\cdot\nabla u_z = 0 \tag{4.17}$$

$$B\cdot\nabla n = 0, \tag{4.18}$$

and using $\widetilde{u}_z$, $\widetilde{n}$ to derive the fluxes. The problem is fundamentally static, and no sound wave dynamics is involved.

Eq. 4.16 describes density evolution. A natural question that arises is how is this related to particle transport, as it is conventionally understood. FGC refers to the density evolution in this problem as 'sound wave transport', yet it is clear that no sound wave dynamics is involved.

To clarify this question, we consider electron particle transport in a stochastic magnetic field. Here, we consider the stochastic field as co-existing with plasma current perturbations which generate it, so that Ampère's law is satisfied. This does not preclude the possibility of external excitation of the stochasticity, as by an RMP. The drift kinetic equation for electrons is

$$\frac{\partial}{\partial t}f + u_z \cdot \nabla_z f - \frac{E_\perp \times \hat{z}}{B_0} \cdot \nabla f - \frac{|e|}{m} E_z \frac{\partial}{\partial u_z} f = C(f), \tag{4.19}$$

so that the electron density evolution due to $\widetilde{b}$ effects is determined by

$$\frac{\partial n_e}{\partial t} = -n_{0,e} \nabla_z u_{z,e}, \tag{4.20}$$

where f is a general distribution function and $u_{z,e}$ is the parallel electron flow. Then for mean electron density, noting that $\nabla_z = \nabla_z^{(0)} + \widetilde{b} \cdot \nabla_\perp$, it follows that

$$\begin{aligned} &\frac{\partial \langle n_e \rangle}{\partial t} + n_{0,e} \frac{\partial}{\partial x} \langle \widetilde{b}_x \widetilde{u}_{z,e} \rangle = 0 \\ \Rightarrow &\frac{\partial \langle n_e \rangle}{\partial t} - \frac{\partial}{\partial x} \frac{\langle \widetilde{b}_x \widetilde{J}_{z,e} \rangle}{|e|} = 0, \end{aligned} \tag{4.21}$$

where $\widetilde{J}_{z,e} = -\widetilde{u}_{z,e} n_{0,e} |e|$ is electron current density. Note that the divergence of the electron current along tilted field lines (Ampère's Law) is what determines $\langle n_e \rangle$ evolution. Ampère's Law states

$$-\nabla_\perp^2 A_z = \mu_0 (J_{z,e} + J_{z,i}). \tag{4.22}$$

Substitution into Eq. 4.21 gives

$$\frac{\partial \langle n_e \rangle}{\partial t} + \frac{1}{\mu_0 |e|} \frac{\partial}{\partial x} \langle \widetilde{b}_x \nabla_\perp^2 \widetilde{A}_{z,e} \rangle + n_{0,i} \frac{\partial}{\partial x} \langle \widetilde{b}_x \widetilde{u}_{z,i} \rangle = 0. \tag{4.23}$$

In the last term on the RHS of Eq. 4.23, we take $u_z = u_{z,i}$ the parallel ion flow, consistent with

our notation. Using the magnetic Taylor identity [9], we then obtain

$$\frac{\partial \langle n_e \rangle}{\partial t} + \frac{\partial}{\partial x}\Gamma_{e,s} = 0, \tag{4.24}$$

where

$$\Gamma_{e,s} = \frac{-B_0}{\mu_0 |e|}\frac{\partial}{\partial x}\langle \widetilde{b}_x \widetilde{b}_y \rangle + n_0 \langle \widetilde{b}_x \widetilde{u}_z \rangle \tag{4.25}$$

is the electron particle flux due to $\widetilde{b}$. Note there are two contributions. The first is the familiar piece due to the divergence of the Maxwell stress [21]. It arises from the flow of current along tilted field lines. The second contribution $\langle \widetilde{b}_x \widetilde{u}_z \rangle$ studied here is due to *ion* flow along tilted lines. Note both total and ion current contributions are required to calculate $\partial_t \langle n_e \rangle$. For the model analyzed here, Eq. 4.12 then gives

$$\Gamma_{e,s} = \frac{-B_0}{\mu_0 |e|}\frac{\partial}{\partial x}\langle \widetilde{b}_x \widetilde{b}_y \rangle - n_0 D_M \frac{\partial}{\partial x}\langle u_z \rangle. \tag{4.26}$$

The first piece adds to the familiar Maxwell force contribution. The second term shows stochastic lines and parallel ion flow gradient drive a net electron particle flux. The discussion here clarifies the relations between Eq. 4.16 and the electron particle flux.

4.4 Calculating the Kinetic Stress and Compressive Energy Flux: Stochastic Fields and Turbulence

In the introduction, we discuss the kinetic stress and compressive energy flux due to stochastic fields. In this section, we consider *fluctuating* $E \times B$ flow effects. These introduce a relatively fast scattering time scale which enters the response to $\widetilde{b}$. We investigate the evolution of mean parallel flow and that of mean ion pressure (in presence of stochastic fields and turbulence) through the kinetic stress and compressive energy flux, respectively. Consider flow and pressure evolution in the basic model presented in the introduction, we have the parallel acceleration and

pressure equations:

$$\frac{\partial}{\partial t}u_z + (\mathbf{u}\cdot\nabla)u_z = -\frac{1}{\rho}\nabla_z p. \tag{4.27}$$

$$\frac{\partial}{\partial t}p + (\mathbf{u}\cdot\nabla)p = -\gamma p(\nabla_z\cdot\mathbf{u}_z), \tag{4.28}$$

where z is set in parallel direction, and x and y are set in perpendicular direction. We decompose velocity and pressure as mean and its perturbation such that $\mathbf{u} = \langle\mathbf{u}\rangle + \widetilde{\mathbf{u}}$, $p = \langle p\rangle + \widetilde{p}$. By using mean field theory, we have

$$\frac{\partial}{\partial t}\langle u_z\rangle + \frac{\partial}{\partial x}\langle\widetilde{u}_x\widetilde{u}_z\rangle = -\frac{1}{\rho}\frac{\partial}{\partial x}\langle\widetilde{b}_x\widetilde{p}\rangle. \tag{4.29}$$

$$\frac{\partial}{\partial t}\langle p\rangle + \frac{\partial}{\partial x}\langle\widetilde{u}_x\widetilde{p}\rangle = -\rho c_s^2\frac{\partial}{\partial x}\langle\widetilde{b}_x\widetilde{u}_z\rangle. \tag{4.30}$$

The right hand side (RHS) of Eq. 4.29 is the divergence of the kinetic stress (K) such that

$$-\frac{1}{\rho}\frac{\partial}{\partial x}\langle\widetilde{b}_x\widetilde{p}\rangle \equiv -\frac{\partial}{\partial x}K$$

The kinetic stress $K \equiv \langle\widetilde{b}_x\widetilde{p}\rangle/\rho$ is determined by the stochastic magnetic field and the turbulence, as pressure perturbation $\widetilde{p}$ is scattered by both the drift-wave turbulence and the stochastic field. However, since it is the coherence of $\widetilde{b}_x$ and $\widetilde{p}$ that determines K, we seek $\widetilde{p} = (\delta p/\delta b)\widetilde{b}$, while including turbulent scattering in $\delta p/\delta b$. Hence, the kinetic stress is derived by considering the $\widetilde{p}$ response to $\widetilde{b}_x$ that evolves in the presence of drift wave turbulence. Notice that both the Reynolds stress $\langle\widetilde{u}_x\widetilde{u}_z\rangle$ and Kinetic stress $\langle\widetilde{p}\widetilde{b}_r\rangle/\rho$ in Eq. 4.29 are affected by stochastic magnetic fields. Chen et al. [10] discussed magnetic stochasticity effects on Reynolds stress. Also, the RHS of Eq. 4.30 contains the *compressive energy flux* $H \equiv \rho c_s^2\langle\widetilde{b}_x\widetilde{u}_z\rangle$, such that

$$-\rho c_s^2\frac{\partial}{\partial x}\langle\widetilde{b}_x\widetilde{u}_z\rangle \equiv -\frac{\partial}{\partial x}H.$$

This compressive energy flux H describes the heat transport effect induced by compression along stochastic magnetic field lines. This effect contributes to the evolution of mean pressure.

We calculate the response of $\widetilde{p}$ and $\widetilde{u}_z$ to $\widetilde{b}_x$, so as to determine K and H. However, we do so *in the presence of scattering by drift-wave turbulence*. Hence, Eq. 4.27 and Eq. 4.28 yield

$$-i\omega\frac{\widetilde{p}}{\rho c_s}+c_s ik_z\widetilde{u}_z+\widetilde{u}_\perp\nabla_\perp\frac{\widetilde{p}}{\rho c_s}=-\widetilde{u}_x\frac{\partial}{\partial x}\frac{\langle p\rangle}{\rho c_s}-\widetilde{b}_x c_s\frac{\partial}{\partial x}\langle u_z\rangle, \tag{4.31}$$

$$-i\omega\widetilde{u}_z+c_s ik_z\frac{\widetilde{p}}{\rho c_s}+\widetilde{u}_\perp\nabla_\perp\widetilde{u}_z=-\widetilde{u}_x\frac{\partial}{\partial x}\langle u_z\rangle-\widetilde{b}_x c_s\frac{\partial}{\partial x}(\frac{\langle p\rangle}{\rho c_s}). \tag{4.32}$$

Note that the response to $\widetilde{u}_x$ on the RHS is not of interest since we take $\langle\widetilde{b}_x\widetilde{u}_x\rangle=0$, i.e. drift waves and stochastic field uncorrelated, for simplicity. By taking Eq. 4.32 $\pm$ Eq. 4.31, we define the Riemann variables $f_{\pm,k\omega}\equiv\widetilde{u}_{z,k\omega}\pm\widetilde{p}_{k\omega}/\rho c_s$ and obtain

$$(-i\omega\pm ic_s k_z+ik_\perp\widetilde{u}_\perp)f_{\pm,k\omega}=-\widetilde{b}_x c_s\big(\frac{\partial}{\partial x}\frac{\langle p\rangle}{\rho c_s}\pm\frac{\partial}{\partial x}\langle u_z\rangle\big). \tag{4.33}$$

This is the evolution equation for the Riemann response to magnetic perturbation $\widetilde{b}_x$. We compute the response of $\widetilde{u}_z$ and $\widetilde{p}$ to $\widetilde{b}_x$, which is *static*—i.e. no time dependence. And $\widetilde{u}_\perp$ is taken as stationary. Then, for $\omega\to 0$, we have:

$$(\pm ic_s k_z+ik_\perp\widetilde{u}_\perp)f_{\pm,k}=-\widetilde{b}_x c_s\big(\frac{\partial}{\partial x}\frac{\langle p\rangle}{\rho c_s}\pm\frac{\partial}{\partial x}\langle u_z\rangle\big). \tag{4.34}$$

Notice that the $\widetilde{u}_\perp\nabla_\perp$ operator in Eq. 4.31 and Eq. 4.32 can be expressed as a cumulant scattering effect on a timescale long, compared to the auto-correlation time of drift-wave turbulence τ_{ac}, i.e.

$$\langle\frac{i}{-c_s k_z\mp\widetilde{u}_\perp k_\perp}\rangle = \int d\tau e^{-ic_s k_z\tau}\langle e^{\mp i\widetilde{u}_\perp k_\perp\int d\tau'}\rangle \tag{4.35}$$

$$= \int d\tau e^{-ic_s k_z\tau}e^{-\underline{k}_i\underline{\underline{D}}_{ij,T}\underline{k}_j\tau}, \tag{4.36}$$

where $D_{ij,T} \equiv \sum_k \widetilde{u}_{i,k}\widetilde{u}_{j,k}\tau_{ac}$ is turbulent fluid diffusivity. For perpendicular transport ($i = j = x$ or y), we have $D_T \equiv \sum_k |\widetilde{u}_{\perp,k}|^2\tau_{ac}$, which generically is the order of the Gyro-Bohm diffusivity $D_{GB} \sim \rho_s^2 c_s/L_{n,\perp}$, as is ν_{turb}. Here, $L_{n,\perp}$ is density scale length. So, we can replace $\widetilde{u}_\perp\nabla_\perp$ with

$$\widetilde{u}_\perp\nabla_\perp \equiv -\underline{\nabla}_\perp \cdot \underline{\underline{D_T}} \cdot \underline{\nabla}_\perp. \tag{4.37}$$

Hence, Eq. 4.33 become

$$(\pm ic_s k_z + k_\perp^2 D_T) f_{\pm,k} = -\widetilde{b}_x c_s \big(\frac{\partial}{\partial x}\frac{\langle p\rangle}{\rho c_s} \pm \frac{\partial}{\partial x}\langle u_z\rangle\big). \tag{4.38}$$

From this equation, we have

$$\begin{aligned}\frac{\widetilde{p}_k}{\rho c_s} &= \frac{1}{2}(f_{+,k} - f_{-,k}) = \frac{-1}{k_\perp^4 D_T^2 + k_z^2 c_s^2}\times \\ &\left[\widetilde{b}_{x,k} c_s k_\perp^2 D_T \frac{\partial}{\partial x}\langle u_z\rangle - ik_z c_s^2 \widetilde{b}_{x,k}\frac{\partial}{\partial x}(\frac{\langle p\rangle}{\rho c_s})\right],\end{aligned} \tag{4.39}$$

$$\begin{aligned}\widetilde{u}_{z,k} &= \frac{1}{2}(f_{+,k} + f_{-,k}) = \frac{-1}{k_\perp^4 D_T^2 + k_z^2 c_s^2}\times \\ &\left[\widetilde{b}_{x,k} c_s k_\perp^2 D_T \frac{\partial}{\partial x}(\frac{\langle p\rangle}{\rho c_s}) - ik_z c_s^2 \widetilde{b}_{x,k}\frac{\partial}{\partial x}\langle u_z\rangle\right].\end{aligned} \tag{4.40}$$

Then, Eq. 4.39 and Eq. 4.40 yield

$$\begin{aligned}K = \frac{1}{\rho}\langle \widetilde{b}_x \widetilde{p}\rangle &= \frac{1}{\rho}\sum_{k_y,k_z} |\widetilde{b}_{x,k}|^2 \frac{-1}{k_\perp^4 D_T^2 + k_z^2 c_s^2} \\ &\left[\rho c_s^2 k_\perp^2 D_T \frac{\partial}{\partial x}\langle u_z\rangle - ik_z c_s^2 \frac{\partial}{\partial x}\langle p\rangle\right].\end{aligned} \tag{4.41}$$

$$\begin{aligned}H \equiv \rho c_s^2\langle \widetilde{b}_x \widetilde{u}_z\rangle &= \rho c_s^2 \sum_{k_y,k_z} |\widetilde{b}_{x,k}|^2 \frac{-1}{k_\perp^4 D_T^2 + k_z^2 c_s^2} \\ &\left[k_\perp^2 D_T \frac{\partial}{\partial x}\frac{\langle p\rangle}{\rho} - ik_z c_s^2 \frac{\partial}{\partial x}\langle u_z\rangle\right],\end{aligned} \tag{4.42}$$

The first term at the denominator of the response function $1/(k_\perp^4 D_T^2 + k_z^2 c_s^2)$ can be approximated as $(k_\perp^2 D_T)^2 \simeq 1/\tau_{c,k}^2$, where τ_c is the decorrelation time due to perpendicular turbulent scattering. The significance of the factor of i in the second term of the source will be apparent when considering reduction to the quasilinear limit (see Sec. 4.7). Non-zero correlations $\langle \widetilde{b}_x \widetilde{u}_z \rangle$ and $\langle \widetilde{b}_x \widetilde{p} \rangle$, which contribute the kinetic stress K and compressive energy flux H, are due to the synergetic effect of the perpendicular turbulent mixing ($k_\perp^2 D_T$) and stochastic magnetic field ($|\widetilde{b}_x|^2$) scattering, via gradients of mean parallel flow $\partial_x \langle u_z \rangle$ and mean pressure $\partial_x \langle p \rangle$. Also, by observing the denominator of the responses, one can notice that K and H can be set by different mechanisms. When $k_\perp^2 D_T > k_z c_s$, the decorrelation due to scattering is stronger than that due to acoustic signal decoherence. For $k_z c_s > k_\perp^2 D_T$, we recover the quasilinear results. These two regimes will be discussed further in Sec. 4.6 and Sec. 4.7.

4.5 Calculating the flux

In the following Sec. 4.5, 4.6, and 4.7, we consider the effect of magnetic shear in presence of stochastic fields. We'll calculate the kinetic stress and compressive energy flux in detail. Sheared magnetic field geometry is used to clarify aspects of the competition between acoustic pulse decorrelation at rate $k_z c_s$ and turbulent scattering, with rate $k_\perp^2 D_T$, and its implication for the structure of the fluxes. Attention here is focused on the interplay of different terms in the expressions for K and H.

The second term in the denominator of the response function in Eq. 4.41 and Eq. 4.42 can be approximated as $k_z^2 c_s^2 = (k_y x/L_s)^2 c_s^2$, where L_s the is magnetic shear length such that $1/L_s = q' r_0/q^2 R_0$, $q' \equiv dq/dx$, q is the safety factor, and x is the *distance from the resonant surface of the perturbation*—i.e. $x = r - r_{m,n}$, where m, n are the poloidal and toroidal mode

numbers, respectively. We decompose Eq. 4.41 into two parts

$$\begin{aligned}\langle \widetilde{b}_x \widetilde{p} \rangle = & \underbrace{\sum_{k_y,k_z} |\widetilde{b}_{x,k}|^2 \frac{\tau_{c,k}}{1+(k_y x/L_s)^2 c_s^2 \tau_{c,k}^2} \left(-\rho c_s^2 \frac{\partial}{\partial x} \langle u_z \rangle \right)}_{\text{ⓐ}} \\ & + \underbrace{\sum_{k_y,k_z} |\widetilde{b}_{x,k}|^2 \frac{1}{(k_\perp^2 D_T)^2 + k_z^2 c_s^2} \left(i k_z c_s^2 \frac{\partial}{\partial x} \langle p \rangle \right)}_{\text{ⓑ}}.\end{aligned} \tag{4.43}$$

The spectral sum relevant to this shear effect is $\sum_{k_y,k_z}$. The radial structure is accounted for by a box function $F(x/w_k)$ for the magnetic perturbation intensity, which we further analyze in the following paragraph. We approximate the discrete summation $\sum_{k_y k_z}$ by a continuous integral:

$$\sum_{k_y k_z} = \sum_{m,n} = \int dm \int dn. \tag{4.44}$$

By using $n = m/q$ and $dn = |m| q' dx/q^2$, we have

$$\int dm \int dn = \int dm \int dx \frac{|m|}{q^2} q' = r_0 \int dk_y \int dx \frac{|k_y|}{q} \hat{s}, \tag{4.45}$$

where $\hat{s}$ is the magnetic shear, i.e. $\hat{s} = \frac{r_0}{q}\frac{dq}{dr}$. Now, we write the magnetic perturbation spectrum $|\widetilde{b}_{x,k}|^2$ as

$$|\widetilde{b}_{x,k}|^2 = C S(k_y) F(x/w_k),$$

where C is a normalization constant, $S(k_y)$ is the k-spectrum of $\widetilde{b}_x$, $F(x/w_k)$ is the spatial spectrum form factor, and w_k is the spatial width of $|\widetilde{b}_{x,k}|^2$ (see figure 4.3) . We assume $|\widetilde{b}_{x,k}|^2$ perturbations are densely packed and take the spatial spectrum $F(x/w_k)$ to be a normalized box function such that $\int dx F(x/w_k) = 1$. Hereafter, we define the intensity of magnetic perturbation

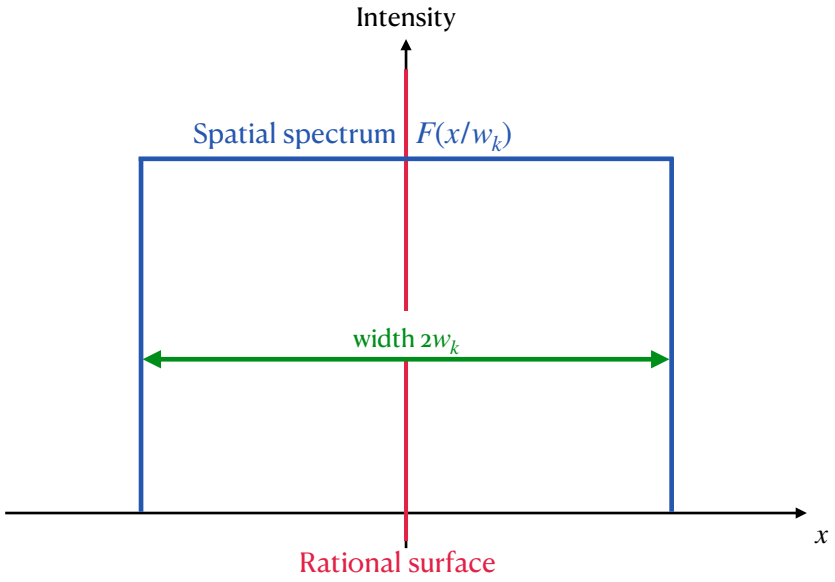

Figure 4.3. $F(x/w_k)$ is spatial spectrum for $|\widetilde{b}_{x,k}|^2$ in radial direction. Here we define $x = r - r_{m,n}$, where $r_{m,n}$ is the location of a rational surface with mode number m, n.

$b^2_{x,0}$ as

$$\begin{aligned} b^2_{x,0} \equiv \sum_{k_y k_z} |\widetilde{b}_{x,k}|^2 &= r_0 \int dk_y \int dx \frac{k_y \hat{s}}{q} \cdot CS(k_y) F(x/w_k) \\ &= C \int dk_y \frac{k_y r_0^2 q'}{q^2} S(k_y) \underbrace{\int dx F(x/w_k)}_{=1} \\ &= C \int dk_y \frac{k_y r_0^2 q'}{q^2} S(k_y). \end{aligned} \tag{4.46}$$

The normalization constant C hence is defined as

$$C \equiv \frac{b^2_{x,0}}{\int dk_y \frac{k_y r_0^2 q'}{q^2} S(k_y)} \tag{4.47}$$

where $m/r_0 \equiv k_y$, R_0 and r_0 are the major and minor radius, respectively. The first term in

equation (4.43) becomes

$$
\begin{aligned}
\text{ⓐ} &= \sum_{k_y k_z} |\widetilde{b}_{x,k}|^2 \frac{\tau_{c,k}}{1+(k_y x/L_s)^2 c_s^2 \tau_{c,k}^2}\left(-\rho c_s^2 \frac{\partial}{\partial x}\langle u_z\rangle\right) \\
&= \underbrace{C\int dk_y \frac{k_y r_0^2 q'}{q^2} S(k_y) \int dx F(x/w_k)}_{\sum_{k_y k_z} |\widetilde{b}_{x,k}|^2} \cdot \\
&\quad \frac{\tau_{c,k}}{1+(k_y x/L_s)^2 c_s^2 \tau_{c,k}^2}\left(-\rho c_s^2 \frac{\partial}{\partial x}\langle u_z\rangle\right)
\end{aligned}
\tag{4.48}
$$

The response function $1/1+(k_y x/L_s c_s \tau_{c,k})^2$ in the equation is the key to understanding the physics of pressure evolution. We define the **acoustic width** (x_s) by

$$
x_s \equiv \frac{L_s}{k_y c_s \tau_{c,k}}, \tag{4.49}
$$

The acoustic width is the value of x for which $k_z c_s(x) = 1/\tau_{c,k}(x)$, where $k_z = k_z(x)$. So, $x_s = L_s/k_y c_s \tau_{c,k}$. Loosely speaking, x_s defines the location where the rate of parallel acoustic streaming equals the decorrelation rate. Here x_s is analogous to the familiar $x_i = \omega L_s/k_y v_{th,i}$—the ion Landau resonance point, where $v_{th,ix}$ is the ion thermal speed [1]. The $\tau_{c,k}$ sets the acoustic width—e.g. in strong fluid turbulence (small τ_c), x_s is large; in weak fluid turbulence, x_s is small. Hence, the first term of Eq. 4.43 becomes

$$
\begin{aligned}
\text{ⓐ} = C\int dk_y \frac{k_y r_0^2 q'}{q^2} S(k_y) \int dx F(x/w_k) \cdot \\
\frac{\tau_{c,k}}{1+(x/x_s)^2}\left(-\rho c_s^2 \frac{\partial}{\partial x}\langle u_z\rangle\right)
\end{aligned}
\tag{4.50}
$$

For strong turbulence, $\tau_{c,k}$ is small such that $x_s \gg w_k$. So w_k is the cutoff length in the integral (see Figure 4.4, green curve). For weak turbulence (i.e. $x_s \ll w_k$), however, the acoustic width x_s is the cutoff length scale (see Figure 4.4, red curve). Let's consider these two limits.

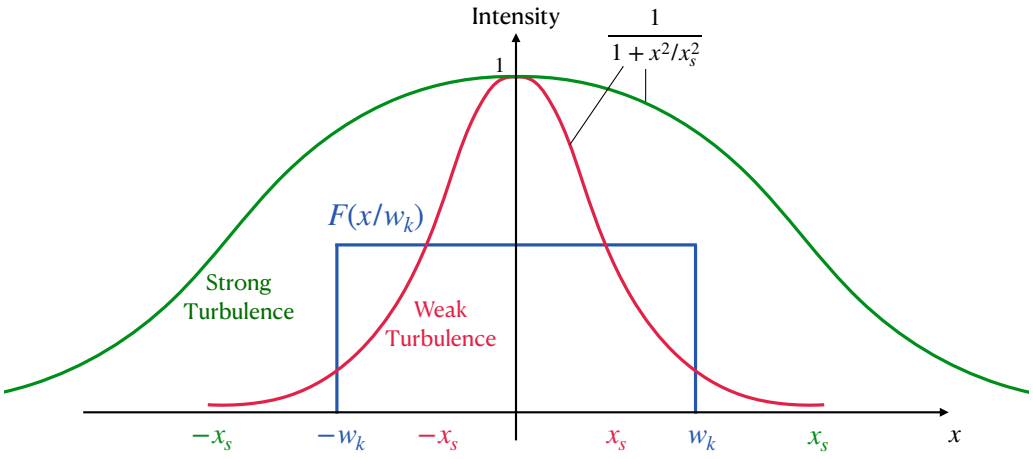

Figure 4.4. The integral of spatial spectrum of stochastic field and the response function $\int dx F(x/w_k)\cdot[1/1+(x/x_s)^2]$. Green and red lines indicate response functions in strong and weak turbulence regime, respectively. For strong turbulence ($x_s \gg w_k$), w_k is the cutoff length in the integral. For weak turbulence ($x_s \ll w_k$), x_s is the cutoff length scale.

4.6 Strong Turbulence

In strong fluid turbulence, we have $x_s \gg w_k$ (or $k_\perp^2 D_T > k_z c_s$). Recall in Eq. 4.43, $\langle \widetilde{b}_x \widetilde{p}\rangle = ⓐ + ⓑ$. Here, the integral $\int d(x)\frac{F(x/w_k)}{1+\cancel{x^2/x_s^2}} \simeq 1$. So, the first term in equation (4.50) becomes

$$\begin{aligned} ⓐ &= \sum_{k_y k_z} |\widetilde{b}_{x,k}|^2 \frac{\tau_{c,k}}{1+(k_y x/L_s)^2 c_s^2 \tau_{c,k}^2}\left(-\rho c_s^2 \frac{\partial}{\partial x}\langle u_z\rangle\right) \\ &\simeq -\rho c_s^2 \sum_{k_y k_z} |\widetilde{b}_{x,k}|^2 \tau_{c,k} \frac{\partial}{\partial x}\langle u_z\rangle \end{aligned} \tag{4.51}$$

The second term in equation (4.50), assuming $k_\perp^4 D_T^2 \gg k_z^2 c_s^2$, becomes small

$$ⓑ = \sum_{k_y k_z} |\widetilde{b}_{x,k}|^2 \frac{1}{(k_\perp^2 D_T)^2 + k_z^2 c_s^2}\left(ik_z c_s^2 \frac{\partial}{\partial x}\langle p\rangle\right) \to 0, \tag{4.52}$$

in the limit $k_\perp^4 D_T^2 \gg k_z^2 c_s^2$. Derivation details can be found in Appendix I. Hence, the kinetic stress can be simplified to

$$\langle \widetilde{b}_x \widetilde{p} \rangle \simeq -\rho c_s^2 \sum_{k_y k_z} |\widetilde{b}_{x,k}|^2 \tau_{c,k} \frac{\partial}{\partial x} \langle u_z \rangle. \tag{4.53}$$

This indicates that *in the presence of strong scattering, the kinetic stress depends on the electrostatic* $\tau_{c,k}$. The kinetic stress hence becomes simply:

$$K \equiv \frac{1}{\rho} \langle \widetilde{b}_x \widetilde{p} \rangle \simeq -\sum_{k_y k_z} |\widetilde{b}_{x,k}|^2 \tau_{c,k} c_s^2 \frac{\partial}{\partial x} \langle u_z \rangle \tag{4.54}$$

From this, we recover a *hybrid viscosity* produced by stochastic magnetic fields $|\widetilde{b}_{x,k}|^2 c_s^2$, with a correlation time set by electrostatic scattering $\tau_{c,k}$. Hence,

$$\begin{aligned} D_{st}(x) &\equiv \frac{b_{x,0}^2 \int dk_y \frac{k_y r_0^2 q'}{q^2} \tau_{c,k} S(k_y) c_s^2}{\int dk_y \frac{k_y r_0^2 q'}{q^2} S(k_y)} \\ &\simeq \sum_{k_y k_z} |\widetilde{b}_{x,k}|^2 (x) \frac{c_s^2}{k_\perp^2 D_T} \end{aligned} \tag{4.55}$$

Eq. 4.55 leads us to notice that the combined effects of stochastic fields in the numerator and (electrostatic) turbulent scattering in the denominator *together* define D_{st}. This hybrid turbulent viscosity is the actual diffusivity that describes how the mean flow is scattered by stochastic magnetic fields. The parallel flow evolution equation then becomes

$$\frac{\partial}{\partial t} \langle u_z \rangle = -\frac{\partial}{\partial x} \langle \widetilde{u}_x \widetilde{u}_z \rangle + \frac{\partial}{\partial x} D_{st}(x) \frac{\partial}{\partial x} \langle u_z \rangle. \tag{4.56}$$

This indicate that the turbulent viscous stress balances $\widetilde{b}_x \partial_x \langle u_z \rangle$.

Similarly, Eq. 4.42 gives the compressive energy flux (H)

$$\begin{aligned} H(x) &\equiv \rho c_s^2 \langle \widetilde{b}_x \widetilde{u}_z \rangle \\ &\simeq -c_s^2 \sum_{k_y k_z} |\widetilde{b}_{x,k}|^2 \tau_{c,k} \frac{\partial}{\partial x} \langle p \rangle \simeq -D_{st}(x) \frac{\partial}{\partial x} \langle p \rangle. \end{aligned} \tag{4.57}$$

This indicates that *the tilting of the magnetic field lines in presence of the pressure gradient (i.e.* $\widetilde{b}_x \partial \langle p \rangle / \partial x \neq 0$*) balances with the turbulent diffusion*. Notice that Eq. 4.57 also shows that $D_T \nabla_\perp^2 \widetilde{u}_z \simeq -\sum_{k_y k_z} \widetilde{b}_{x,k} \partial_x (\langle p \rangle / \rho)$. This again indicates that the *change in mean pressure* ($\partial_x \langle p \rangle / \rho$) *due to the stochastic fields is balanced by turbulent mixing of parallel flow* ($\nabla_\perp^2 \widetilde{u}_z$, see Figure 4.2). The pressure equation now can be written as

$$\frac{\partial}{\partial t} \langle p \rangle = -\frac{\partial}{\partial x} \langle \widetilde{u}_x \widetilde{p} \rangle + \frac{\partial}{\partial x} D_{st}(x) \frac{\partial}{\partial x} \langle p \rangle, \tag{4.58}$$

again a diffusion equation.

4.7 Weak Turbulence

For weak fluid turbulence, we have $w_k \gg x_s$ (or $k_z c_s > k_\perp^2 D_T$). Recall Eq. 4.50)

$$\begin{aligned} \text{ⓐ} = & C \int dk_y \frac{k_y r_0^2 q'}{q^2} S(k_y) \int dx F(x/w_k) \cdot \\ & \frac{\tau_{c,k}}{1 + (x/x_s)^2} \cdot \left(-\rho c_s^2 \frac{\partial}{\partial x} \langle u_z \rangle \right) \end{aligned} \tag{4.59}$$

Since in the weak turbulence limit, the cutoff of integral is set by x_s and hence $F(x/w_k) \simeq F(x_s/w_k \to 0)$. So, ⓐ is simplified as follows:

$$\begin{aligned}
\text{ⓐ} &\simeq \frac{b_{x,0}^2 \cancel{\int dk_y \frac{k_y r_0^2 q'}{q^2} S(k_y)}}{\cancel{\int dk_y \frac{k_y r_0^2 q'}{q^2} S(k_y)}} \cdot \tau_{c,k} \frac{x_s}{w_k} F(0) \cdot \\
&\underbrace{\int_0^{x=x_s} d(x/x_s) \frac{1}{1+(x/x_s)^2}}_{=arctan(x_s/x_s)=\pi/4} \left(-\rho c_s^2 \frac{\partial}{\partial x} \langle u_z \rangle \right) \\
&\simeq -b_{x,0}^2 \tau_{d,k} \frac{x_s}{w_k} F(0) \frac{\pi}{4} \left(\rho c_s^2 \frac{\partial}{\partial x} \langle u_z \rangle \right)
\end{aligned} \tag{4.60}$$

where $\tau_{d,k} \equiv L_s/k_y c_s w_k$ is dispersal timescale of an acoustic wave packet propagating along the stochastic magnetic field. This dispersal timescale $\tau_{d,k}$ defines the width of the acoustic signal 'cone'. The second term in equation (4.50) becomes

$$\begin{aligned}
\text{ⓑ} &= \sum_{k_y k_z} |\widetilde{b}_{x,k}|^2 \frac{1}{\cancel{(k_\perp^2 D_T)^2} + k_z^2 c_s^2} \left(i k_z c_s^2 \frac{\partial}{\partial x} \langle p \rangle \right) \\
&\simeq -D_M \frac{\partial}{\partial x} \langle p \rangle,
\end{aligned} \tag{4.61}$$

where $D_M(x) \equiv \sum_{k_y k_z} |\widetilde{b}_{x,k}|^2 \tau_{d,k}(x) c_s$ is the magnetic diffusivity. Hence, the kinetic stress flux is

$$\langle \widetilde{b}_x \widetilde{p} \rangle = -b_{x,0}^2 \tau_{d,k} F(0) \frac{\pi}{4} \rho c_s^2 \frac{\partial}{\partial x} \langle u_z \rangle - D_M \frac{\partial}{\partial x} \langle p \rangle. \tag{4.62}$$

The first term on the RHS is asymptotically small, so ⓐ $\to 0$ for $x_s/w_k \to 0$ in this limit. The detailed calculation is shown in Appendix II. Notice that Eq. B.13 also shows that $\nabla_z \widetilde{p} \simeq -\sum_k \widetilde{b}_{x,k} \partial_x \langle p \rangle$, by approximating $1/\tau_{d,k} c_s$ with operator ∇_z. This indicates that the *change in mean pressure ($\partial_x \langle p \rangle$) due to the stochastic fields is balanced by a parallel pressure gradient*

($\nabla_z \widetilde{p}$, see Figure 4.2). The kinetic stress in this limit can be simplified as

$$K(x) \equiv \frac{1}{\rho}\langle \widetilde{b}_x \widetilde{p} \rangle \simeq -\frac{1}{\rho} D_M(x) \frac{\partial}{\partial x}\langle p \rangle. \tag{4.63}$$

Hence, we have the parallel flow evolution

$$\frac{\partial}{\partial t}\langle u_z \rangle \simeq -\frac{\partial}{\partial x}\langle \widetilde{u}_x \widetilde{u}_z \rangle + \frac{\partial}{\partial x}\frac{D_M(x)}{\rho}\frac{\partial}{\partial x}\langle p \rangle. \tag{4.64}$$

Similarly, we have the compressive energy flux

$$H(x) = \rho c_s^2 \langle \widetilde{b}_x \widetilde{u}_z \rangle = -\rho c_s^2 D_M(x) \frac{\partial}{\partial x}\langle u_z \rangle. \tag{4.65}$$

Notice that this equation shows the response of mean parallel flow, due to stochastic field tilting ($\widetilde{b}_x \partial \langle u_z \rangle / \partial x$), is balanced by the parallel flow compression ($\nabla_\parallel \widetilde{u}_z$), i.e. equivalent to $\underline{B_z} \cdot \underline{\nabla} u_z = 0$ or $\nabla_\parallel \widetilde{u}_z = -\widetilde{b}_x \partial \langle u_z \rangle / \partial x$. Hence the pressure equation can be written as

$$\frac{\partial}{\partial t}\langle p \rangle = -\frac{\partial}{\partial x}\langle \widetilde{u}_x \widetilde{p} \rangle + \frac{\partial}{\partial x}\rho c_s^2 D_M(x)\frac{\partial}{\partial x}\langle u_z \rangle. \tag{4.66}$$

Eq. 4.63 and Eq. 4.65 indicate that for weak scattering, momentum and energy transport occur only through stochastic fields, with the familiar transport coefficient $c_s D_M$. There is no dependence on D_T for $k_\perp^2 D_T \ll k_z c_s$. This result is equivalent to that in FGC [28]. Note, however, that the key effect for $\langle u_z \rangle$ is residual stress; and for $\langle p \rangle$, it is an off-diagonal flux. The comparison of K and H in strong and weak turbulence regime is shown in Table 4.1.

4.8 Summary for parallel momentum and ion heat transport

In this Chapter (all the work are presented in Chen et al. (2022)[8]), we develop the theory of ion heat and parallel momentum transport due to stochastic magnetic fields and

Table 4.1. A comparison of strong and weak turbulent MHD for Kinetic stress and compressive energy flux.

	Weak Turbulence	Strong Turbulence
Kinetic Stress $K \equiv \langle \widetilde{b}_x \widetilde{p} \rangle / \rho$	$K = -D_{st} \frac{\partial}{\partial x} \langle u_z \rangle$	$K = -D_M \frac{\partial}{\partial x} \langle p \rangle$
Compressive energy flux $H \equiv \rho c_s^2 \langle \widetilde{b}_x \widetilde{u}_z \rangle$	$H = -D_{st} \frac{\partial}{\partial x} \langle p \rangle$	$H = -\rho c_s^2 D_M \frac{\partial}{\partial x} \langle u_z \rangle$

turbulence. We focus on the kinetic stress (K) and the compressional flux (H) due to stochastic fields in the presence of (electrostatic) turbulence. The responses $\delta p/\delta b$ and $\delta u_{\|}/\delta b$ are calculated by integration over *perturbed* particle trajectories and then used to close the fluxes. Interestingly, this analysis renders moot one of the deepest questions in stochastic-field-induced transport. Recall that Rechester and Rosenbluth [77] showed that irreversibility requires some means to scatter particles off magnetic field lines, lest they bounce back and undergo no net excursion. Here, ambient cross-field electrostatic scattering supplies this needed effect. Thus, $\delta p/\delta b$ and $\delta u_{\|}/\delta b$ should be viewed as statistically averaged nonlinear responses. Here, we posit an ambient ensemble of drift waves, which specifies $\langle \widetilde{u}_{\perp}^2 \rangle$. The probability distribution functions (PDFs) of $\langle \widetilde{u}_{\perp}^2 \rangle$ and $\langle \widetilde{b}_x^2 \rangle$ are assumed to be quasi-Gaussian and independent. General results are obtained and shown to recover the dynamic balance limit (viscous dissipation vs. $\widetilde{b}_x \partial \langle p \rangle / \partial x$, for $k_{\perp}^2 D_T > k_z c_s$) and the parallel pressure balance limit ($\nabla_z \widetilde{p}$ vs. $\widetilde{b}_x \partial \langle p \rangle / \partial x$, for $k_z c_s > k_{\perp}^2 D_T$), as appropriate. In reality, dynamic balance is the relevant case, and the quasilinear regime is of very limited practical interest. We calculate the explicit form of the turbulent viscous flux and compressive energy flux, and show both are diffusive with a hybrid diffusivity $D_{st} \equiv \sum_k |\widetilde{b}_{x,k}^2| c_s^2 / k_{\perp}^2 D_T$—i.e. determined by magnetic fluctuations but with correlation time set by turbulent scattering. The hybrid diffusivity D_{st} is sensitive to the long wavelength content of $|\widetilde{b}_k^2|$. The analysis is extended to the case of a sheared mean magnetic field. We show that the critical comparison is between the $|\widetilde{b}|^2$ spatial spectral width (w_k) and the acoustic width, i.e.

$x_s = L_s/k_y c_s \tau_{c,k}$, where $\tau_{c,k}$ is decorrelation time due to perpendicular turbulent scattering.

This Chapter [8] relatively untouched issues, namely the interaction of stochastic magnetic field and turbulence, and how they together drive transport. As such several of the results merit further discussion. First, while the analysis is in the spirit of a resonance broadening calculation, the basic *form* of the flux-gradient relation charges with the ratio of $k_z c_s$ to $k_\perp^2 D_T$. Indeed, the kinetic stress changes from a residual stress to a turbulence viscous stress. Also, given that $k_\perp^2 D_T \simeq \omega \gg k_z c_s$, the strong turbulence regime results are surely the relevant ones, and it is unlikely that the pure quasilinear predictions are ever observed. This point is the major *prediction* of this paper. This outcome is in contrast to the case for the quasilinear predictions for electromagnetic turbulence [71], which are more robust since ω, not $k_z c_s$, is the relevant base rate there. Second, the sensitivity of the hybrid diffusivity $D_{st} \equiv \sum_k |\widetilde{b}_{x,k}^2| c_s^2/k_\perp^2 D_T$ to long wavelength (i.e. 'slow modes') is interesting and reminiscent of the results of Taylor and McNamara [94]. Further study, including coupling to $E \times B$ shearing, is needed.

4.9 Future works

Several questions and extensions for further study naturally suggest themselves. Magnetic drifts could be included in theory, which could then be used to study the effect of stochastic magnetic fields and turbulence upon geodesic acoustic modes (GAMs) [98, 41, 59, 63, 104]. This topic is of obvious relevance to edge turbulence and transitions. Second, we have assumed throughout the magnetic perturbations and electrostatic turbulence are uncorrelated, i.e. $\langle \widetilde{b}_x \widetilde{\phi} \rangle = 0$. Recent results, however, indicate that the constraint of $\nabla \cdot J = 0$ naturally forces the generation of small scale convective cells by the interaction of long wavelength flows with turbulence. As a consequence, $\langle \widetilde{b}_x \widetilde{\phi} \rangle \neq 0$ develops, indicative of small-scale correlations between turbulence and stochastic fields. These may induce novel cross-coupling in the fluxes. Work on this question is ongoing. Finally, since the system studied here essentially is one of gas dynamics in a stochastic field, we note it may have relevance to problems in cosmic ray acceleration and propagation

[56]. In those problems, magnetic irregularities are thought to be scatter particles in turbulent environments—similar to the physics discussed in this paper.

Chapter 4, in full, is a reprint of the material as it appears in Chang-Chun Chen, Patrick H. Diamond, and Steven M. Tobias, *Plasma Physics and Controlled Fusion* 64, 015006 (2022). The dissertation author was the primary investigator and author of this paper.

Chapter 5

Summary and Future Work

5.1 Summary

This dissertation is about momentum and heat transport in presence of small-scale disordered/irregular magnetic fields. It focuses particularly on turbulent momentum transport influenced by disordered magnetic fields, which may be found in the interstellar/intergalactic medium, the solar tachocline, and at the edge of fusion devices. Tachocline stochastic fields are thought to from due to the occur from 'pumping' by the convective zone in the solar tachocline, while in fusion devices, resonant magnetic perturbations (RMPs) are imposed to control the edge localized modes (ELMs). Such ELMs produce high transient heat loads and damage wall components of a fusion device. Thus, the RMP is as developed to mitigate them.

In the study of the solar tachocline [9], I studied stochastic magnetic-field effects on momentum transport in β-plane magnetohydrodynamics (MHD) turbulence at high magnetic Reynolds number and low Prandtl number. Simulation results showed that Reynolds stress and momentum transport are suppressed by stochastic fields at a mean-field intensity lower than that required for a fully Alvénized system at which fluid and magnetic energy reach near equipartition. By developing an effective 'mean-field theory' for this high magnetic perturbation regime, I obtained an explicit form for the PV flux suppression due to stochastic magnetic fields, and hence—via the Taylor identity— the Reynolds stress suppression. This result explained that the Reynolds stress (or flow generation) suppression is due to disordered magnetic fields in the

relevant case of a relatively weak mean-field intensity. I also found that the dispersion relation can be rewritten in a form that represents the dissipation and drag from stochastic fields. These "dissipation" and "drag" effects suggest that stochastic fields form an effective resisto-elastic network, in which Alfvén wave dynamics evolves. They also suggest that turbulent momentum transport in the tachocline is suppressed by the enhanced memory of stochastically induced elasticity (i.e. the random elastic network) and drag. A critical dimensionless parameter which pinpoints at which intensity of mean field the growth of zonal flow ceases is obtained. These results suggest that turbulent momentum transport in the tachocline is suppressed by the enhanced memory of stochastically induced elasticity. This leaves no viscous or mixing mechanism to oppose 'burrowing' of the tachocline due to meridional cells driven by baroclinic torque. This finding suggests that the Spiegel & Zahn (1992) [91] scenario of burrowing opposed by latitudinal viscous diffusion and the Gough & McIntyre (1998) [31] suggestion of that PV mixing opposed burrowing *both fail*. Finally, by process of elimination, the enhanced memory-induced suppression of momentum transport allows the Gough & McIntyre (1998) [31] suggestion that a residual fossil field in the radiation zone is what ultimately limits tachocline burrowing.

Further, I asked how stochastic fields affect strongly magnetized 3D turbulence? Experiments in fusion devices showed that Reynolds stress bursts—which may lead to the L-H transition suppression—drop when RMPs are applied at the edge of DIII-D in pre-L-H transition stage. Experiments also found that an increase in the L-H power threshold occurs in fusion devices. In my second paper [10], we shed light on these two phenomena and addressed the more general question of the physics of Reynolds stress decoherence by stochastic fields. This decoherence requires stochastic-field-induced broadening to exceed the natural turbulence linewidth. By considering the effect of the "shear-eddy tilting feedback loop" for self-generation of shear flows in presence of stochastic fields, I found that stochastic fields at or beyond the critical magnitude can break this feedback loop, since then the phase correlation in Reynolds stress is no longer set by flow shear, but rather by the mean-squre stochastic field $\langle \widetilde{B}^2 \rangle$, which is not related to the tilting. This explains the strong suppression of poloidal Reynolds stress at

the edge of a tokamak with RMPs in DIII-D. Note that the Alfvén speed follows from charge balance, which determines Reynolds stress. A natural threshold condition for Reynolds stress decoherence emerges as $k_\perp^2 v_A D_M/\Delta\omega > 1$. Finally, a *critical parameter* $\alpha \equiv b^2 q/\rho_*^2\sqrt{\beta\varepsilon}$ for the increment in L-H power threshold was calculated—the stochastic magnetic field raises the power thresholds linearly in proportional to the mean-square value of normalized stochastic field intensity.

My third project [8] explored relatively untouched issues—the interaction of stochastic magnetic fields and turbulent flow, and how they together drive transport in MHD turbulence. I studied the transport of ion heat and parallel momentum via the pressure and parallel flow responses to stochastic fields in strong/weak turbulence regimes. Regimes are separated by a critical comparison between the mean-squre stochastic field $|\widetilde{b}|^2$ spatial spectral width (w_k) and the acoustic width, i.e. $x_s = L_s/k_y c_s \tau_{c,k}$, where $\tau_{c,k}$ is decorrelation time due to perpendicular turbulent scattering. I found in a strong turbulent regime (i.e. turbulent viscosity dissipation rate larger than other rates), the turbulent viscosity will dissipate the parallel flow perturbation, in response to the pressure excess. I explicitly derived that the transport mechanism is dominated by a *hybrid turbulent diffusivity*, which contains a stochastic magnetic scattering term and a turbulent fluid scattering term. While in a weak turbulence regime, a pressure gradient builds up along the mean field line in response to a pressure excess. The momentum and energy transport occur only through magnetic fields in this regime, with the familiar transport coefficient $C_s D_M$, where C_s is the sound speed and D_M is the magnetic diffusivity. Results of this paper are amenable to testing via computer simulations. Such studies would necessarily be non-trivial, as they require simulation of turbulence in stochastic fields. Studies might compare the kinetic stress and compressive energy flux calculated directly from the simulation to the predictions made here. Turbulence intensity could be scanned by varying the deviation from marginality. In this way, one should be able to pass smoothly from the weak turbulence/quasilinear regime ($k_\perp^2 D_T \ll k_z c_s$) to the strong turbulence/nonlinear regime ($k_\perp^2 D_T \gg k_z c_s$), and evaluate scaling trends in both limits.

In general terms, we see that 42 years after the influential paper by Rechester and Rosenbluth [77] the physics of plasma dynamics in a stochastic magnetic field remains theoretically challenging and vital to both astrophysical and magnetic fusion energy (MFE) plasma physics. Transport in a state of coexisting turbulence and stochastic magnetic field is a topic of intense interest. Overall, this dissertation summarizes my PhD works focus on the turbulent momentum transport in 2D/quasi-2D MHD in presence of highly disordered magnetic fields. In these three journal articles, I discussed aspects of momentum transport, heat transport, and zonal flow generation in two systems with low effective Rossby number, where dynamics evolve in the presence of a stochastic magnetic field. I proposed an analytical model based on a renormalized mean-field theory—a theory well beyond the quasi-linear theory—to approach this daunting non-linear problem. I derived critical parameters for the zonal flow suppression [9], for the power threshold increment in L-H transition [10], and the hybrid turbulent diffusivity [8]. These have not been stated explicitly before.

5.2 Future Work

Chen & Diamond [9] suggests a novel model of transport and mixing in 2D MHD turbulence derived from considering the coupling of turbulent hydrodynamic motion to a fractal elastic network [7, 76, 74, 75, 58, 3]. Both the network connectivity and the elasticity of the network elements can be distributed statistically and can be intermittent and multiscale. These would introduce a packing fractional factor to Ck in the cross-phaase, i.e., $\langle \widetilde{B}^2 \rangle \to p\langle \widetilde{B}^2$ in C_k, where $0 < p < 1$ are the probabilities of sites. This admittedly crude representation resembles that of the mean field limit for "fractons" [2]. Somewhat more sophisticated might be the form $\langle \widetilde{B}^2 \rangle \to (p - p_c)^{\gamma} \langle \widetilde{B} \rangle^{2\varepsilon}$, where p_c iss the magnetic activity percolation threshold, and γ, ε are scaling exponent to be determine [92]. We also speculate that the back- reaction (at high Rm) of the small-scale magnetic field on the fluid dynamics may ultimately depend heavily on whether or not the field is above the packing "percolation threshold" for long-range Alfvén wave

propagation. Such a long-range propagation would induce a radiative damping of fluid energy by Alfvénic propagation through the stochastic network.

From Chen et al. (2022) [8] Several questions and extensions for further study naturally suggest themselves. Magnetic drifts could be included in theory, which could then be used to study the effect of stochastic magnetic fields and turbulence upon geodesic acoustic modes (GAMs) [98, 41, 59, 57, 63, 104]. This topic is of obvious relevance to edge turbulence and transitions. Second, we have assumed throughout the magnetic perturbations and electrostatic turbulence are uncorrelated, i.e. $\langle \widetilde{b}_x \widetilde{\phi} \rangle = 0$. Recent results, however, indicate that the constraint of $\nabla \cdot J = 0$ naturally forces the generation of small scale convective cells by the interaction of long wavelength flows with turbulence. As a consequence, a non-zero $\langle \widetilde{b}_x \widetilde{\phi} \rangle$ develops, indicative of small- scale correlations between turbulence and stochastic fields. These may induce novel cross-coupling in the fluxes. Work on this question is ongoing. Finally, since the system studied here essentially is one of gas dynamics in a stochastic field, we note it may have relevance to problems in cosmic ray acceleration and propagation (cite). In those problems, magnetic irregularities are thought to be scatter particles in turbulent environments—similar to the physics discussed in this paper [8].

A project currently in preparation is to study stochastic field effect in a β-plane partially ionized MHD (PIMHD) system. Examples can be found in Jupiter-like gas giant planet atmospheres, which are characterized by two regions—the outer neutral envelop and the fully ionized interior, or in the tail of heliosphere where solar wind and interstellar medium (ISM) interact. This transition from neutral to fully ionized regime happens continuously as a function of radius. In this transition region, physics are depicted by PIMHD which contains neutral and charged flows interaction. Compared with studies in β-plane MHD, this two-fluid interaction yields a nonlinear ambipolar diffusion in the induction equation, and a Lorentz drag in the equation of motion for neutral particles. Methods and ideas from momentum transport studies can be also applied to the interstellar/intergalactic plasma. In the future, I would be interested in studying the effects of perturbed/irregular magnetic fields on cosmic ray hydrodynamics and cosmic ray

transport, or other related problems.

Another project in preparation is the shear layer and staircase formation in a stochastic magnetic field. This staircase is analogous to the "salinity staircases" observed in oceanography. The staircase-like structure of particle density and pressure (or density/pressure corrugation) will form a "barrier" that prevents momentum transport and hence quenches the turbulence at the edge of fusion devices. I will study the spatial scale of the layer and how resilient this barrier is in the presence of a prescribed stochastic field. This study can be started using a turbulence mixing length that involves two scales—the forcing scale and the Rhines scale. A preliminary calculation suggests a large magnetic Kubo number is required for significant change in mean field-turbulence coupling. For cases where the magnetic Kubo number is small, this result indicates the staircase is *resilient*.

Chapter 5, in full, is currently being prepared for submission for publication of the material. Chang-Chun Chen & Patrick H. Diamond (2022). The dissertation author was the primary investigator and author of this material.

Appendix A

I Collective Random Magnetic Fields

We check the validity of the assumption for ignoring changes in random fields on the small, stochastic scales (lst) due to Rossby wave straining, after applying the random-field average method. Here we turn off the mean field (i.e. $B = 0$) and consider random fields only ($B_{\rm tot} = 0 + \widetilde{B} + B_{\rm st}$). Since the Rossby wave may perturb the small-scale random field, we can write the total magnetic field as

$$B_{\rm tot} = B_{\rm st} + \widetilde{B}, \tag{A.1}$$

where $B_{\rm tot}$ is the total random field including effect of the Rossby turbulence, $B_{\rm st}$ is stochastic fields, and $\widetilde{B}$ is the change of the magnetic field induced by $B_{\rm st}$. Also, we define the linear response of collective fields ($\delta\overline{B_{\rm tot}}$) and of the random fields ($\delta\overline{B_{\rm st}}$) has relation

$$\frac{\delta\overline{B_{\rm tot}}}{\overline{B_{\rm tot}}} = \frac{\delta\overline{B_{\rm st}}}{\widetilde{B}}. \tag{A.2}$$

Note that collective fields $\overline{B_{tot}}$ are at Rossby-wave scale (k_{Rossby}) after applying the **random-field average method**. Combining Eq. A.1 and A.2, we have

$$B_{tot} \equiv B_{st} + \frac{\delta B_{st}}{\delta\overline{B_{tot}}}\overline{B_{tot}}. \tag{A.3}$$

Since the magnetic field is dominated by random fields, the average total field is small ($\overline{B_{tot}} \to 0$), rendering the second term of RHS in Eq. A.3 small. Eq. A.3 indicates that the collective field at Rossby-scale ($\overline{B_{tot}}$) is not large enough to alter the structure of the random fields ($\widetilde{B} \to 0$). Thus, we can approximate the total magnetic field as the small-scale stochastic field $\overline{B_{tot}} \sim \overline{B_{st}}$. This suggests that the perturbation of the Rossby wave has a minor influence on random fields. So, the averaged magnetic stress tensor remains unchanged:

$$\overline{B_{tot}^2} = \overline{(B_{st} + \frac{\delta B_{st}}{\delta \overline{B_{tot}}} \overline{B_{tot}})^2} \simeq \overline{B_{st}^2}. \tag{A.4}$$

This indicates that the random field energy is fixed under the influence of the Rossby turbulence, as described by the random-field average method. Thus, one can simplify the calculation by ignoring the perturbation of random fields $\widetilde{B}$.

Appendix B

I Strong Turbulence Limit

In strong fluid turbulence, we have $x_s > w_k$ (or $k_\perp^2 D_T > k_\| c_s$)—w_k sets a cut-off for the integral $\int dx$. The first term in Eq. 4.43 becomes

$$\begin{aligned} ⓐ &= \sum_{k_y k_z} |\widetilde{b}_{x,k}|^2 \frac{\tau_{c,k}}{1+(k_y x/L_s)^2 c_s^2 \tau_{c,k}^2} \left(-\rho c_s^2 \frac{\partial}{\partial x} \langle u_z \rangle \right) \\ &= -C \int dk_y \frac{k_y r_0^2 q'}{q^2} \tau_{c,k} S(k_y) \cdot \int_0^{x=w_k} dx \frac{F(x/w_k)}{1+(x/x_s)^2} \left(\rho c_s^2 \frac{\partial}{\partial x} \langle u_z \rangle \right) \end{aligned} \tag{B.1}$$

We ignore the $(x/x_s)^2$ in the denominator for that in the integration of step function $F(x/w_k)$, the $1/(1+x^2/x_s^2) \to 1$ (see Figure 4.4). Hence, in this limit, we obtain

$$\int_0^{x=w_k} dx \frac{F(x/w_k)}{1+(x/x_s)^2} \simeq \int_0^{x=w_k} dx F(x/w_k) = 1. \tag{B.2}$$

Hence, we have

$$
\begin{aligned}
ⓐ &= C\int dk_y \frac{k_y r_0^2 q'}{q^2}\tau_{c,k}S(k_y)\cdot\left(-\rho c_s^2\frac{\partial}{\partial x}\langle u_z\rangle\right)\\
&= \frac{b_{x,0}^2 \cancel{\int dk_y \frac{k_y r_0^2 q'}{q^2}S(k_y)}\tau_{c,k}}{\cancel{\int dk_y \frac{k_y r_0^2 q'}{q^2}S(k_y)}}\left(-\rho c_s^2\frac{\partial}{\partial x}\langle u_z\rangle\right)\\
&= -\rho c_s^2\sum_{k_y k_z}|\widetilde{b}_{x,k}|^2\tau_{c,k}\frac{\partial}{\partial x}\langle u_z\rangle
\end{aligned}
\tag{B.3}
$$

Also, the second term in Eq. 4.43 becomes

$$
\begin{aligned}
ⓑ &= \sum_{k_y k_z}|\widetilde{b}_{x,k}|^2\frac{1}{(k_\perp^2 D_T)^2+k_z^2c_s^2}\left(ik_z c_s^2\frac{\partial}{\partial x}\langle p\rangle\right)\\
&= -i\sum_{k_y k_z}\frac{|\widetilde{b}_{x,k}|^2}{k_z}(-1+\frac{k_\perp^4 D_T^4}{k_\perp^4 D_T^4+k_z^2c_s^2})\left(\frac{\partial}{\partial x}\langle p\rangle\right),
\end{aligned}
\tag{B.4}
$$

In this limit, we have $k_\perp^2 D_T \gg k_z^2 c_s^2$ such that

$$
-1+\frac{k_\perp^4 D_T^4}{k_\perp^4 D_T^4+\cancel{k_z^2c_s^2}}\simeq 0. \tag{B.5}
$$

Hence, the second term can be approximated as ⓑ $\simeq 0$, and $\langle\widetilde{b}_x\widetilde{p}\rangle$ can be simplified to

$$
\langle\widetilde{b}_x\widetilde{p}\rangle \simeq -\rho c_s^2\sum_{k_y k_z}|\widetilde{b}_{x,k}|^2\tau_{c,k}\frac{\partial}{\partial x}\langle u_z\rangle. \tag{B.6}
$$

II Weak Turbulence Limit

In weak fluid turbulence, we have $w_k \gg x_s$ (or $k_\| c_s > k_\perp^2 D_T$). The integral in equation (4.50) becomes

$$\begin{aligned}
ⓐ &= \sum_{k_y k_z} |\widetilde{b}_{x,k}|^2 \frac{\tau_{c,k}}{1+(k_y x/L_s)^2 c_s^2 \tau_{c,k}^2}\left(-\rho c_s^2 \frac{\partial}{\partial x}\langle u_z\rangle\right) \\
&= -C\int dk_y \frac{k_y r_0^2 q'}{q^2} S(k_y) \int dx F(x/w_k) \frac{\tau_{c,k}}{1+(x/x_s)^2}\cdot\left(\rho c_s^2 \frac{\partial}{\partial x}\langle u_z\rangle\right) \\
&\simeq -\frac{b_{x,0}^2 \cancel{\int dk_y \frac{k_y r_0^2 q'}{q^2} S(k_y)}}{\cancel{\int dk_y \frac{k_y r_0^2 q'}{q^2} S(k_y)}} \cdot \tau_{c,k}\frac{x_s}{w_k} F(0) \cdot \underbrace{\int_0^{x=x_s} \frac{d(x/x_s)}{1+(x/x_s)^2}}_{=arctan(x_s/x_s)=\pi/4} \cdot\left(\rho c_s^2 \frac{\partial}{\partial x}\langle u_z\rangle\right)
\end{aligned} \tag{B.7}$$

where $\arctan(x_s/x_s) = \arctan(1) = \pi/4$ and $\tau_{d,k} \simeq L_s/k_y c_s w_k$ is dispersal timescale of acoustic packet propagating along stochastic magnetic field. Hence,

$$ⓐ \simeq -b_{x,0}^2 \tau_{d,k}\left(\frac{x_s}{w_k}\right) F(0)\frac{\pi}{4}\left(\rho c_s^2 \frac{\partial}{\partial x}\langle u_z\rangle\right). \tag{B.8}$$

Note that this term scales $\propto x_s/w_k$, which is asymptotically small as $x_s/w_k \to 0$. Then ⓐ $\to 0$, so the first term is negligible. The second term in equation (4.50) becomes

$$\begin{aligned}
ⓑ &= \sum_{k_y k_z} |\widetilde{b}_{x,k}|^2 \frac{1}{(k_\perp^2 D_T)^2 + k_z^2 c_s^2}\left(ik_z c_s^2 \frac{\partial}{\partial x}\langle p\rangle\right) \\
&= \sum_{k_y k_z} |\widetilde{b}_{x,k}|^2 \frac{-i}{k_z}\Big(-1 + \underbrace{\frac{(k_\perp^2 D_T)^2}{(k_\perp^2 D_T)^2 + k_z^2 c_s^2}}_{=0}\Big)\Big(\frac{\partial}{\partial x}\langle p\rangle\Big),
\end{aligned} \tag{B.9}$$

where the response term is approximated as i/k_z, since in this limit turbulent scattering is weak—i.e. $k_\perp^2 D_T \to 0$. So, we obtain

$$\begin{aligned} ⓑ &= \sum_{k_y k_z} |\widetilde{b}_{x,k}|^2 \frac{1}{(k_\perp^2 D_T)^2 + k_z^2 c_s^2} \left(i k_z c_s^2 \frac{\partial}{\partial x} \langle p \rangle \right) \\ &\simeq \sum_{k_y k_z} |\widetilde{b}_{x,k}|^2 \frac{i}{k_z} \frac{\partial}{\partial x} \langle p \rangle. \end{aligned} \tag{B.10}$$

Here, $\sum\limits_{k_z} i/k_z$ can be approximate as

$$\begin{aligned} \sum_{k_z} \frac{i}{k_z - i\delta} &= \sum_{k_z} iPV \left[\frac{1}{k_z} \right] - \pi \delta(k_z) \\ &= 0 - \pi \delta(k_z), \end{aligned} \tag{B.11}$$

where PV is Cauchy principle value and $\pi\delta(k_z c_s)$ as $\tau_{d,k}$. So, we have

$$\begin{aligned} ⓑ &\simeq - \sum_{k_y k_z} |\widetilde{b}_{x,k}|^2 \pi \delta(k_z) \frac{\partial}{\partial x} \langle p \rangle \\ &\simeq - D_M \frac{\partial}{\partial x} \langle p \rangle, \end{aligned} \tag{B.12}$$

where D_M is the magnetic diffusivity. Hence, the kinetic stress flux is

$$\langle \widetilde{b}_x \widetilde{p} \rangle = - b_{x,0}^2 \tau_{d,k} F(0) \frac{\pi}{4} \rho c_s^2 \frac{\partial}{\partial x} \langle u_z \rangle - D_M \frac{\partial}{\partial x} \langle p \rangle. \tag{B.13}$$

The first term on RHS is approximate ⓐ $\simeq 0$ for $F(0) \simeq 0$ in this limit. So, we obtain .

$$\langle \widetilde{b}_x \widetilde{p} \rangle = - D_M \frac{\partial}{\partial x} \langle p \rangle \tag{B.14}$$

in this limit.

Bibliography

[1] 61 - on the vibrations of the electronic plasma. In D. TER HAAR, editor, *Collected Papers of L.D. Landau*, pages 445–460. Pergamon, 1965.

[2] Shlomo Alexander and Raymond Orbach. Density of states on fractals:≪fractons≫. *Journal de Physique Lettres*, 43(17):625–631, 1982.

[3] JA Ashraff and BW Southern. Density of states and dynamic scaling on the vicsek snowflake fractal. *Journal of Physics A: Mathematical and General*, 21(10):2431, 1988.

[4] Armstrong R. C. Bird, R. B. and O. Hassager. Dynamics of polymeric liquids. volume i : Fluid mechanics. *AIChE Journal*, 34(6):1052–1053, 1987.

[5] D. Biskamp and H. Welter. Dynamics of decaying two-dimensional magnetohydrodynamic turbulence. *Physics of Fluids B*, 1(10):1964–1979, Oct 1989.

[6] Stanislav Boldyrev, Don Huynh, and Vladimir Pariev. Analog of astrophysical magnetorotational instability in a Couette-Taylor flow of polymer fluids. *Physical Review E*, 80(6):066310, Dec 2009.

[7] S. R. Broadbent and J. M. Hammersley. Percolation processes: I. crystals and mazes. *Mathematical Proceedings of the Cambridge Philosophical Society*, 53(3):629–641, 1957.

[8] Chang-Chun Chen, P H Diamond, and S M Tobias. Ion heat and parallel momentum transport by stochastic magnetic fields and turbulence. *Plasma Physics and Controlled Fusion*, 64(1):015006, dec 2021.

[9] Chang-Chun Chen and Patrick H. Diamond. Potential vorticity mixing in a tangled magnetic field. *The Astrophysical Journal*, 892(1):24, mar 2020.

[10] Chang-Chun Chen, Patrick H. Diamond, Rameswar Singh, and Steven M. Tobias. Potential vorticity transport in weakly and strongly magnetized plasmas. *Physics of Plasmas*, 28(4):042301, 2021.

[11] Boris V Chirikov. A universal instability of many-dimensional oscillator systems. *Physics Reports*, 52(5):263–379, 1979.

[12] Jørgen Christensen-Dalsgaard and Michael J. Thompson. *Observational results and issues concerning the tachocline*, pages 53–86. Cambridge University Press, 2007.

[13] Navid C. Constantinou and Jeffrey B. Parker. Magnetic Suppression of Zonal Flows on a Beta Plane. *Astrophysical Journal*, 863(1):46, Aug 2018.

[14] Pierre-Gilles De Gennes. On a relation between percolation theory and the elasticity of gels. *Journal de Physique Lettres*, 37(1):1–2, 1976.

[15] P. H. Diamond, S.-I. Itoh, K. Itoh, and T. S. Hahm. TOPICAL REVIEW: Zonal flows in plasma a review. *Plasma Physics and Controlled Fusion*, 47:35–+, May 2005.

[16] P H Diamond, S-I Itoh, K Itoh, and T S Hahm. Zonal flows in plasma—a review. *Plasma Physics and Controlled Fusion*, 47(5):R35–R161, apr 2005.

[17] Patrick H. Diamond, Sanae-I. Itoh, Kimitaka Itoh, and Lara J. Silvers. *β-Plane MHD turbulence and dissipation in the solar tachocline*, pages 213–240. Cambridge University Press, 2007.

[18] Patrick H Diamond, Y Kosuga, ÖD Gürcan, CJ McDevitt, TS Hahm, N Fedorczak, JE Rice, WX Wang, S Ku, JM Kwon, et al. An overview of intrinsic torque and momentum transport bifurcations in toroidal plasmas. *Nuclear Fusion*, 53(10):104019, 2013.

[19] P.H. Diamond, Y. Kosuga, Ö.D. Gürcan, C.J. McDevitt, T.S. Hahm, N. Fedorczak, J.E. Rice, W.X. Wang, S. Ku, J.M. Kwon, G. Dif-Pradalier, J. Abiteboul, L. Wang, W.H. Ko, Y.J. Shi, K. Ida, W. Solomon, H. Jhang, S.S. Kim, S. Yi, S.H. Ko, Y. Sarazin, R. Singh, and C.S. Chang. An overview of intrinsic torque and momentum transport bifurcations in toroidal plasmas. *Nuclear Fusion*, 53(10):104019, sep 2013.

[20] PH Diamond, Y-M Liang, BA Carreras, and PW Terry. Self-regulating shear flow turbulence: A paradigm for the l to h transition. *Physical review letters*, 72(16):2565, 1994.

[21] W. X. Ding, D. L. Brower, D. Craig, B. E. Chapman, D. Ennis, G. Fiksel, S. Gangadhara, D. J. Den Hartog, V. V. Mirnov, S. C. Prager, J. S. Sarff, V. Svidzinski, P. W. Terry, and T. Yates. Stochastic magnetic field driven charge transport and zonal flow during magnetic reconnection. *Physics of Plasmas*, 15(5):055901, 2008.

[22] W. X. Ding, L. Lin, D. L. Brower, A. F. Almagri, B. E. Chapman, G. Fiksel, D. J. Den Hartog, and J. S. Sarff. Kinetic stress and intrinsic flow in a toroidal plasma. *Phys. Rev. Lett.*, 110:065008, Feb 2013.

[23] T Estrada, C Hidalgo, T Happel, and PH Diamond. Spatiotemporal structure of the interaction between turbulence and flows at the lh transition in a toroidal plasma. *Physical review letters*, 107(24):245004, 2011.

[24] T. E. Evans, R. A. Moyer, P. R. Thomas, J. G. Watkins, T. H. Osborne, J. A. Boedo, E. J. Doyle, M. E. Fenstermacher, K. H. Finken, R. J. Groebner, M. Groth, J. H. Harris, R. J. La Haye, C. J. Lasnier, S. Masuzaki, N. Ohyabu, D. G. Pretty, T. L. Rhodes, H. Reimerdes, D. L. Rudakov, M. J. Schaffer, G. Wang, and L. Zeng. Suppression of large edge-localized

modes in high-confinement diii-d plasmas with a stochastic magnetic boundary. *Phys. Rev. Lett.*, 92:235003, Jun 2004.

[25] T.E. Evans, M.E. Fenstermacher, R.A. Moyer, T.H. Osborne, J.G. Watkins, P. Gohil, I. Joseph, M.J. Schaffer, L.R. Baylor, M. Bécoulet, J.A. Boedo, K.H. Burrell, J.S. deGrassie, K.H. Finken, T. Jernigan, M.W. Jakubowski, C.J. Lasnier, M. Lehnen, A.W. Leonard, J. Lonnroth, E. Nardon, V. Parail, O. Schmitz, B. Unterberg, and W.P. West. RMP ELM suppression in DIII-d plasmas with ITER similar shapes and collisionalities. *Nuclear Fusion*, 48(2):024002, jan 2008.

[26] T.E Evans, R.A Moyer, J.G Watkins, T.H Osborne, P.R Thomas, M Becoulet, J.A Boedo, E.J Doyle, M.E Fenstermacher, K.H Finken, R.J Groebner, M Groth, J.H Harris, G.L Jackson, R.J. La Haye, C.J Lasnier, S Masuzaki, N Ohyabu, D.G Pretty, H Reimerdes, T.L Rhodes, D.L Rudakov, M.J Schaffer, M.R Wade, G Wang, W.P West, and L Zeng. Suppression of large edge localized modes with edge resonant magnetic fields in high confinement DIII-d plasmas. *Nuclear Fusion*, 45(7):595–607, jun 2005.

[27] Todd E Evans, Richard A Moyer, Keith H Burrell, Max E Fenstermacher, Ilon Joseph, Anthony W Leonard, Thomas H Osborne, Gary D Porter, Michael J Schaffer, Philip B Snyder, et al. Edge stability and transport control with resonant magnetic perturbations in collisionless tokamak plasmas. *nature physics*, 2(6):419–423, 2006.

[28] John M Finn, Parvez N Guzdar, and Alexander A Chernikov. Particle transport and rotation damping due to stochastic magnetic field lines. *Physics of Fluids B: Plasma Physics*, 4(5):1152–1155, 1992.

[29] David Fyfe and David Montgomery. High-beta turbulence in two-dimensional magnetohydrodynamics. *Journal of Plasma Physics*, 16(2):181–191, 1976.

[30] P. Gohil, T.E. Evans, M.E. Fenstermacher, J.R. Ferron, T.H. Osborne, J.M. Park, O. Schmitz, J.T. Scoville, and E.A. Unterberg. L–h transition studies on DIII-d to determine h-mode access for operational scenarios in ITER. *Nuclear Fusion*, 51(10):103020, aug 2011.

[31] D. O. Gough and M. E. McIntyre. Inevitability of a magnetic field in the Sun's radiative interior. *Nature*, 394:755–757, August 1998.

[32] A. V. Gruzinov and P. H. Diamond. Nonlinear mean field electrodynamics of turbulent dynamos. *Physics of Plasmas*, 3(5):1853–1857, 1996.

[33] Ö D Gürcan and P H Diamond. Zonal flows and pattern formation. *Journal of Physics A: Mathematical and Theoretical*, 48(29):293001, jul 2015.

[34] Akira Hasegawa and Kunioki Mima. Pseudo-three-dimensional turbulence in magnetized nonuniform plasma. *The Physics of Fluids*, 21(1):87–92, 1978.

[35] K Ida and T Fujita. Internal transport barrier in tokamak and helical plasmas. *Plasma Physics and Controlled Fusion*, 60(3):033001, jan 2018.

[36] K. Ida, N. Ohyabu, T. Morisaki, Y. Nagayama, S. Inagaki, K. Itoh, Y. Liang, K. Narihara, A. Yu. Kostrioukov, B. J. Peterson, K. Tanaka, T. Tokuzawa, K. Kawahata, H. Suzuki, and A. Komori. Observation of plasma flow at the magnetic island in the large helical device. *Phys. Rev. Lett.*, 88:015002, Dec 2001.

[37] K. Ida, M. Yoshinuma, K. Nagaoka, M. Osakabe, S. Morita, M. Goto, M. Yokoyama, H. Funaba, S. Murakami, K. Ikeda, H. Nakano, K. Tsumori, Y. Takeiri, and O. Kaneko and. Spontaneous toroidal rotation driven by the off-diagonal term of momentum and heat transport in the plasma with the ion internal transport barrier in LHD. *Nuclear Fusion*, 50(6):064007, may 2010.

[38] K. Ida, M. Yoshinuma, H. Tsuchiya, T. Kobayashi, C. Suzuki, M. Yokoyama, A. Shimizu, K. Nagaoka, S. Inagaki, and K. Itoh. Erratum: Flow damping due to stochastization of the magnetic field. *Nature Communications*, 6:6531, March 2015.

[39] Y. In, J.-K. Park, Y.M. Jeon, J. Kim, G.Y. Park, J.-W. Ahn, A. Loarte, W.H. Ko, H.H. Lee, J.W. Yoo, J.W. Juhn, S.W. Yoon, and H. Park and. Enhanced understanding of non-axisymmetric intrinsic and controlled field impacts in tokamaks. *Nuclear Fusion*, 57(11):116054, aug 2017.

[40] P. S. Iroshnikov. Turbulence of a Conducting Fluid in a Strong Magnetic Field. *Soviet Astronomy*, 7:566–+, February 1964.

[41] K Itoh, K Hallatschek, and S-I Itoh. Excitation of geodesic acoustic mode in toroidal plasmas. *Plasma Physics and Controlled Fusion*, 47(3):451–458, feb 2005.

[42] E Joffrin, C.D Challis, G.D Conway, X Garbet, A Gude, S Günter, N.C Hawkes, T.C Hender, D.F Howell, G.T.A Huysmans, E Lazzaro, P Maget, M Marachek, A.G Peeters, S.D Pinches, S.E Sharapov, and JET-EFDA contributors. Internal transport barrier triggering by rational magnetic flux surfaces in tokamaks. *Nuclear Fusion*, 43(10):1167–1174, sep 2003.

[43] I. Joseph, T.E. Evans, A.M. Runov, M.E. Fenstermacher, M. Groth, S.V. Kasilov, C.J. Lasnier, R.A. Moyer, G.D. Porter, M.J. Schaffer, R. Schneider, and J.G. Watkins. Calculation of stochastic thermal transport due to resonant magnetic perturbations in DIII-d. *Nuclear Fusion*, 48(4):045009, mar 2008.

[44] B. B. Kadomtsev and O. P. Pogutse. Electron heat conductivity of the plasma across a 'braided' magnetic field. In *Plasma Physics and Controlled Nuclear Fusion Research 1978, Volume 1*, volume 1, pages 649–662, Jan 1979.

[45] Y Kaspi, E Galanti, William B Hubbard, DJ Stevenson, SJ Bolton, L Iess, T Guillot, J Bloxham, JEP Connerney, H Cao, et al. Jupiter's atmospheric jet streams extend thousands of kilometres deep. *Nature*, 555(7695):223–226, 2018.

[46] S.M. Kaye, R. Maingi, D. Battaglia, R.E. Bell, C.S. Chang, J. Hosea, H. Kugel, B.P. LeBlanc, H. Meyer, G.Y. Park, and J.R. Wilson. L–h threshold studies in NSTX. *Nuclear Fusion*, 51(11):113019, oct 2011.

[47] Eun-jin Kim and PH Diamond. Mean shear flows, zonal flows, and generalized kelvin–helmholtz modes in drift wave turbulence: A minimal model for l→ h transition. *Physics of Plasmas*, 10(5):1698–1704, 2003.

[48] Andrei Nikolaevitch Kolmogorov. Entropy per unit time as a metric invariant of automorphisms. In *Dokl. Akad. Nauk SSSR*, volume 124, pages 754–755, 1959.

[49] R. H. Kraichnan. Inertial Range Spectrum of Hydromagnetic Turbulence. *Physics of Fluids*, 8:1385–1387, July 1965.

[50] D. M. Kriete, G. R. McKee, L. Schmitz, D. R. Smith, Z. Yan, L. A. Morton, and R. J. Fonck. Effect of magnetic perturbations on turbulence-flow dynamics at the l-h transition on diii-d. *Physics of Plasmas*, 27(6):062507, 2020.

[51] David Kriete, George McKee, Lothar Schmitz, Raymond Fonck, David Smith, and Zheng Yan. Effect of radial magnetic perturbations on turbulence-flow dynamics at the L-H transition on DIII-D. In *APS Division of Plasma Physics Meeting Abstracts*, volume 2019 of *APS Meeting Abstracts*, page BI2.00003, Oct 2019.

[52] Ryogo Kubo. Stochastic liouville equations. *Journal of Mathematical Physics*, 4(2):174–183, 1963.

[53] Lev Davidovich Landau and E. M. Lifshitz. *Fluid mechanics*. 1959.

[54] A.W. Leonard, A.M. Howald, A.W. Hyatt, T. Shoji, T. Fujita, M. Miura, N. Suzuki, and S. Tsuji and. Effects of applied error fields on the h-mode power threshold of JFT-2m. *Nuclear Fusion*, 31(8):1511–1518, aug 1991.

[55] Nicolas Leprovost and Eun-jin Kim. Effect of rossby and alfvén waves on the dynamics of the tachocline. *The Astrophysical Journal*, 654(2):1166, 2007.

[56] MA Malkov and PH Diamond. Nonlinear dynamics of acoustic instability in a cosmic ray shock precursor and its impact on particle acceleration. *The Astrophysical Journal*, 692(2):1571, 2009.

[57] M.A. Malkov and P.H. Diamond. Weak hysteresis in a simplified model of the lh transition. *Physics of Plasmas*, 16(1):012504, 2009.

[58] Benoit B Mandelbrot and James A Given. Physical properties of a new fractal model of percolation clusters. *Physical review letters*, 52(21):1853, 1984.

[59] A V Melnikov, V A Vershkov, L G Eliseev, S A Grashin, A V Gudozhnik, L I Krupnik, S E Lysenko, V A Mavrin, S V Perfilov, D A Shelukhin, S V Soldatov, M V Ufimtsev, A O Urazbaev, G Van Oost, and L G Zimeleva. Investigation of geodesic acoustic mode oscillations in the t-10 tokamak. *Plasma Physics and Controlled Fusion*, 48(4):S87–S110, mar 2006.

[60] Leon Mestel. *Stellar magnetism*, volume 410. Cambridge University Press, 1999.

[61] Mark S. Miesch. Numerical modeling of the solar tachocline. i. freely evolving stratified turbulence in a thin rotating spherical shell. *The Astrophysical Journal*, 562(2):1058–1075, dec 2001.

[62] Mark S. Miesch. Numerical modeling of the solar tachocline. II. forced turbulence with imposed shear. *The Astrophysical Journal*, 586(1):663–684, mar 2003.

[63] K. Miki and P. H. Diamond. Role of the geodesic acoustic mode shearing feedback loop in transport bifurcations and turbulence spreading. *Physics of Plasmas*, 17(3):032309, 2010.

[64] S Mordijck, T L Rhodes, L Zeng, E J Doyle, L Schmitz, C Chrystal, T J Strait, and R A Moyer. Effects of resonant magnetic perturbations on turbulence and transport in DIII-d l-mode plasmas. *Plasma Physics and Controlled Fusion*, 58(1):014003, oct 2015.

[65] Tsuneyoshi Nakayama, Kousuke Yakubo, and Raymond L Orbach. Dynamical properties of fractal networks: Scaling, numerical simulations, and physical realizations. *Reviews of modern physics*, 66(2):381, 1994.

[66] T. F. Neiser, F. Jenko, T. A. Carter, L. Schmitz, D. Told, G. Merlo, A. Bañón Navarro, P. C. Crandall, G. R. McKee, and Z. Yan. Gyrokinetic gene simulations of diii-d near-edge l-mode plasmas. *Physics of Plasmas*, 26(9):092510, Sep 2019.

[67] Gordon I. Ogilvie and Michael R. E. Proctor. On the relation between viscoelastic and magnetohydrodynamic flows and their instabilities. *Journal of Fluid Mechanics*, 476:389–409, Feb 2003.

[68] Yoshiaki Ohtani, Kenji Tanaka, Hiroe Igami, Katsumi Ida, Yasuhiro Suzuki, Yuki Takemura, Hayato Tsuchiya, Mike Sanders, Mikirou Yoshinuma, Tokihiko Tokuzawa, Ichihiro Yamada, Ryo Yasuhara, Hisamichi Funaba, Mamoru Shoji, Takahiro Bando, and LHD Experimental Group. Effects of core stochastization on particle and momentum transport. *Nuclear Fusion*, 61(3):034002, feb 2021.

[69] James G Oldroyd. On the formulation of rheological equations of state. *Proceedings of the Royal Society of London. Series A. Mathematical and Physical Sciences*, 200(1063):523–541, 1950.

[70] JG Oldroyd. The motion of an elastico-viscous liquid contained between coaxial cylinders. i. *The Quarterly Journal of Mechanics and Applied Mathematics*, 4(3):271–282, 1951.

[71] Shuitao Peng, Lu Wang, and Yuan Pan. Intrinsic parallel rotation drive by electromagnetic ion temperature gradient turbulence. *Nuclear Fusion*, 57(3):036003, dec 2016.

[72] Henri Poincare. *Chapitre premier: Théorème de helmholtz*, pages 3–29. Cours de physique mathematique. G. Carre, Paris, 1893.

[73] KR Rajagopal and RK Bhatnagar. Exact solutions for some simple flows of an oldroyd-b fluid. *Acta Mechanica*, 113(1-4):233–239, 1995.

[74] R Rammal. Nature of eigenstates on fractal structures. *Physical Review B*, 28(8):4871, 1983.

[75] Rammal Rammal. Spectrum of harmonic excitations on fractals. *Journal de Physique*, 45(2):191–206, 1984.

[76] Rammal Rammal and Gérard Toulouse. Random walks on fractal structures and percolation clusters. *Journal de Physique Lettres*, 44(1):13–22, 1983.

[77] A. B. Rechester and M. N. Rosenbluth. Electron heat transport in a tokamak with destroyed magnetic surfaces. *Phys. Rev. Lett.*, 40:38–41, Jan 1978.

[78] A. B. Rechester and M. N. Rosenbluth. Electron heat transport in a tokamak with destroyed magnetic surfaces. *Phys. Rev. Lett.*, 40:38–41, Jan 1978.

[79] Peter B. Rhines. Waves and turbulence on a beta-plane. *Journal of Fluid Mechanics*, 69(3):417–443, 1975.

[80] J.E Rice, P.T Bonoli, J.A Goetz, M.J Greenwald, I.H Hutchinson, E.S Marmar, M Porkolab, S.M Wolfe, S.J Wukitch, and C.S Chang. Central impurity toroidal rotation in ICRF heated alcator c-mod plasmas. *Nuclear Fusion*, 39(9):1175–1186, sep 1999.

[81] J.E Rice, W.D Lee, E.S Marmar, P.T Bonoli, R.S Granetz, M.J Greenwald, A.E Hubbard, I.H Hutchinson, J.H Irby, Y Lin, D Mossessian, J.A Snipes, S.M Wolfe, and S.J Wukitch. Observations of anomalous momentum transport in alcator c-mod plasmas with no momentum input. *Nuclear Fusion*, 44(3):379–386, feb 2004.

[82] M.N. Rosenbluth, R.Z. Sagdeev, J.B. Taylor, and G.M. Zaslavski. Destruction of magnetic surfaces by magnetic field irregularities. *Nuclear Fusion*, 6(4):297–300, dec 1966.

[83] Carl-Gustaf Rossby. Relation between variations in the intensity of the zonal circulation of the atmosphere and the displacements of the semi-permanent centers of action. *J. Mar. Res.*, 2:38–55, 1939.

[84] F. Ryter, S.K. Rathgeber, L. Barrera Orte, M. Bernert, G.D. Conway, R. Fischer, T. Happel, B. Kurzan, R.M. McDermott, A. Scarabosio, W. Suttrop, E. Viezzer, M. Willensdorfer, and E. Wolfrum and. Survey of the h-mode power threshold and transition physics studies in ASDEX upgrade. *Nuclear Fusion*, 53(11):113003, sep 2013.

[85] R Scannell, A Kirk, M Carr, J Hawke, S S Henderson, T O'Gorman, A Patel, A Shaw, and A Thornton and. Impact of resonant magnetic perturbations on the l-h transition on MAST. *Plasma Physics and Controlled Fusion*, 57(7):075013, jun 2015.

[86] L. Schmitz, D.M. Kriete, R.S. Wilcox, T.L. Rhodes, L. Zeng, Z. Yan, G.R. McKee, T.E. Evans, C. Paz-Soldan, P. Gohil, B. Lyons, C.C. Petty, D. Orlov, and A. Marinoni. L–h transition trigger physics in ITER-similar plasmas with applied n = 3 magnetic perturbations. *Nuclear Fusion*, 59(12):126010, sep 2019.

[87] O. Schmitz, T. E. Evans, M. E. Fenstermacher, E. A. Unterberg, M. E. Austin, B. D. Bray, N. H. Brooks, H. Frerichs, M. Groth, M. W. Jakubowski, C. J. Lasnier, M. Lehnen, A. W. Leonard, S. Mordijck, R. A. Moyer, T. H. Osborne, D. Reiter, U. Samm, M. J. Schaffer, B. Unterberg, and W. P. West. Resonant pedestal pressure reduction induced by a thermal transport enhancement due to stochastic magnetic boundary layers in high temperature plasmas. *Phys. Rev. Lett.*, 103:165005, Oct 2009.

[88] KELLY SERVICK. Brain parasite may strip away rodents' fear of predators—not just of cats. *Nature News*, 2020.

[89] Yakov G Sinai. On the notion of entropy of a dynamical system. In *Doklady of Russian Academy of Sciences*, volume 124, pages 768–771, 1959.

[90] A. S. Skal and B. I. Shklovskii. Influence of the impurity concentration on the hopping conduction in semiconductors. *Semiconductors*, 7(8):1058–1061, 1 1974.

[91] E. A. Spiegel and J.-P. Zahn. The solar tachocline. *Astronomy and Astrophysics*, 265:106–114, November 1992.

[92] H Eugene Stanley. Cluster shapes at the percolation threshold: and effective cluster dimensionality and its connection with critical-point exponents. *Journal of Physics A: Mathematical and General*, 10(11):L211, 1977.

[93] Geoffrey Ingram Taylor. I. eddy motion in the atmosphere. *Philosophical Transactions of the Royal Society of London. Series A, Containing Papers of a Mathematical or Physical Character*, 215(523-537):1–26, 1915.

[94] JB Taylor and B McNamara. Plasma diffusion in two dimensions. *The Physics of Fluids*, 14(7):1492–1499, 1971.

[95] S. M. Tobias, P. H. Diamond, and D. W. Hughes. β-Plane Magnetohydrodynamic Turbulence in the Solar Tachocline. *The Astrophysical Journal Letters*, 667:L113–L116, September 2007.

[96] Lu Wang and P. H. Diamond. Gyrokinetic theory of turbulent acceleration of parallel rotation in tokamak plasmas. *Phys. Rev. Lett.*, 110:265006, Jun 2013.

[97] John Wesson and David J Campbell. *Tokamaks*, volume 149. Oxford university press, 2011.

[98] Niels Winsor, John L. Johnson, and John M. Dawson. Geodesic acoustic waves in hydromagnetic systems. *The Physics of Fluids*, 11(11):2448–2450, 1968.

[99] R C Wolf. Internal transport barriers in tokamak plasmas. *Plasma Physics and Controlled Fusion*, 45(1):R1–R91, nov 2002.

[100] R.C Wolf, W Biel, M.F.M. de Bock, K.H Finken, S Günter, G.M.D Hogeweij, S Jachmich, M.W Jakubowski, R.J.E Jaspers, A Krämer-Flecken, H.R Koslowski, M Lehnen, Y Liang, B Unterberg, S.K Varshney, M. von Hellermann, Q Yu, O Zimmermann, S.S Abdullaev, A.J.H Donné, U Samm, B Schweer, M Tokar, E Westerhof, and the TEXTOR Team. Effect of the dynamic ergodic divertor in the TEXTOR tokamak on MHD stability, plasma rotation and transport. *Nuclear Fusion*, 45(12):1700–1707, nov 2005.

[101] Richard B Wood and Michael E McIntyre. A general theorem on angular-momentum changes due to potential vorticity mixing and on potential-energy changes due to buoyancy mixing. *Journal of the atmospheric sciences*, 67(4):1261–1274, 2010.

[102] X. Z. Yang, B. Z. Zhang, A. J. Wootton, P. M. Schoch, B. Richards, D. Baldwin, D. L. Brower, G. G. Castle, R. D. Hazeltine, J. W. Heard, R. L. Hickok, W. L. Li, H. Lin, S. C. McCool, V. J. Simcic, Ch. P. Ritz, and C. X. Yu. The space potential in the tokamak TEXT. *Physics of Fluids B: Plasma Physics*, 3(12):3448–3461, 1991.

[103] Q Yu, S Günter, K Lackner, A Gude, and M Maraschek. Interactions between neoclassical tearing modes. *Nuclear Fusion*, 40(12):2031–2039, dec 2000.

[104] D. Zarzoso, Y. Sarazin, X. Garbet, R. Dumont, A. Strugarek, J. Abiteboul, T. Cartier-Michaud, G. Dif-Pradalier, Ph. Ghendrih, V. Grandgirard, G. Latu, C. Passeron, and O. Thomine. Impact of energetic-particle-driven geodesic acoustic modes on turbulence. *Phys. Rev. Lett.*, 110:125002, Mar 2013.

[105] Y. B. Zel'dovich. Percolation properties of a random two-dimensional stationary magnetic field. *ZhETF Pisma Redaktsiiu*, 38:51, July 1983.

[106] Ya B Zel'dovich. The magnetic field in the two-dimensional motion of a conducting turbulent fluid. *Sov. Phys. JETP*, 4:460–462, 1957.